

Final Report

AIR QUALITY IMPACTS OF LOW VAPOR PRESSURE- VOLATILE ORGANIC COMPOUNDS

(Contract Number: 13-302)

Principal Investigator:
David R. Cocker III
951 231 0729

Prepared for:

State of California Air Resources Board
Research Division
PO Box 2815
Sacramento, CA 95812

Prepared by:

David Cocker, Weihua Li, Lijie Li, Mary Kacarab, Weihan Peng

University of California, Riverside

College of Engineering Center for Environmental Research and Technology (CE-CERT)
1084 Columbia Ave
Riverside, CA 92507
Phone: (951) 781 5791
Fax: (951) 781-5790

December 13, 2016

ACKNOWLEDGEMENTS AND DISCLAIMER

This work was funded by the California Air Resources Board (ARB) through contract number 13-302.

The UCR EPA chamber experiments were carried out at the College of Engineering, Center for Environmental Research and Technology (CE-CERT) primarily by Weihua Li, Lijie Li, and Mary Kacarab with assistance from Weihan Peng, Dana Maxie, Robert Espinoza, and Kurt Bumiller.

Helpful discussions with Jin Xu and Eileen McCauley of the ARB staff, Doug Fratz of the Consumer Specialty Products Association, and Naveen Berry of the SCAQMD staff concerning research directions for the project are acknowledged. We also acknowledge input from other members of the LVP-VOC advisory group concerning selection of compounds for this project and other input. Helpful discussions with Dr. William P.L. Carter concerning the experimental protocols and chemical reactivity modeling are also gratefully acknowledged.

Although this work was funded primarily by the ARB, it reflects only the opinions and conclusions of the author. Mention of trade names and commercial products does not constitute endorsement or recommendation for use.

Table of Contents

List of Tables	5
List of Figures	6
EXECUTIVE SUMMARY	11
I. INTRODUCTION	15
II. EXPERIMENTAL SET-UP	19
1. Investigation of LVP-VOC volatilization rates using an evaporation chamber.....	19
2. Selection of LVP-VOCs and mixtures:.....	20
3. Laboratory chamber experiments on LVP-VOCs.....	22
a. Environmental chamber facility	22
b. Analytical methods	24
c. Gas-phase analysis	24
d. Particle-phase analysis	24
e. LVP-VOC injection	26
III. RESULTS AND DISCUSSION	28
1. Atmospheric availability	28
a. Individual LVP-VOCs	28
b. LVP-VOC in consumer product surrogate mixtures.....	31
c. Wall effects	42
d. Chamber background	42
e. LVP-VOC stability within the UCR environmental chamber	42
f. Particle wall loss correction	44
g. Chamber characterization run	44
h. Experimental types.....	45
2. Individual LVP-VOC experiments	52
a. Ozone experimental results.....	52
b. Ozone modeling results.....	55
c. SOA results	62
d. Seeded experiment-vapor wall loss effects	69
e. In depth glycol ether study.....	71

f.	Individual LVP-VOC with NO and UV only	73
g.	Individual LVP-VOC with H ₂ O ₂ only	74
3.	Consumer products	76
a.	Ozone results.....	76
b.	SOA results	78
c.	Comparison with single compounds	80
4.	Hydrocarbon solvent mixtures	81
a.	Ozone formation	81
b.	SOA formation.....	83
c.	Hydrocarbon solvent mixture experimental repeatability	85
5.	Overall ozone and SOA formation comparison	87
6.	Chemical composition characteristics of SOA formation.....	90
a.	Volume fraction remaining (VFR).....	90
b.	Average oxidation state of carbon (OSc).....	90
c.	SOA density	91
IV.	SUMMARY	95
V.	REFERENCES.....	98

List of Tables

Table 1: Individual LVP-VOCs tested.....	20
Table 2: Surrogate consumer products studied.....	20
Table 3: The recipes of selected consumer products	21
Table 4: The recipe and manufacturing process of hand lotion	21
Table 5: List of analytical and characterization instrumentation used in this project.....	24
Table 6: Individual LVP-VOCs tested.....	29
Table 7 : Viscosity and diffusivity of water, honey and propylene glycol at room condition.....	40
Table 8: Stability run	43
Table 9 : Tested LVP-VOCs.....	43
Table 10: Summary of types of characterization experiments.....	45
Table 11 : EPA run table for LVP-VOCs	47
Table 12: Yield for individual LVP-VOC runs	68
Table 13: Ozone and SOA formation relative to surrogate runs for individual LVP-VOC runs.....	69
Table 14: SOA characteristics.....	91

List of Figures

Figure 1: Volatility distribution (gas/particle) for low vapor pressure compounds as function of organic aerosol concentration. Example is for a-pinene ozonolysis (Donahue, 2010, AAAR tutorial). Green shaded areas represent aerosol partitioned component, clear represents gas-phase.....	16
Figure 2: Schematic for LVP-VOC volatilization measurement.	19
Figure 3: Schematic of the UCR EPA chamber, showing the two side-by-side 90 m ³ Teflon bags (right), the light source (upper left), and the area flushed with purified air to control temperature and humidity, and minimize background effects.	23
Figure 4: Blacklight (used in this work), UCR EPA (argon arc-lamp), and ground-level outdoor spectra.	23
Figure 5: Injection system currently used (valid for methods 1 and 2).....	27
Figure 6: Average Structure Activity for Organic Aerosol (Donahue 2010).....	29
Figure 7: Weight Loss in Evaporation chamber	30
Figure 8: Evaporation Rate (calculated from weight loss results (Figure 7).	31
Figure 9: DBE-5 concentration versus the volumetric amount of DBE-5 as pure compound and as component of paint stripper.	32
Figure 10: DBE-5 concentration versus volumetric amount of DBE-5 in pure form and as component of caulk remover.....	33
Figure 11: DEGBE concentration versus volumetric amount of DEGBE in pure form and as component of general purpose spray cleaner	33
Figure 12: Propylene glycol concentration versus volumetric amount of propylene glycol pure form and as component of laundry detergent.....	34
Figure 13: The relation of initial liquid LVP-VOC and final gas concentration	35
Figure 14: The relation of initial liquid LVP-VOC and final gas concentration in equilibrium zone	35
Figure 15: Evaporation results of three pure LVP-VOCs.....	36
Figure 16: Diagram of a evaporation chamber	37
Figure 17: The co-relation of viscosity, diffusivity, mixing time and evaporation particle scale. (Koop et al. 2011)	39
Figure 18: Evaporation results of pure LVP-VOC and its mixture	41
Figure 19: Stability test for LVP-VOCs in chamber.....	44
Figure 20: Ozone formation from individual LVP-VOCs with surrogate	53
Figure 21: Ozone repeatability observed for repeat experiments within this work.	53
Figure 22: Ozone formation from individual LVP-VOCs with surrogate and H ₂ O ₂	54
Figure 23: Typical ozone formation comparison between runs with or without H ₂ O ₂	55
Figure 24: The summary of O ₃ prediction results during experiment (elapsed time in hour) for LVP-VOCs by the SAPRC-11 model.....	61
Figure 25: SOA formation from individual LVP-VOCs with surrogate.....	63
Figure 26: SOA formation in surrogate only experiments.....	64
Figure 27: SOA formation from repeat surrogate experiments with H ₂ O ₂	64
Figure 28: SOA formation from individual LVP-VOCs with surrogate and H ₂ O ₂	65
Figure 29: Comparison of SOA formation with and without H ₂ O ₂ for select LVP-VOCs.....	65
Figure 30: Typical yield curve showing changes in aerosol formation as a function of M _o (Aerosol mass).	66
Figure 31: Yield curves for C6-C9 aromatics.....	67
Figure 32: Vapor Wall Loss Effects – Seeded Experiments.....	70
Figure 33: Molecular structure of ethers investigated.....	72
Figure 34: SOA yield from glycol ethers and relative ethers in absence of NO _x . (Colored by the amount of ether (precursor) reacted to aid in visual comparison of which ethers on a per ether reacted basis is producing the greatest relative amount of SOA).....	73
Figure 35: SOA formation from individual LVP-VOCs with NO.....	74

Figure 36: SOA formation from individual LVP-VOCs with H ₂ O ₂	75
Figure 37: Comparison of SOA formation from DEGEE at different conditions	76
Figure 38: Ozone formation trends for each consumer product injected into surrogate mixture.	77
Figure 39: Ozone formation from consumer products in surrogate mixture with enhanced H ₂ O ₂	78
Figure 40: Aerosol volume formation for consumer products corrected for wall loss.	79
Figure 41: PM volume formation from consumer products in surrogate mixture with H ₂ O ₂ added.	79
Figure 42: Ozone and aerosol formation from repeat experiments of hand lotion with and without added H ₂ O ₂	80
Figure 43: Comparison of SOA formation from single LVP-VOCs with that from mixtures in the presence of surrogate	81
Figure 44: Ozone formation for solvent mixtures. Two Conosol C200 mixtures were investigated for ozone formation (local vendor (*) and large vendor (**)). Aromatic-200 is not shown due to interferences of the Aromatic 200 with the UV absorption of the ozone analyzer.	82
Figure 45: Ozone formation from surrogate with solvent mixtures and H ₂ O ₂ added.	83
Figure 46: PM volume formation corrected for wall loss for solvent mixtures added to surrogate mixture	84
Figure 47: Aerosol formation for hydrocarbon solvent mixtures added to surrogate mixture with enhanced H ₂ O ₂	85
Figure 48: SOA formation from repeat Aromatic 200 solvent mixtures. Ozone is not shown as the aromatic content of the aromatic 200 interfered with the UV absorption of the ozone analyzer due to the conjugate double bonds.....	86
Figure 49: Ozone and SOA formation from repeat experiments of Isopar M plus surrogate with and without H ₂ O ₂	86
Figure 50: Comparison of ozone formation from individual LVP-VOCs under different scenarios.....	88
Figure 51: Comparison of ozone formation from consumer products and hydrocarbon solvents under different scenarios.....	89
Figure 52: Comparison of SOA formation from individual LVP-VOCs under different scenarios. (*: No experiment)	89
Figure 53: Comparison of SOA formation from consumer products and hydrocarbon solvents under different scenarios. (*: No experiment)	90

Glossary of abbreviations

LVP-VOCs	Low vapor pressure-volatile organic compounds
AADCO	AADCO 737-SERIES PURE AIR GENERATORS
APM	Air Particle Monitor
ARB	Air Resources Board
CARB	California Air Resources Board
CE-CERT	College of Engineering, Center for Environmental Research and Technology
CSPA	Consumer Specialty Product Association
CSTR	Continuous stirred tank reactor
CSTRs	Continuous stirred tank reactors
DBE-5	Dimethyl Glutarate
DEGBE	Diethylene Glycol Monobutyl Ether
DEGDME	Diethylene Glycol Dimethyl Ether
DEGEE	Diethylene Glycol Ethyl Ether
DEGME	2-(2-Methoxyethoxy)ethanol
DPGBE	Dipropylene Glycol Butyl Ether
DPGMEA	Dipropylene Glycol Methyl Ether Acetate
EDTA	Ethylenediaminetetraacetic acid
ELVOC	Extremely low vapor pressure volatile organic compound
EPA	Environmental Protection Agency
EU	European Union
FID	Flame ionization detectors
GC	Gas chromatographs
GC- FID	GC with Flame Ionization Detector
GSQ	ACEM
HR-ToF-AMS	High resolution time-of flight aerosol mass spectrometer
IVOC	Intermediate volatile organic compound

LVOC	Low vapor pressure volatile organic compound
LVP	Low vapor pressure
m/z	Mass to charge ratio
MIR	Maximum incremental reactivity
MOIR	Maximum ozone incremental reactivity
n-C13	n-Tridecane
n-C17	n-Heptadecane
OSc	Average Oxidation State of Carbon
OTC	Ozone Transport Commission
PEG	Polyethylene glycol
PM	Particular Matter
RH	Relative humidity,
ROG	Reactive organic gas
SAPRC-07	Statewide Air Pollution Research Center, Model Version 2007
SAPRC-11	Statewide Air Pollution Research Center, Model Version 2011
SCAQMD	South Coast Air Quality Management District
SMPS	Scanning mobility particle sizers
SOA	Secondary organic aerosol
SVOC	Semi-volatile organic compound
SYFT SIFT-MS	Selected ion flow tube mass spectrometry
TDMA	Tandem differential mobility analyzer
TEA	Triethanolamine
UV	Ultraviolet
VBS	Volatility basis set
VFR	Volume Fraction Remaining
VOC	Volatile organic compound

EXECUTIVE SUMMARY

A primary objective of this study was to provide critical experimental data on the atmospheric availability of low vapor pressure-volatile organic compounds (LVP-VOCs) from the use of consumer products. LVP-VOCs identified by the ARB working group to be studied within this work include: Benzyl Alcohol, Dipropylene Glycol Methyl Ether Acetate (DPGMEA), Diethylene Glycol Monobutyl Ether (DEGBE), n-Tridecane, n-Heptadecane, Diethylene Glycol Ethyl Ether (DEGEE), Dimethyl Glutarate (DBE-5), Propylene Glycol, Triethanolamine, 2,2,4-trimethyl-1,3-pentanediol monoisobutyrate (Texanol), diethylene glycol, glyceryl triacetate, Glycerol, and Methyl Palmitate. Triethanolamine, Glyceryl Triacetate, and Methyl Palmitate did not show appreciable evaporation rates after six months and were replaced in the program by three hydrocarbon solvents (Conosol 200, Aromatic 200, and Isopar M). Generic consumer products (Caulk Remover, Laundry Detergent, Paint Stripper, General Purpose Spray Cleaner Mixture and Hand Lotion) were formulated with guidance from the Consumer Specialty Products Association (CSPA) and their individual members and used to investigate differences in behaviors of individual LVP-VOCs and more complex mixtures. This study proceeded to evaluate the evaporation rate, and therefore atmospheric availability, of LVP-VOCs in pure form and as part of mixtures as they are used in consumer products. A semi-empirical formula using vapor pressure and molecular weight of the LVP-VOC was identified from the scientific literature and found to be sufficient to accurately estimate evaporation rates for the wide range of LVP-VOCs studied within this program. LVP-VOC evaporation rates were influenced by the presence of other chemicals in the consumer product mixtures. The effect appears to be related to mass transfer rates of the LVP-VOC to the air-mixture interface as opposed to significant changes in the thermodynamic equilibrium of those LVP-VOCs studied as increasing surface area increased the partitioning of the LVP-VOC to the air from the consumer product.

Another primary objective of the program was to evaluate the ozone and secondary organic aerosol (SOA) formation from the select individual LVP-VOCs, hydrocarbon solvent mixtures, and generic consumer products described above. Environmental chamber experiments were conducted within the advanced environmental chamber facility housed at the College of Engineering, Center for Environmental Research and Technology (CE-CERT) at UC Riverside designed to investigate atmospheric reactivity, ozone formation, and SOA formation at relevant atmospheric concentrations.

The influence of chamber walls on gas-phase reactivity and SOA formation was assessed by conducting multiple characterization experiments. CO experiments were used to identify the rate of NO_x offgassing from the chamber walls. CO- NO_x experiments were conducted to quantify the HONO radical source. Clean air experiments were performed to screen for background VOC effects combined with chamber wall NO_x offgassing. m-Xylene-NO experiments were carried out to demonstrate the repeatability of chamber SOA experiments. Combined, this suite of experiments characterized the UCR environmental chamber performance and provided critical model inputs into the SAPRC-2011 mechanism.

Losses of LVP-VOCs to the chamber surfaces were evaluated and found to be negligible through chamber stability tests by monitoring the decay of the LVP-VOC precursors in the absence of light and oxidants over the course of multiple hours. All LVP-VOCs monitored maintained a constant concentration within measurement error during stability tests. Additional experiments performed with and without inorganic seed showed little impact on SOA formation for LVP-VOCs producing significant quantities of aerosol (e.g. DEGBE, DEGEE) indicating that the walls were not significantly contributing to losses of LVP-VOC oxidation products. However, differences were observed in experiments with and without seed when the nucleation intensity was low (few particle numbers formed) and for LVP-VOCs with generally low SOA formation (e.g., Glyceryl triacetate, DPGMEA, and DBE-5). Therefore, the environmental chambers used in this work were deemed suitable to study ozone and SOA formation from the LVP-VOCs investigated within this work.

A simplified ROG surrogate commonly used to study maximum incremental reactivity was utilized within this work to mimic total atmospheric reactivity for select experiments. The ROG surrogate used included seven representative compounds: n-butane, n-octane, ethene, propene, trans-2-butene, toluene, and m-xylene with a total surrogate concentrations of 1.1 ppmC. This represents one of the first reported works for secondary organic aerosol formation in the presence of a surrogate mixture and was used to parallel work previously conducted determining ozone formation. Further, surrogate experiments with additional H₂O₂ added were used to offset losses in hydroxyl radical concentrations due to the addition of select LVP-VOCs.

The formed ozone concentration from photo-oxidation of individual LVP-VOCs with surrogate and NO_x ranged from 145 to 222 ppb. The ozone formation from photo-oxidation of individual LVP-VOCs with surrogate and NO_x at elevated hydroxyl radical concentration was also evaluated with ozone formation ranging from 135 to 193 ppb. Several LVP-VOCs formed less ozone compared with surrogate only experiments, even after addition of H₂O₂ experiments. But this does not necessarily indicate that the LVP-VOC will suppress (or enhance) ozone formation in the atmosphere—only that it is negatively (or positively) impacting the specific surrogate mixture ozone formation. This may be attributed to larger changes in radical concentrations, NO_x loadings, etc. than expected to occur within the more complex ambient atmosphere with its more significant reservoir of other atmospheric species.

Surrogate-NO_x only experiments did not form noticeable SOA. SOA formation from photo-oxidation of individual LVP-VOCs with surrogate and NO_x ranged widely among LVP-VOCs with n-Heptadecane, Benzyl Alcohol, Diethylene Glycol Monobutyl Ether generally forming the most aerosol while DEGEE, DBE-5, and n-Tridecane show relatively more moderate aerosol formation. Propylene Glycol, Diethylene Glycol, and Texanol formed only minimal SOA. More aerosols formed after injecting H₂O₂ for all LVP-VOCs that formed measurable SOA.

Aerosol yield (Y) is often reported as the ratio of the organic mass concentration of aerosol formed to mass concentration of hydrocarbon consumed. The yield data provides a comparative basis to determine which LVP-VOCs are most likely to contribute to SOA formation. SOA yield data are reported for individual LVP-VOC experiments with or without H₂O₂ added. Based on the starting vapor pressure of LVP-VOCs relative to other aerosol forming atmospheric precursors (e.g., monocyclic aromatics, isoprene, and monoterpenes) it was originally hypothesized that LVP-VOCs would form significant SOA. However, only propylene glycol, DEGBE, n-Tricane, n-Heptadecane, and benzyl alcohol had yields greater than or equal to 0.1 (typical of low-yield aromatic precursors) without added H₂O₂ and only n-heptadecane and benzyl alcohol had higher yields relative to common VOC SOA precursors. Addition of H₂O₂ to the chamber experiments adds DBE-5 and DEGBE to the list of SOA precursors with measurable SOA formation.

We also present an in-depth glycol ether study to further investigate the impact of molecular structure on SOA formation from glycol ethers. It was determined that SOA formation from the photo-oxidation of selected ethers was associated with the presence and location of –OH on the glycol ether backbone. Further, the molecular structure of the glycol ethers determined the branching ratio among carbonyl formation, cyclization and fragmentation thereby determining their propensity to form SOA.

Selected LVP-H₂O₂ and LVP-NO experiments were conducted as part of this study to provide additional SOA formation and chemical composition data without the presence of other VOCs in the surrogate. These tests provided the simplest evaluation of SOA formation from individual LVP-VOCs performed following classical SOA environmental chamber procedures and the most direct measure of the chemical composition and aerosol properties of SOA from LVP-VOC precursors.

The SAPRC-2011 mechanism was used to predict O₃ formation within the environmental chamber studies conducted and to evaluate the ability of current models to accurately predict observed ozone formation for the experiments conducted. The modelling results were found to predict well the gas-phase chemistry and ozone formation from the individual LVP-VOCs studied. Therefore, no major changes to the SAPRC-2011 mechanism or MIRs for these precursors is recommended based on this work.

Five hydrocarbon mixtures were included as part of this study to mimic the evaporation and atmospheric reactivity of select LVP-VOC containing consumer products. Simulated products included paint stripper, caulk remover, laundry detergent, hand lotion, and general purpose spray cleaner. Caulk remover was investigated with and without water added to the caulk remover. Only the laundry detergent (15% propylene glycol) measurably influenced ozone formation with the laundry detergent increasing ozone formation. These trends are consistent with the impacts of the LVP-VOCs investigated as propylene glycol (major LVP-VOC component) also enhanced ozone formation in the surrogate mixture. Select consumer products were also evaluated for ozone formation with increased H₂O₂. Hand lotion was found to elevate ozone produced by the surrogate mixture while laundry detergent was found to have little effect with added H₂O₂. Difficulty in injection of hand lotion and laundry detergent may have reduced the availability of these mixtures in the atmospheric chamber thereby limiting their measured impacts.

The particle formation for the surrogate consumer products was also investigated within the environmental chamber. Laundry detergent, spray cleaner, and paint stripper (from most to least) each formed appreciable amounts of SOA compared to the surrogate while the hand lotion and caulk remover (with or without water) formed only minimal amounts of SOA compared to the surrogate only experiments. SOA formation exceeded that of the individual LVP-VOC indicating that there were other SOA forming components of these three consumer products in addition to the LVP-VOC precursors investigated in this work. Two consumer products (laundry detergent and caulk remover) were studied in the presence of the surrogate mixture with enhanced H₂O₂. The hand lotion still produced little SOA while the laundry detergent SOA formation was further enhanced from the baseline measurements.

Three hydrocarbon solvents were identified by ARB staff for further evaluation of their ozone and SOA forming potentials. The three hydrocarbon solvents selected were Isopar M (low-aromatic mixture of alkanes, iso-alkanes, and cycloalkanes), Conosol 200 (low-aromatic mixture of cycloparaffinic and isoparaffinic hydrocarbons), and Aromatic 200 (predominantly aromatic compounds, b.p. 230°C). C-200* refers to a custom mixture of C-70* and C-400* blended to create C-200* with appropriate viscosity and was used prior to obtaining C-200 (labelled in report as C-200**) from a major vendor. Ozone formation was suppressed by both Isopar M and Conosol 200 hydrocarbon solvents (as expected) due to the ability of the solvent mixture to reduce the reactivity by scavenging hydroxyl radicals. Similar to the individual LVP-VOCs, additional surrogate experiments were performed with added H₂O₂ to enhance the OH reactivity of the system and offset some of the losses of OH to the solvent mixtures. Increases in ozone were observed with injection of H₂O₂. Differences between observed ozone for these experiments were also reduced.

The SOA formation from each hydrocarbon solvent mixture in the presence of the surrogate was evaluated. Significant aerosol formation was observed for all three solvent mixtures with Aromatic 200 greater than Conosol 200 which was greater than Isopar M. Similar experiments with large alkanes n-Tridecane and n-n-Heptadecane were seen to bracket the aerosol formation of the Conosol 200 and Isopar M and are provided as reference points. Differences in SOA formation between C-200* (blended from C-70 and C-400) and C-200** (obtained directly as C-200 from manufacturer) is attributed to compositional differences between the two blends. These experiments were repeated with added H₂O₂. As seen for individual LVP-VOCs, the enhanced H₂O₂ increased the amount of aerosol formed, likely due to a combination of increased kinetics (greater consumption of precursors) and increased radical oxidant concentrations leading to the formation of more condensable products for PM formation.

In this report, we also provide chemical composition characterization data, including volume fraction remaining (VFR), oxygen to carbon ratio (O/C), hydrogen to carbon ratio (H/C), average oxidation state of carbon (OSc), and SOA density. The VFR is used to study aerosol volatility. Information on the aerosol volatility also gives indirect indications of the aerosol composition and provides insights on the vapor pressure of the condensable species. The VFR at the end of the experiment typically ranged between 0.2 – 0.7, indicating that the SOA formed in the experiments were semi-volatile with 30 – 80% of the aerosol returning to the gas-phase at temperatures of 100°C. The OSc is an ideal metric for the degree of oxidation of organic species in the atmosphere, and regarded as a key quantity to describe mixtures of organic aerosol. The OSc also provides insight into the extent of functionalization (e.g., addition of OH, =O, etc.) leading to the SOA formation. The greater the functionalization, the lower the expected vapor pressure (per number of carbon) of the SOA.

I. INTRODUCTION

Atmospheric emissions of low vapor pressure-volatile organic compounds (LVP-VOCs) from consumer products and their impacts on ozone and secondary organic aerosol (SOA) formation are inadequately understood at this time. According to the ARB Consumer Products Regulation (Regulation for Reducing Emissions from Consumer Products. Title 17, California Code of Regulations, Article 2, section 94508),” LVP-VOC is defined as follows:

“LVP-VOC” means a chemical “compound” or “mixture” that contains at least one carbon atom and meets one of the following:

- (A) has a vapor pressure less than 0.1 mm Hg at 20°C as determined by ARB Method 310; or
- (B) is a chemical “compound” with more than 12 carbon atoms, or a chemical “mixture” comprised solely of “compounds” with more than 12 carbon atoms, as verified by formulation data, and the vapor pressure and boiling point are unknown; or
- (C) is a chemical “compound” with a boiling point greater than 216° C, as determined by ARB Method 310; or
- (D) is the weight percent of a chemical “mixture” that boils above 216° C, as determined by ARB Method 310.

For the purposes of the definition of LVP-VOC, chemical “compound” means a molecule of definite chemical formula and isomeric structure, and chemical “mixture” means a substance comprised of two or more chemical “compounds”.

Chemical compounds or mixtures that meet the definition of LVP-VOC are not counted towards compliance with the volatile organic compound (VOC) standards, i.e., towards the total VOC content of consumer product. However, recent work (Vö and Morris, 2012) has raised concerns that certain compounds currently receiving VOC exemptions as LVP-VOCs may have greater atmospheric impacts than previously understood. Further, their evaluation of a number of methods to determine VOC volatility including GC analysis, boiling point, carbon number, and vapor pressure led them to conclude that these methods provide contradictory evaluations as to whether a number of compounds currently classified as LVP-VOCs should be provided the LVP-VOC exemption (e.g., “Currently, EPA, California Air Resources Board (CARB), and the Ozone Transport Commission (OTC) exempt LVP solvents in consumer products with a vapor pressure less than 0.1 mmHg, a boiling point greater than 216 °C or 12 or more carbon atoms. The European Union (EU) and Canada exempt solvents with a boiling point greater than 250 °C. Green Seal exempts solvents with boiling point greater than 280 °C.”) Many of these compounds have high maximum incremental reactivity (MIR) values (Carter et al. 1995; Carter, 2008) relative to ethane and if available for atmospheric oxidation would be expected to participate in the formation of ozone (based on available MIR values) and SOA (based on the low vapor pressure of LVP-VOC precursors). Therefore, it is essential to revisit and improve estimates of the atmospheric availability and potential atmospheric impacts of LVP-VOCs.

The concept of vapor pressure and atmospheric availability can also be evaluated in the context of gas-particle equilibria that occur during SOA formation. The concept for a gas-particle partitioning model for atmospheric organic aerosol was first introduced by Odum et al. (1996) using the foundations laid by Pankow (1994a,b) to describe the SOA formation by using a thermodynamic equilibrium scheme and two semi-empirically lumped compounds of different vapor pressures. This concept has been applied to over one hundred atmospherically relevant compounds including aromatics (Cocker et al., 2001; Song et al., 2005; Na et al., 2006; Ng et al., 2007; Song et al., 2007; Warren et al., 2008), alkenes (Matsunaga et al., 2009), and terpenes (Cocker et al., 2001; Na et al., 2007; Ng et al., 2007) and other compounds (Chan et al., 2009; Lim and Ziemann, 2009). More recently, Song et al. (2005) suggested that atmospheric

chemistry involving both the VOC and NO_x may play a pivotal role in determining SOA yield from parent compounds.

Over the last decade, another concept, the volatility basis set (VBS), has been used to visualize the atmospheric behavior of semi-volatile organic species (Donahue et al., 2006). The VBS allows one to envision a complex mixture of organic aerosol evaporating and condensing over many orders of magnitude of compound vapor pressures depending on parameters such as temperature and organic aerosol concentration. The VBS is most often constructed using basis sets with bins of volatilities separated by one order of magnitude and spanning many orders of magnitude. The overall partitioning is given by

$$C_{OA} = \sum_i C_i \xi_i \quad \text{Eq. 1}$$

$$\xi_i = \left(1 + \frac{C_i^*}{C_{OA}}\right)^{-1} \quad \text{Eq. 2}$$

where C_i^* ($\mu\text{g}/\text{m}^3$) is the condensed-phase mass concentration of compound i , C_{OA} ($\mu\text{g}/\text{m}^3$) is the total condensed-phase concentration of all compounds in condensed-phase mixture, and ξ_i is defined as a partitioning coefficient for compound i given an effective saturation concentration C_i^* under a certain C_{OA} . The VBS can easily be used to demonstrate how compounds volatilize based on surrounding atmospheric concentrations. Shown below are two volatility distributions for SOA from α -pinene ozonolysis (Donahue et al., 2007). Figure 1 (left) shows the volatility distribution of the same mixture of products when only $1 \mu\text{g m}^{-3}$ of organic aerosol is present while the Figure 1 (right) shows the distribution when $100 \mu\text{g}/\text{m}^3$ of organic aerosol is present.

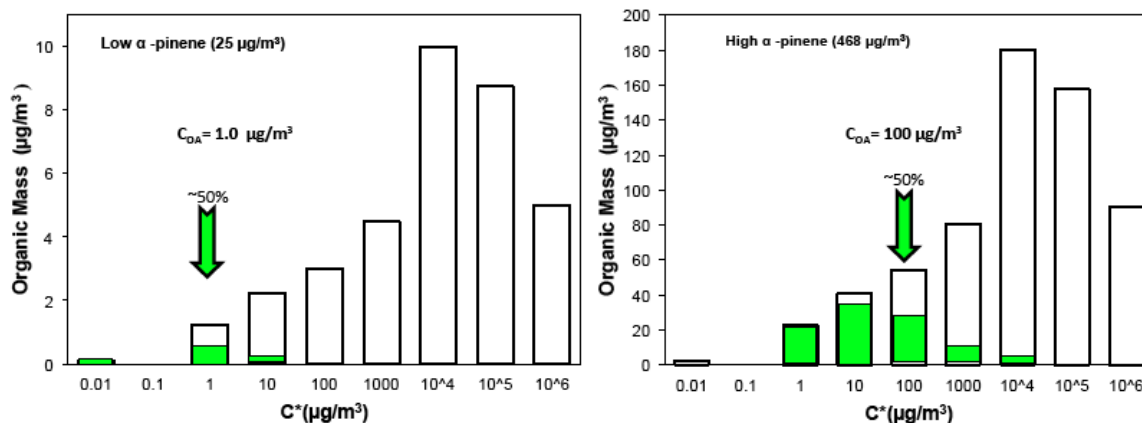


Figure 1: Volatility distribution (gas/particle) for low vapor pressure compounds as function of organic aerosol concentration. Example is for α -pinene ozonolysis (Donahue, 2010, AAAR tutorial). Green shaded areas represent aerosol partitioned component, clear represents gas-phase.

As C^* is related to the vapor pressure of the compound,

$$C^* = \frac{M_i 10^6 \zeta_i'}{760 RT} p_i^0 \left(\frac{\mu\text{g}}{\text{m}^3}\right) \quad \text{Eq. 3}$$

p_i^0 : Vapor pressure of pure compound

ζ_i' : Activity coefficient of a compound i

M_i : Molecular weight of a compound i

It can be seen how chemicals that would be measured in the particle phase (low vapor pressure) begin to evaporate (species with C^* of 1 are now partitioned 50-50 between the gas and particle phase) when

the organic aerosol concentration is lowered to $1 \mu\text{g m}^{-3}$ whereas the same species with C^* of 1 would be 99% in particle phase for organic aerosol concentrations of $100 \mu\text{g m}^{-3}$. Similarly, compounds with “low” vapor pressure with LVP-VOC exemptions may be more readily available for atmospheric degradation resulting in ozone and fine particle formation. The VBS tool therefore provides a conceptual framework for the chemical availability of “low” vapor pressure LVP-VOCs, which may subsequently participate in atmospheric chemistry and secondary pollutant formation.

Atmospheric environmental chambers have been utilized for several decades as the gold standard approach toward the evaluation of atmospheric reactivity of VOC precursors and their propensity to form ozone and SOA. These chambers provide the platform to evaluate the atmospheric chemical oxidation processes under well controlled conditions in the absence of meteorological impacts such as dilution. The UCR/CE-CERT environmental chamber was carefully designed in 2001 to allow for the study of these processes at more atmospherically relevant concentrations (Carter et al., 2005). Environmental chamber experiments are designed to closely simulate atmospheric conditions leading to the oxidation of test VOC (or LVP-VOC) precursors. However, practical experimental constraints (e.g., size of experimental matrix) require that select environmental conditions be investigated to provide critical information necessary for extrapolation to the outside world.

Data on SOA formation in well-characterized environmental chamber experiments representing a range of atmospheric conditions are essential to test and improve our theories and models for predicting SOA in the atmosphere. Emerging evidence obtained from such experiments demonstrates that NO_x levels during atmospheric simulations impact the extent of gas-to-particle conversion measured for atmospherically relevant hydrocarbons (Chen et al., 2007; Hurley et al., 2001). Previous work widely cited and used in atmospheric airshed models are derived from atmospheric chamber simulations at elevated NO_x concentrations far exceeding those typically encountered in urban airsheds (e.g., Odum et al., 1996, 1997; Griffin et al., 1999; Cocker et al., 2001; Izumi and Fukuyama, 1990; Jang and Kamens, 2001). Recent data from our group (Song et al., 2005) and at EUPHORE (Johnson et al., 2005) indicate that current environmental chamber data obtained under elevated NO_x conditions may significantly underestimate SOA formation. For aromatic systems, Song et al. (2005, 2007) has performed a series of experiments demonstrating that aerosol production is elevated at low NO_x concentrations and that this cannot simply be predicted by ozone (O_3), hydroxyl (OH), and nitrate (NO_3) concentrations present in the chamber. A significant portion of the underprediction in aerosol formation may be resulting from improperly evaluating aerosol formation at atmospherically relevant VOC to NO_x ratios.

Work by the Ziemann group at UCR (now at Colorado University) (Matsunaga and Ziemann, 2010) has more recently challenged the conventional assumption that the highly hydrophobic Teflon surfaces used for chamber wall material do not participate in the gas-particle equilibrium achieved within the reaction mixture inside the chamber. Matsunaga and Ziemann (2010) point out that sufficiently low vapor pressure products (C8–C16 n-alkanes and 1-alkenes and C8–C13 2-alcohols and 2-ketones) could participate in an equilibrium process with the wall, providing a sink for VOCs during the initial part of the experiment and a possible source later in the experiment. More recently, papers by (Yeh and Ziemann, (2014); Krechmer et al, (2016); Ye et al, (2016); and Zhang et al, (2014) have provided additional insight into the potential effects of chamber walls with their impacts ranging from very significant to minor. The impacts of the Teflon wall are evaluated and addressed in this work given the greater potential of the lower volatility precursor LVP-VOCs to interact with the wall than VOCs studied in environmental chambers to date.

Maximum Incremental Reactivity (MIR) is currently used to evaluate the reactivity of chemical compounds and their propensity to form ozone. MIR values have been developed for many compounds relevant for consumer products by Carter et al. and have been updated in 2008. However, in this earlier work, mechanism development and accurate MIR representations for LVP-VOCs were difficult to achieve due to challenges in analytical instrumentation for measuring these low-volatility compounds and

the lack of a chamber wall model to account for the partitioning of these species between the chamber surfaces, fine particles, and the gas-phase (Carter, 2008). This work revisits the ability of the current models to evaluate ozone performance within the environmental chamber.

Data on ozone formation and SOA formation have been obtained for individual LVP-VOCs, surrogate consumer product mixtures, and hydrocarbon solvents and analyzed for use in ozone and SOA model development from the UCR/CE-CERT environmental chamber. Further, evaporation rates of individual LVP-VOCs and LVP-VOCs within surrogate consumer product mixtures have been evaluated within a custom built evaporation chamber. This report details observations of ozone formation, evaluation of ozone formation from LVP-VOCs using the current SAPRC-11, and chemical and physical characterization of SOA formation. (The SAPRC-11 model is based on a kinetic and equilibrium approach with OH concentration estimated from the decay of m-xylene. The current completed model version is designated as SAPRC-11 and includes the rate constant and reactions updates based on current data, SAPRC-07 chemical mechanism and chamber evaluations (Carter and Heo, 2013; Carter, 2010). Chamber experiments conducted within this study include studies of oxidation of individual LVP-VOCs, oxidation of LVP-VOCs within a surrogate atmosphere with and without enhanced oxidation, and oxidation of mixtures of surrogate consumer products containing defined quantities of LVP-VOCs.

II. EXPERIMENTAL SET-UP

1. Investigation of LVP-VOC volatilization rates using an evaporation chamber

Evaporation rates of individual LVP-VOCs were evaluated gravimetrically within miniature (~30 L) evaporation chambers operating as continuous stirred tank reactors (CSTRs, Figure 2). This approach is based on the recent work by SCAQMD scientists (Võ and Morris, 2012). This work aimed to determine an empirical relationship between LVP-VOC chemical properties and evaporation rates since VOC content exemptions for LVP-VOCs are based on atmospheric availability.

The evaporative mass flux of the pure compound was simply determined through a mass balance approach with the pure compounds being placed on aluminum boats (capacity 20 ml, top I.D. 43 mm, Sigma-Aldrich) and weighed. Samples were weighed daily for the first ten days and then weekly thereafter for compounds with slow evaporative rates for a period of six months. The residence time of the chambers was set to 3.5 exchange of air per hour. Exchange rates were controlled by metering the flow of dilution air into the CSTR. The air entering the chambers was purified (see pure air system description as part of task 2) with very low humidity (dew point < -60 °C) to reduce the impacts of water or VOC sorption by the LVP-VOCs measured. The system was maintained at room temperature (25°C), which was tightly controlled in the environmental chamber building. A bank of 10 of these systems was utilized in parallel.

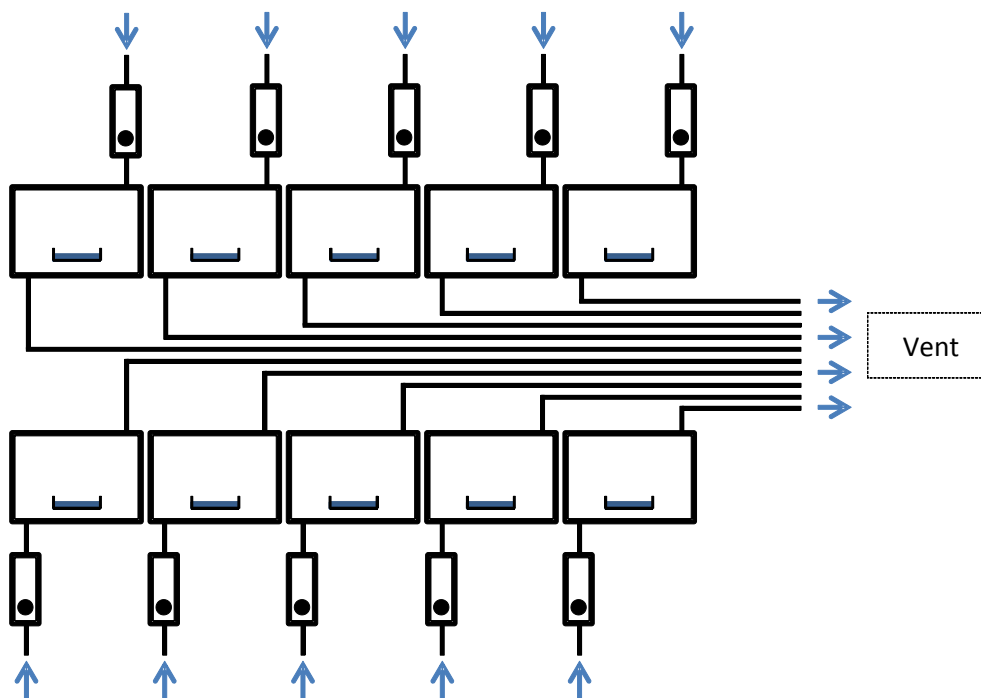


Figure 2: Schematic for LVP-VOC volatilization measurement.

2. Selection of LVP-VOCs and mixtures:

The selection of individual LVP-VOCs and consumer products was made in direct consultation with ARB staff and the advisory committee set-up by ARB. Fourteen LVP-VOCs were initially selected for analysis (Table 1); however as three (glycerol, methyl palmitate, and triethanolamine) were not atmospherically available over a six-month time period they were not studied as part of the subsequent environmental chamber work. Three hydrocarbon solvents (Isopar M, Conosol 200, Aromatic 200) were selected to replace these LVP-VOCs. Additionally, five LVP-VOC containing consumer products were selected (Table 2). The recipes for the four surrogate consumer products (Table 3) synthesized by mixing ingredients at room temperature along with the manufacturing process used for hand lotion (Table 4) are provided below.

Table 1: Individual LVP-VOCs tested

LVP-VOC Compound Name	CAS #
Diethylene Glycol	111-46-6
Propylene Glycol	57-55-6
Diethylene Glycol Ethyl Ether (DEGEE)	111-90-0
Diethylene Glycol Monobutyl Ether (DEGBE)	112-34-5
n-Tridecane (n-C13)	629-50-5
n-Heptadecane (n-C17)	629-78-7
Dimethyl Glutarate (DBE-5)	1119-40-0
Dipropylene Glycol Methyl Ether Acetate (DPGMEA)	88917-22-0
2,2,4-Trimethyl-1,3-Pentanediol Monoisobutyrate (Texanol)	25265-77-4
Glyceryl Triacetate	102-76-1
Benzyl Alcohol	100-51-6
Methyl Palmitate	112-39-0
Triethanolamine (TEA)	102-71-6
Glycerol	56-81-5

Table 2: Surrogate consumer products studied

Consumer Product Name
Laundry detergent
General-Purpose Spray Cleaner
Caulk Remover
Paint Stripper Gel
Hand Lotion

Table 3: The recipes of selected consumer products

Product Name	Formulations (weight percent)
Laundry detergent	51% water; 15% propylene glycol; 5% coconut fatty acid; 25% Pareth 25-9; 4% triethanolamine.
General-Purpose Spray Cleaner	90.2% water; 5% diethylene glycol monobutyl ether; 0.5% tetrasodium EDTA; 1% ethylene glycol butyl ether; 3% cocamidopropylamine oxide (34% active); 0.3 % triethanolamine.
Caulk Remover	30% dimethyl glutarate, 10% dimethyl succinate, 5% dimethyl adipate, 1% ethanolamine, 1% ethylene glycol, 53% water.
Paint Stripper Gel	40% N-methylpyrrolidone, 30% dimethyl glutarate, 20% dimethyl adipate, 5% PEG-15 cocamine, 5% d-limonene.

- The recipes of selected consumer products were in consultation with industry stakeholders.

Table 4: The recipe and manufacturing process of hand lotion

	Raw Material description	Weight percent (%)	Comments
Water Phase - Main Tank			
1	Water, Purified	82.6700	
2	Carbopol Ultrez 20 Polymer (Acrylates/C10-30 Alkyl Acrylates Crosspolymer)	0.2500	Sprinkle on top of water at RT. Let wet without agitation.
Premix A			
3	Propylene Glycol	4.0000	Can heat premix to get powders in.
4	Glycerol, USP	2.0000	
5	Chlorphenesin Powder	0.2800	
6	Methylparaben	0.2500	
End Premix A			
Add Premix A to the Main Tank.			
7	Xanthan Gum	0.2000	Sprinkle into Main Tank with good agitation.
Start heating water phase to 165-170F.			
Oil Phase			
8	Sorbitan Laurate	0.5000	Heat the oil phase to 165-175F
9	Behenyl Alcohol	0.2500	
10	Petrolatum	1.0000	
11	Squalane	4.0000	
12	Dimethicone	0.2500	
End Oil Phase			
Add Oil Phase to Water Phase at 165 - 175F. Mix 15 minutes.			
Begin Cooling to 130-140F and then add premix B.			
Premix B			
13	Water, Purified	4.0000	Make extra Premix, may need to add more for pH (5.8 - 6.8)
	Arginine	0.3500	
End Premix B			
		100.0000	

3. Laboratory chamber experiments on LVP-VOCs

a. Environmental chamber facility

The environmental chamber experiments were carried out using the UCR EPA chamber. This chamber was constructed under EPA funding to address the needs for an improved environmental chamber database for mechanism evaluation (Carter et al., 1999). The objectives, design, construction, and initial evaluation of this chamber facility are described in more detail elsewhere (Carter et al, 1999, Carter, 2002, 2004). This chamber was successfully utilized in our “low NO_x” mechanism evaluation study for the CARB (Carter, 2004), for experiments to reduce uncertainties in reactivities of coatings VOCs (Carter and Malkina, 2005; Carter et al, 2005c), pesticides (Carter and Malkina, 2007; Carter, 2007c), and amines (Carter, 2007b), and is being continuously utilized for ongoing PM studies (Carter et al, 2005c; Song et al, 2005, 2007a-c). Detailed description of the chamber and procedures are given in the references cited above, and are briefly summarized below.

The UCR EPA chamber consists of two ~90,000-liter Teflon® reactors located inside a 16,000 cubic foot temperature-controlled “clean room” that is continuously flushed with purified air. The clean room design is employed in order to minimize background contaminants into the reactor due to permeation or leaks. The light source used in this study consists of 272 115W Sylvania 350BL blacklights. The interior of the enclosure is covered with reflective aluminum panels in order to maximize the available light intensity and to attain sufficient light uniformity, which is estimated to be ±10% or better in the portion of the enclosure where the reactors are located (Carter, 2002). The reactors are attached to a semi-flexible moveable framework that allows the reactors to be emptied between experiments and reduces the volume under positive pressure control to prevent dilution due to sampling or leaks during experiments. A high-volume mixing system with Teflon® pipes and Teflon®-coated flanges is used to mix the reactors and to exchange reactants between the reactors to achieve equal concentrations when desired. A diagram of the enclosure and reactors is shown on Figure 3, and the spectra of different light sources (blacklights, current study; UCR EPA, Ar arc-lamp; Solar z=0, ground level light intensity at zenith angle 0°) are shown on Figure 4. Variations in light-intensity by the artificial lights across the light spectrum can lead to differential photolysis rates of chemicals within the chamber; however, this is only a concern for chemicals subject to direct photolysis by these wavelengths. It is expected that the main atmospheric chemistry is driven by NO₂ photolysis; the measured k_1 (NO₂ photolysis rate) in the chamber is 0.401 min⁻¹, similar to k_1 (~0.39 min⁻¹) measured on July 1, 1997 as part of the Southern California Ozone Study (SCOS) (Vuilleumier et al., 2001) following identical measurement procedures.

An AADCO air purification system that provides dry purified air at flow rates up to 1500 liters min⁻¹ is used to supply the air to flush the enclosure and to flush and fill the reactors between experiments. The air is further purified by passing it through cartridges filled with Purafil® and heated Carulite 300® which is a Hopcalite®-type catalyst and also through a filter to remove particulate matter. The measured NO_x, CO, and non-methane organic concentrations in the purified air were found to be less than the detection limits of the instrumentation employed. The ultra-low humidity is expected to minimize the sorptive influence of the Teflon walls. It is noted that it is possible that changes in atmospheric water content will impact gas-particle partitioning and/or chemical reactions leading to ozone formation. Analysis of these impacts would be the subject of future work and was beyond the scope of this program.

The chamber enclosure is located on the second floor of a two-floor laboratory building that was designed and constructed specifically to house this facility (Carter, 2002). Analytical instrumentation (except for the PM instrumentation) is located on the ground floor beneath the chamber or on the second floor immediately adjacent to the chamber enclosure. The particle sizing instrumentation is located within the enclosure to ensure sizing is conducted at the same temperature as the experiment to prevent evaporation and/or condensation during analysis.

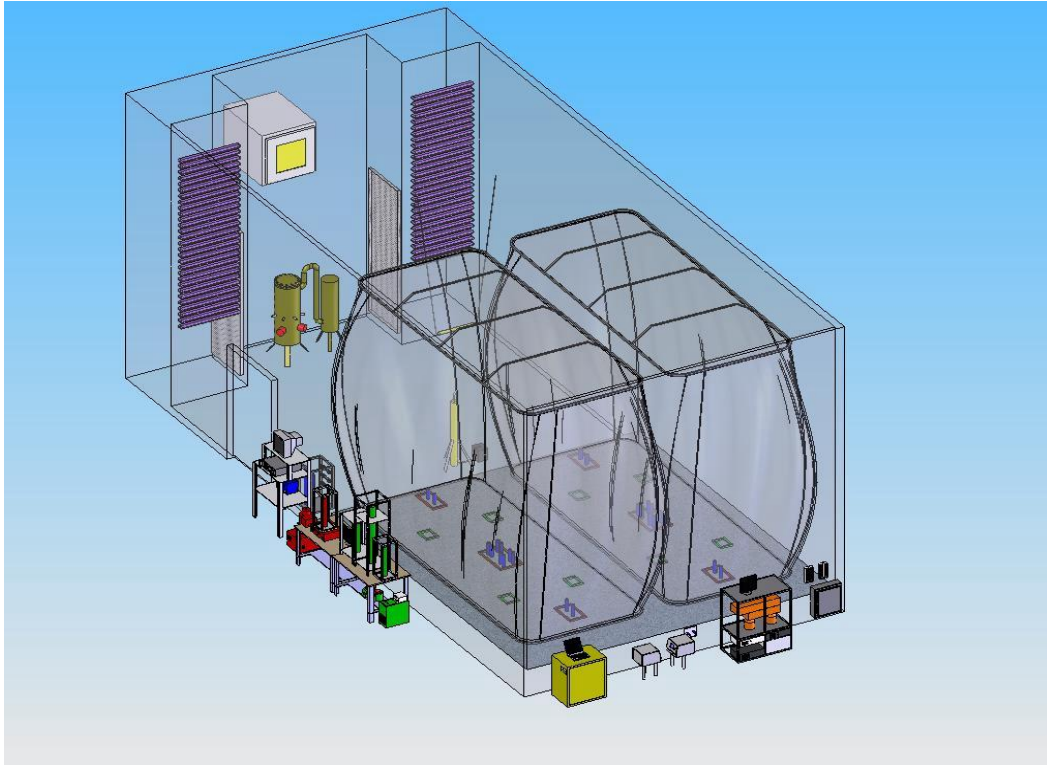


Figure 3: Schematic of the UCR EPA chamber, showing the two side-by-side 90 m³ Teflon bags (right), the light source (upper left), and the area flushed with purified air to control temperature and humidity, and minimize background effects.

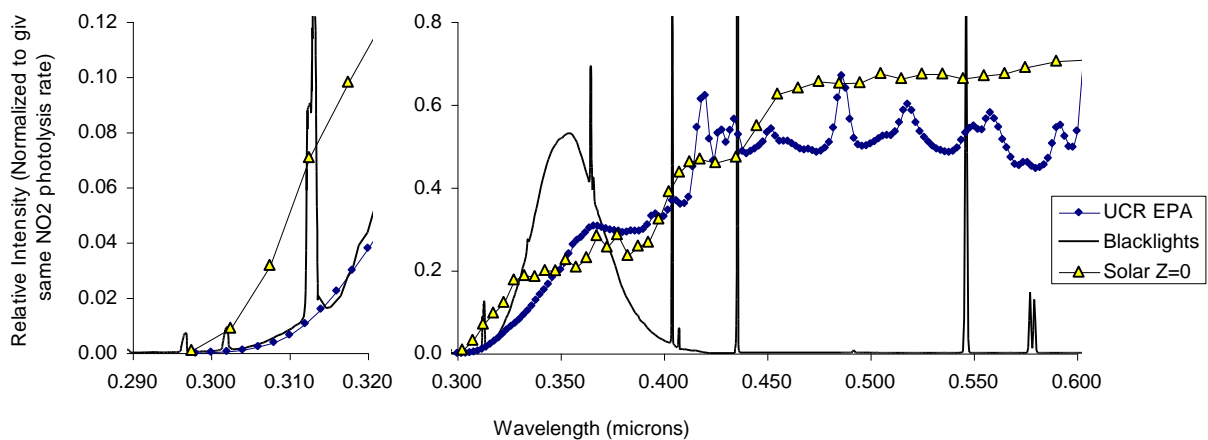


Figure 4: Blacklight (used in this work), UCR EPA (argon arc-lamp), and ground-level outdoor spectra.

b. Analytical methods

A summary of the instrumentation used in this project is given in Table 5 along with the compounds, parameters, or properties measured and typical sensitivities. The gas-phase and particle-phase analysis and data analysis methods are discussed in more detail below.

c. Gas-phase analysis

Decay of select VOCs (and LVP-VOCs) was monitored using dual Agilent 6890 (Palo Alto, CA) gas chromatographs (GC) equipped with flame ionization detectors (FID). A Thermal Environmental Instruments Model 42C chemiluminescence NO_x analyzer was used to measure NO, NO₂ and NO_x. Ozone concentration was monitored by a Dasibi Environmental Corp. Model 1003-AH O₃ analyzer. We used the SYFT SIFT-MS to monitor volatile oxygenated reaction products (and in some cases parent hydrocarbons (e.g., LVP-VOCs) for comparison with GC- FID analyses).

d. Particle-phase analysis

Aerosol growth was monitored using a pair of scanning mobility particle sizers (SMPS). The particle sampling equipment is located inside the enclosure to ensure that instrumentation temperature is identical to the reaction temperature. Total number counts were used to correct for particle wall losses assuming a first order wall loss decay as described in Cocker et al. (2001). A tandem differential mobility analyzer (TDMA) also tracked routinely the evolving volatility of SOA produced within the reaction chamber. The system was designed following the original work of Stolzenburg and McMurry (1989) and is quite similar to that reported in Cocker et al. (2001), with the key change being the use of a Dekati® thermal denuder (residence time = 17 sec; temperature 100°C) in lieu of a humidification tube.

Table 5: List of analytical and characterization instrumentation used in this project

Type	Model or Description	Species	Sensitivity	Comments
Gas Calibrator	Model 146C Thermo Environmental Dynamic Gas Calibrator	N/A	N/A	Used for calibration of NO _x and other analyzers.
Data Acquisition System	Windows PC with custom LabView software, 16 analog input, 40 I/O, 16 thermo-couple, and 8 RS-232 channels.	N/A	N/A	Used to collect data from most monitoring instruments and control sampling solenoids. In-house LabView software.
Temperature sensors	Various thermocouples, radiation shielded thermocouple housing	Temperature	~0.1 °C	Primary measurement is thermocouples inside reactor. Corrections made for radiative heating effect with arc light irradiation.
Ozone Analyzer	Dasibi Model 1003-AH. UV absorption analysis. Monitor Labs Chemiluminescence Ozone Analyzer Model 8410	O ₃	2 ppb	Standard monitoring instruments.

NO - NO _y Analyzer	Teco Model 42 C with external converter. Chemiluminescent analysis for NO, NO _y by catalytic conversion.	NO	1 ppb	Useful for NO and initial NO ₂ monitoring. Converter close-coupled to the reactors so the “NO _y ” channel should include HNO ₃ as well as NO ₂ , PANs, organic nitrates, and other species converted to NO by the catalyst.
		NO _y	1 ppb	
GC-FID #1	HP 6890 Series II GC with dual columns, loop injectors and FID detectors. Various megabore GC columns available. Controlled by computer interfaced to network.	VOCs	~10 ppbC	Equipped with: 30 m x 0.53 mm GS-Alumina column used for the analysis of light hydrocarbons and 30 m x 0.53 mm DB-5 column used for the analysis of C ₅₊ alkanes and aromatics. Loop injection suitable for low to medium volatility VOCs that are not too “sticky” to pass through valves.
GC-FID #2	HP 6890 Series II GC with dual columns and FID detectors, one with loop sampling and one set up for cartridge sampling. Various megabore GC columns available. Controlled by computer interfaced to network.	VOCs	~10 ppbC	30 m x 0.53 mm GSQ column. Loop injection suitable for low to medium volatility VOCs that are not too “sticky”. Not used as primary analysis for most of these experiments.
		VOCs	1 ppbC	Sorption cartridge sampling was used for low volatility or moderately “sticky” VOCs that cannot go through GC valves but can go through GC columns. Equipped with a 30 m x 0.53 mm DB-1701 column. Uses Dynatherm ACEM model 9305 (thermal desorption system).
Humidity Monitor	LiCor Li-840	Humidity	Dew point range: -60 - 50°C	Used for determination of RH in system. RH for dry experiments often below detection limit (<0.1% RH).
Spectro-radiometer	LiCor LI-1800 Spectroradiometer	300-850 nm Light Spectrum	Adequate	Resolution relatively low but adequate for its purpose. Used to obtain relative spectrum. Also gives an absolute intensity measurement at Teflon surface useful for assessing relative trends.
Spherical Irradiance Sensors	Biospherical QSL-2100 PAR Irradiance Sensor or related product. Responds to 400-700 nm light. Spectral response curve included.	Spherical Broad-band Light Intensity	Adequate	Provides a measure of absolute intensity and light uniformity that is more directly related to photolysis rates than light intensity on surface. Gives more precise measurement of light intensity trends than NO ₂ actinometry, but is relatively sensitive to small changes in position.
Scanning Mobility Particle Sizer (SMPS)	Uses matrix inversion program. Consists of TSI 3081L differential mobility analyzer, TSI 3077 ⁸⁵ Kr neutralizer, TSI 3760A condensation particle counter.	Aerosol Number and Volume concentration	Adequate	Provides information on size distribution of aerosols in the 28-730 nm size range, which accounts for most of the aerosol mass formed in our experiments. Data can be used to estimate secondary aerosol formation.
Tandem Differential Mobility	Comprised of two TSI 3081L differential mobility analyzer, TSI 3077 ⁸⁵ Kr	Aerosol volatility	Adequate	Provides information on the volatility of SOA produced during the reaction.

Analyzer (TDMA)	neutralizer, TSI 3760A condensation particle counter and thermal denuder.			
APM-SMPS	Kanomax APM coupled to custom SMPS similar to that described above	Aerosol Density	Requires $\sim 5 \mu\text{g m}^{-3}$ PM	Used to obtain real time (every 100 sec) density data necessary to convert aerosol volume (from SMPS) to aerosol mass
SIFT-MS	SYFT Voice200 single ion flow tube mass spectrometer	VOCs	Sub ppb	Online, real time (1 Hz) acquisition of VOC data including LVP-VOCs
HR-ToF-AMS	Aerodyne High Resolution (W and V-mode) time of flight aerosol mass spectrometer	PM chemical composition	Requires $\sim 5 \mu\text{g m}^{-3}$ PM	Online measurement of aerodynamic particle mobility and EI mass fragmentation pattern from chamber aerosol.

Particle density was obtained using the Kanomax APM. This analyzer classifies the mass of a single aerosol based on the balance between centrifugal and electrostatic forces. When coupled to an SMPS, this method provides a rapid, accurate determination of particle density within the chamber. Density can also be calculated by analysis of simultaneous SMPS and HR-ToF-MS data; this method will provide comparison for the APM-derived value. These methods provide insight into the changing nature of the aerosol produced within the chamber and allows for direct conversion of SMPS data into particle mass. (Malloy et al., 2008)

The high resolution time-of flight aerosol mass spectrometer HR-ToF-AMS is a real-time chemical aerosol analyzer capable of quantitatively sampling, sizing, and chemically analyzing aerosol with fast time resolution and sufficient mass spectral resolution to directly distinguish elemental composition of ions having the same mass (DeCarlo, 2006). The V-mode offers high sensitivity ($0.04 \mu\text{g m}^{-3}$) for all species with mass to charge (m/z) resolving power of approximately 2100, while the W-mode offers sensitivity of $0.4 \mu\text{g m}^{-3}$ for all species with m/z resolving powers approaching 5000. It is especially suited for quantification of C_xH_y , $\text{C}_x\text{H}_y\text{O}_z$, $\text{C}_x\text{H}_y\text{N}_z$, and $\text{C}_x\text{H}_y\text{O}_z\text{N}_p$ with direct identification of organonitrogen and organosulfur content (DeCarlo et al., 2006).

e. LVP-VOC injection

Due to their inherent low-volatility, the injection of LVP-VOCs into atmospheric chambers is challenging. Challenges include vaporization of the LVP-VOCs without thermal degradation (especially into smaller, reactive VOCs) and transport losses during injection into the chamber.

To overcome concerns of thermal degradation, we injected the LVP-VOCs in situ with the chamber. The injections were accomplished by

- 1) For compounds that have relatively “high” vapor pressures, above 10 ppm (or 0.00076 torr), the compounds were gently heated (35-40C) in a small oven through glass wool (tube) and evaporated into a nitrogen stream (~ 5 LPM), which is shown in Figure 5.



Figure 5: Injection system currently used (valid for methods 1 and 2)

- 2) For compounds with very low vapor pressures (<10 ppm), the compounds were heated through glass wool gradually (oven temperature approx. 150 °C) and injected through a heated transfer line into the chamber (55 °C). For these compounds, we used the scanning mode of the SIFT-MS to confirm that the LVP-VOCs did not undergo thermal degradation through vaporization.

III. RESULTS AND DISCUSSION

1. Atmospheric availability

a. Individual LVP-VOCs

LVP-VOCs, as defined by the regulatory communities, are excluded in determining compliance with VOC limits due to their limited ability to evaporate into the atmosphere. As discussed previously, the definition is generally based on boiling point, vapor pressure, or carbon number. Figure 6 presents a SOA point of view of volatility. As described in the introduction, C^* is a useful parameter to identify the propensity of a compound to partition between the gas-phase and an organic containing aerosol. Within this SOA community, the acronyms VOC (volatile organic compound), IVOC (intermediate volatile organic compound), SVOC (semi-volatile organic compound), LVOC (low vapor pressure volatile organic compound), and ELVOC (extremely low vapor pressure volatile organic compound) are often used. SVOC generally refers to the class of compounds that partition between gas and aerosol-phase with IVOC and VOC generally residing in the gas-phase and LVOC and ELVOC generally residing in the aerosol-phase. Using the definition of an LVP-VOC within this context, a LVP-VOC such as n-tridecane has a C^* value $\sim 5.54 \times 10^5 \mu\text{g m}^{-3}$ or $\log C^*$ of approximately 5.7, near the border between IVOC and VOC. Triethanolamine, with the lowest C^* of the LVP-VOCs investigated in this study, has a C^* is $\sim 67 \mu\text{g m}^{-3}$ or $\log C^*$ of approximately 1.8, falling just within the SVOC range.

Evaporation rates of the fourteen pure compounds (Table 6) were evaluated gravimetrically (See Section II-1) from evaporation chambers operating as CSTRs. All individual LVP-VOC evaporation experiments began with 200 μL placed into a weighing boat. The weight loss results are shown in Figure 7.

- n-Tridecane ● DEGBE ● Texanol ● Diethylene glycol ● Glycerol
- n-Heptadecane ● DEGEE ● Benzyl Alcohol ● Methyl Palmitate
- Propylene glycol ● DPGMEA ● Triethanolamine ● Glyceryl Triacetate

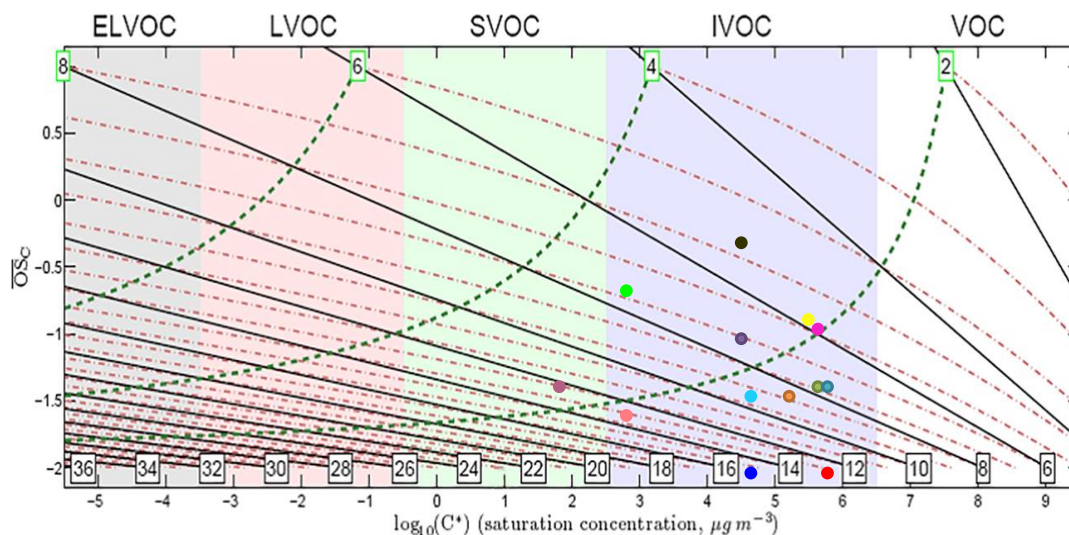


Figure 6: Average Structure Activity for Organic Aerosol (Donahue 2010)

Table 6: Individual LVP-VOCs tested

LVP-VOC Compound Name	CAS #	BP, °C	VP, mm Hg
First regime			
Propylene Glycol	57-55-6	188	0.08
Diethylene Glycol Ethyl Ether (DEGEE)	111-90-0	202	<0.1
Benzyl Alcohol	100-51-6	204.7	0.094 @ 25 °C
Dipropylene Glycol Methyl Ether Acetate (DPGMEA)	88917-22-0	209	0.08
Dimethyl Glutarate (DBE-5)	1119-40-0	215	0.097
Diethylene Glycol Monobutyl Ether (DEGBE)	112-34-5	230	0.02
n-Tridecane (n-C13)	629-50-5	234	0.08 @ 25 °C
2,2,4-Trimethyl-1,3-Pentanediol Monoisobutyrate (Texanol)	25265-77-4	244	0.01
Second Regime			
Diethylene Glycol	111-46-6	245	0.002
Glyceryl Triacetate	102-76-1	258-260	0.0025 @ 25 °C
n-Heptadecane (n-C17)	629-78-7	302	<0.001
Third Regime			
Glycerol	56-81-5	290	0.003@50 °C
Triethanolamine (TEA)	102-71-6	335.4	8.38e-06 @ 25 °C
Methyl Palmitate	112-39-0	417	0.038 @ 25 °C

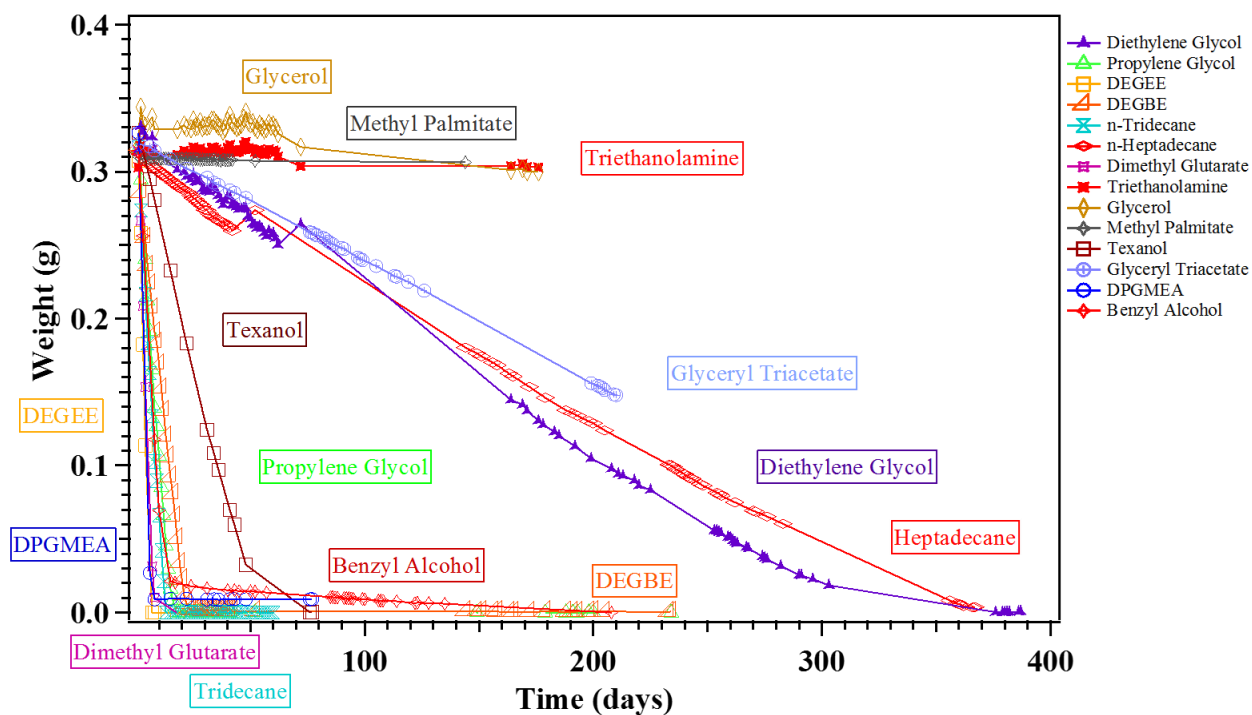


Figure 7: Weight Loss in Evaporation chamber

The evaporative losses of the LVP-VOCs generally fell into three regimes. The first regime includes benzyl alcohol, DEGBE, n-tridecane, DBE-5, DPGMEA, DEGEE, and propylene glycol, which lost more than 95% of their mass within one month and Texanol within three months. The second regime includes glyceryl triacetate, diethylene glycol, and n-heptadecane with loss of half of their weight on the order of six months. Glycerol, triethanolamine, and methyl palmitate lost less than 5% of their mass within six months and, after discussion with ARB staff and members of the Consumer Products advisory group were removed from the environmental chamber portion of the study.

Correlations of the LVP-VOC evaporation rates with physical and chemical properties of the LVP-VOCs was explored in an effort to provide semi-empirical prediction of the evaporation behavior for LVP-VOCs studied. The best correlation (equation 4, below; $R^2=0.98$, Figure 8) used both the vapor pressure and the molecular weight of the LVP-VOC with a linear trend obtained plotting molecular weight * vapor pressure versus evaporation rate (Mackay and Wesenbeeck, 2014), which is consistent with the literature. Evaporation rate is calculated from the initial loss rate (initial slope) in Figure 7 for each individual LVP-VOC.

$$\text{Evaporation Rate (g day}^{-1}\text{)} = 0.00284 * \text{Molecular weight (g mol}^{-1}\text{)} * \text{Vapor Pressure (mmHg)} \quad \text{Eq. 4}$$

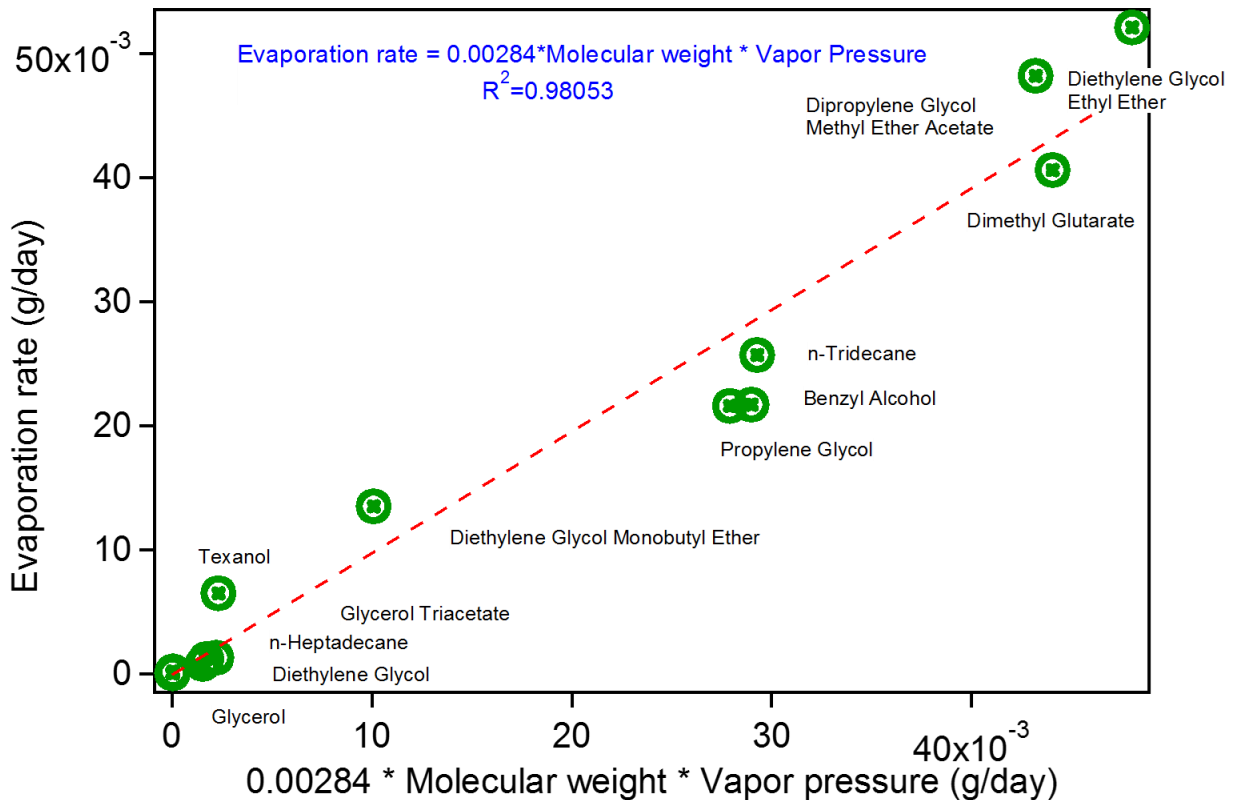


Figure 8: Evaporation Rate (calculated from weight loss results (Figure 7)).

b. LVP-VOC in consumer product surrogate mixtures

The evaporation of the individual LVP-VOCs from a consumer product mixture was evaluated next. Consumer products were placed into the evaporation chambers with measurement of the evaporating LVP-VOCs commencing immediately. Concentrations in the evaporation chamber and the SIFT were allowed to equilibrate (typically on order of 1 hour) prior to recording LVP-VOC concentrations. The time constant for evaporation of the LVP-VOC from the consumer product was many times greater than the measurement timescale so changes in LVP-VOC concentrations during measurement were assumed to be negligible. Tables 2 and 6 above summarizes the consumer products and LVP-VOC compounds measured. Since there are multiple compounds in each mixture, gravimetric analysis was no longer practical to evaluate the loss of individual LVP-VOCs. Therefore, a SIFT-MS was calibrated and utilized to directly measure the emissions of each LVP-VOC present in each consumer product studied. An additional challenge was identifying the appropriate methodology to use to make direct comparisons between losses of the individual LVP-VOCs and the LVP-VOCs present in the consumer products. Therefore, a series of experiments were performed with varying quantities of individual LVP-VOC placed into the evaporation chamber to explore the relationship between the concentration of LVP-VOC in the evaporation chamber and the liquid quantity injected. A plot of the concentration of the individual LVP-VOC within the atmosphere as a function of volume injected is shown in Figures 9-12 below. For each individual LVP-VOC, a linear increase is observed with increasing volume of LVP-VOC placed into the

evaporation chamber. The linear increase implies that the release rate of the LVP-VOC is sufficiently slow that kinetics and not equilibrium thermodynamics is establishing the atmospheric concentration for the LVP-VOC.

Next, varying amounts of each consumer product were injected into the evaporation chamber following the same injection protocol used for individual LVP-VOCs (Figures 9-12). Hand lotion did not release the LVP-VOC as the cooking portion of the recipe for making hand lotion likely chemically converted the LVP-VOC not detected by the SIFT-MS. The other four consumer products were simple mixtures with the LVP-VOC studied as a component of the mixture. Notable results are seen with the evaporation of the consumer products containing LVP-VOCs. First, since the LVP-VOC is typically a minor component of the mixture, far greater liquid volumes of each consumer product were needed to have the equivalent volume of LVP-VOC present in the chamber. Similar amounts of LVP-VOC were used as evaporation rate was observed to be a function of the amount of LVP-VOC present (see Figure 7 (decreasing slope over time or Figure 9 below) and direct comparison to measured evaporation rates of pure LVP-VOC were desired. Note that the x-axis is the equivalent volume of LVP-VOC present in the consumer product placed into the evaporation chamber. The relative evaporation of the LVP-VOC into the chamber as measured by gas-phase concentrations varied (some higher, some lower) for each LVP-VOC present in the evaporation chamber compared to that measured above the pure LVP-VOC.

The duration of each of these series of experiments was short (on the order of a few hours); therefore, given the relatively low-volatility of the consumer product, the relative composition (or mole-fraction) of the consumer product was not modified by evaporation of the LVP-VOC or other components. (E.g., the release of ppb levels of the LVP-VOCs measured by the SIFT-MS represents an insignificant amount of the LVP-VOC evaporated from consumer product on a mass conservation basis.) Measured values reported after steady-state concentrations achieved.

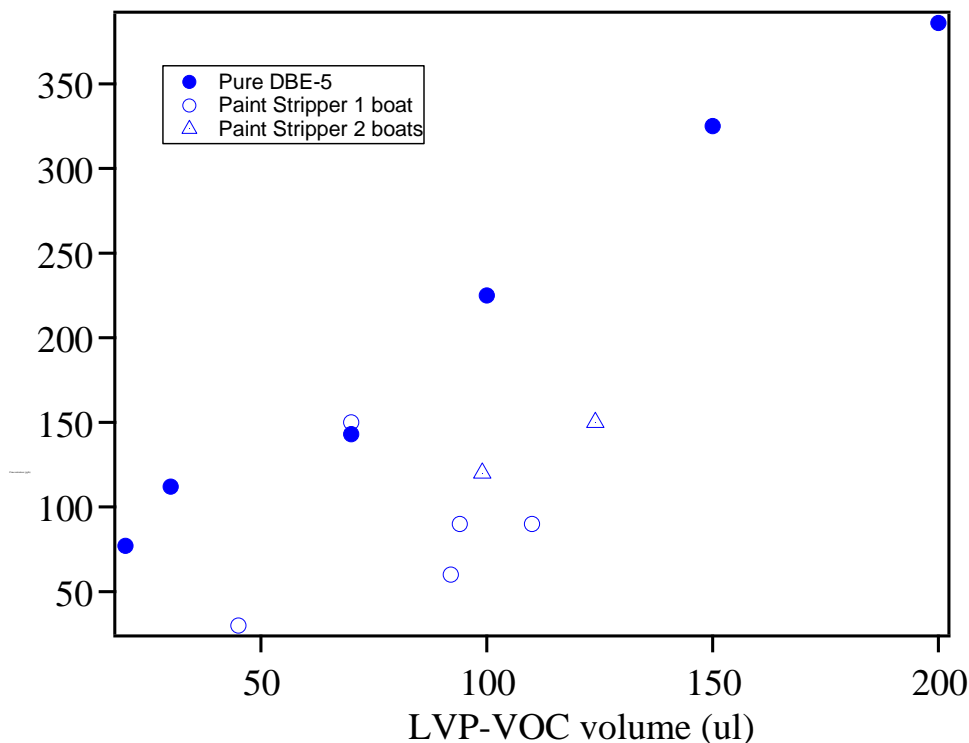


Figure 9: DBE-5 concentration versus the volumetric amount of DBE-5 as pure compound and as component of paint stripper.

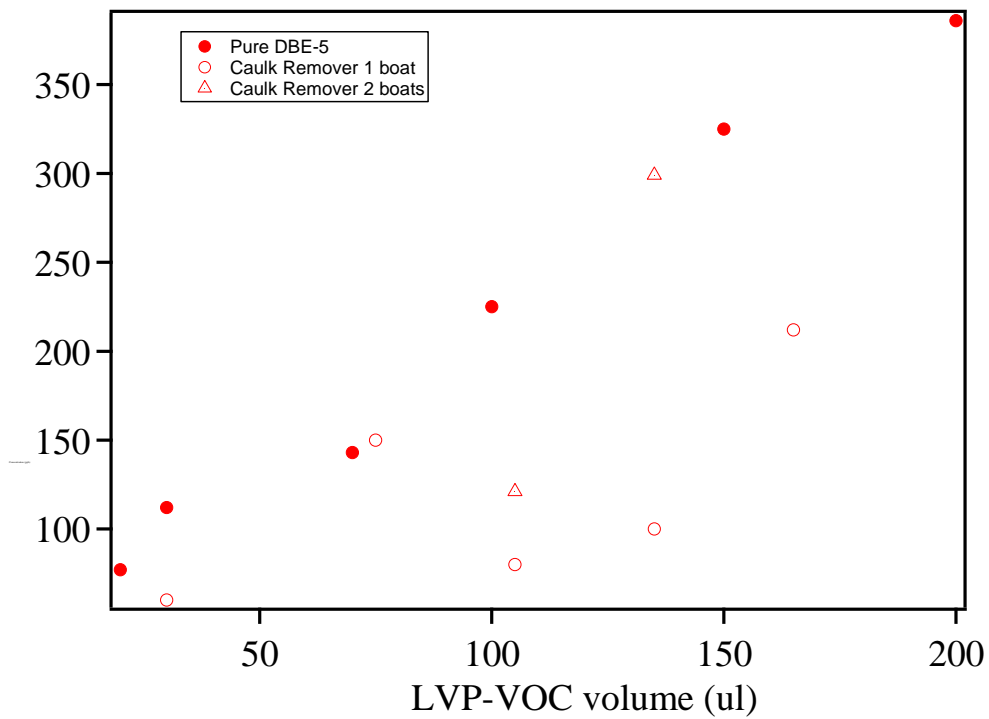


Figure 10: DBE-5 concentration versus volumetric amount of DBE-5 in pure form and as component of caulk remover

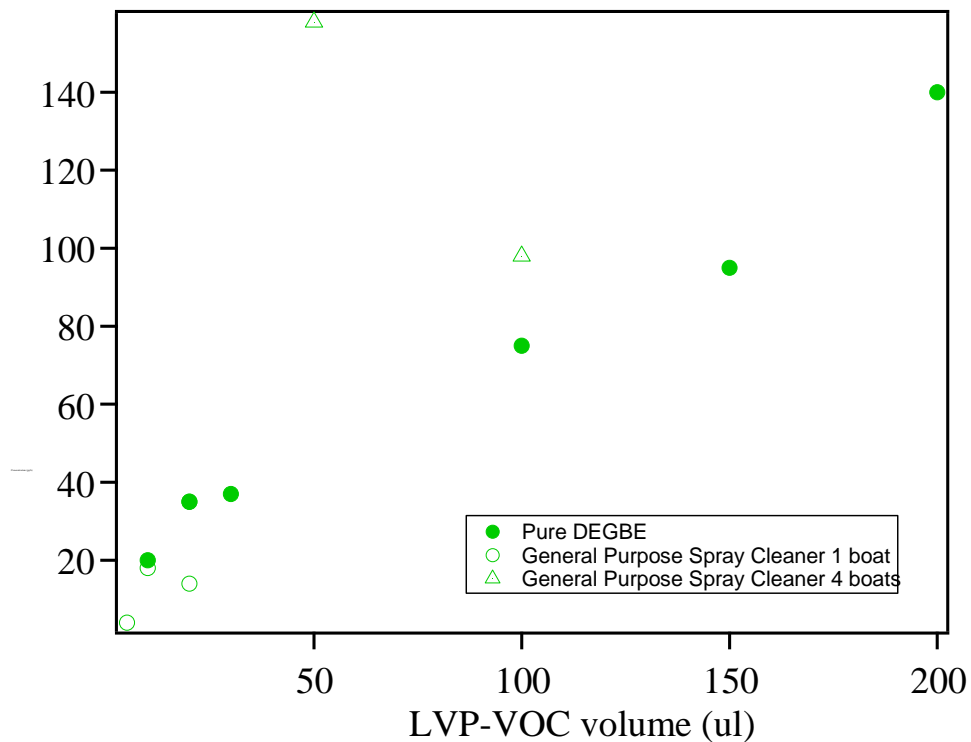


Figure 11: DEGBE concentration versus volumetric amount of DEGBE in pure form and as component of general purpose spray cleaner

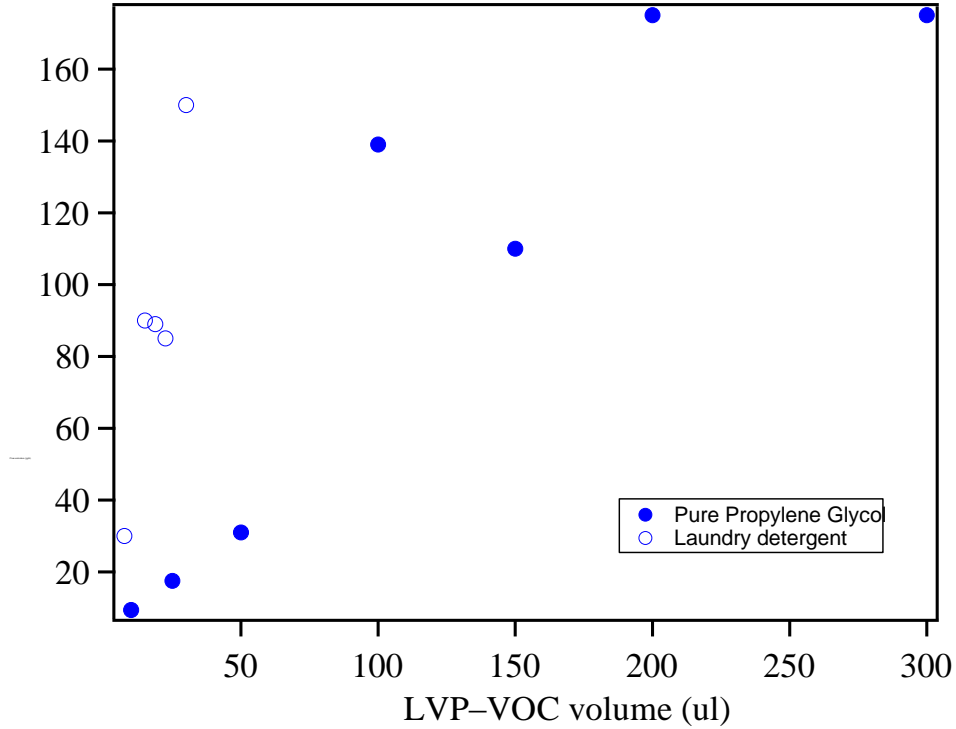


Figure 12: Propylene glycol concentration versus volumetric amount of propylene glycol pure form and as component of laundry detergent

From a mass transfer point of view, the gas phase LVP-VOC concentration in the evaporation chamber with respect the volume of the liquid material is schematically shown in Figure 13 below. When achieving equilibrium (right hand side of the Figure), the gas concentration or partial pressure of component α does not change with liquid volume present. However, should the ability of the LVP-VOC to achieve equilibrium be inhibited, a lower concentration than predicted by equilibrium will be achieved as shown on the left hand side of Figure 13.

Along with mass transfer, the equilibrium condition for the LVP-VOC must also be evaluated as it also impacts the total transfer of LVP-VOC between phases. The chemical equilibrium between gas-phase and liquid-phase LVP-VOC concentrations is described by equation 5 below. The concentration at equilibrium of gas-phase LVP-VOC in the chamber is different when pure LVP-VOC or mixture was put in by a factor of $x_a\gamma_a$. This relationship is expressed as:

$$P_\alpha * \Phi_\alpha = x_\alpha * \gamma_\alpha * P_\alpha^{sat} \quad \text{Eq. 5}$$

Φ_α : Gas phase activity, 1 for high dilution system;
 x_α : Mole fraction of α component in mixture, 1 for pure compound;
 γ_α : Aqueous phase activity, 1 for pure compound;
 P_α^{sat} : Saturation pressure of component α in air.
 P_α : Partial pressure of component α in air.

Therefore, the expected measured concentration, for equilibrium conditions, is shown in Figure 14.

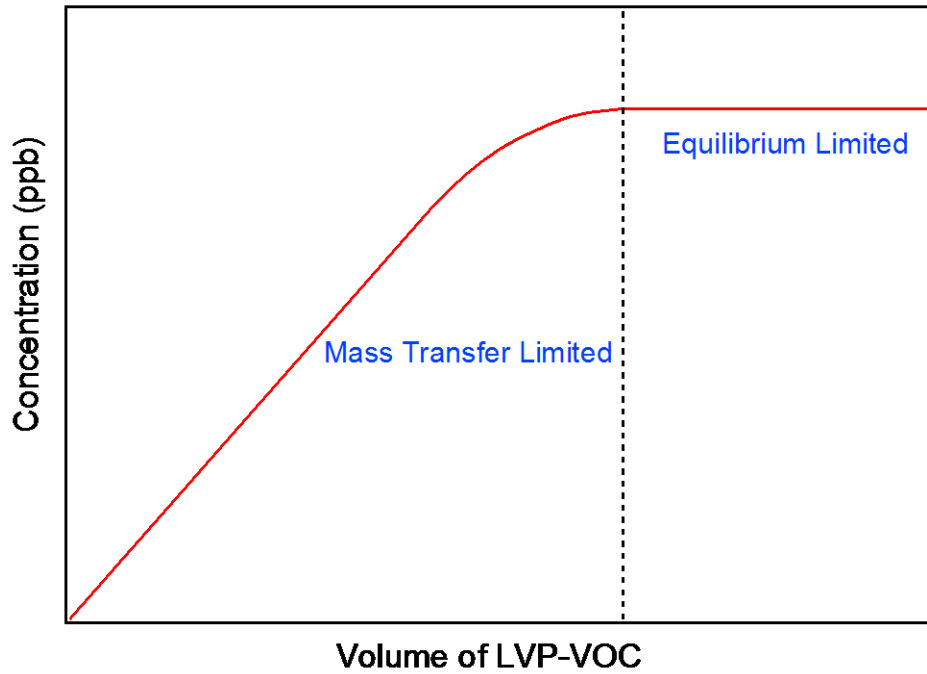


Figure 13: The relation of initial liquid LVP-VOC and final gas concentration

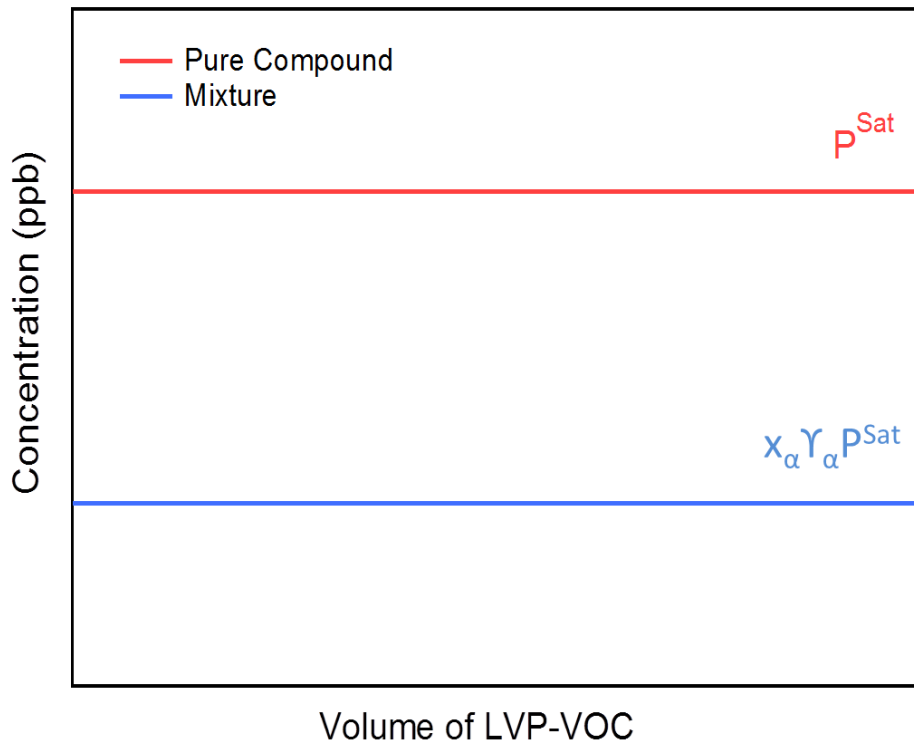


Figure 14: The relation of initial liquid LVP-VOC and final gas concentration in equilibrium zone

Revisiting the pure LVP-VOC evaporation, the evolution of the three LVP-VOCs studied that were present in the consumer product mixtures are replotted in Figure 15 below. The final concentration of gaseous LVP-VOC increases with the initial volume of LVP-VOC, so the evaporation chamber experiment results are clearly in mass transfer limited zone. Excellent agreement is observed between measured LVP-VOC (DBE-5, propylene glycol, and DEGBE) concentrations and equation 4 above when mass balance principles and equation 4 are applied. Observed concentrations are well below saturation concentrations of the individual LVP-VOC estimated from vapor pressure data as 1.31×10^5 ppb, 1.08×10^5 ppb, and 2.7×10^4 ppb for DBE-5, propylene glycol, and DEGBE, respectively. The much lower measured concentrations also suggest a severe kinetic limitation to evaporation of the compounds—i.e., that the compounds are not at thermodynamic equilibrium.

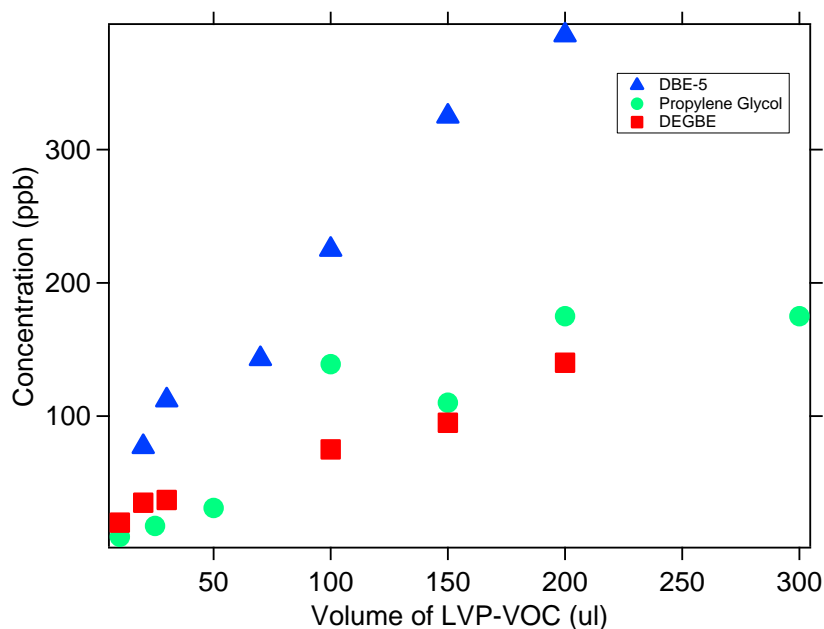


Figure 15: Evaporation results of three pure LVP-VOCs

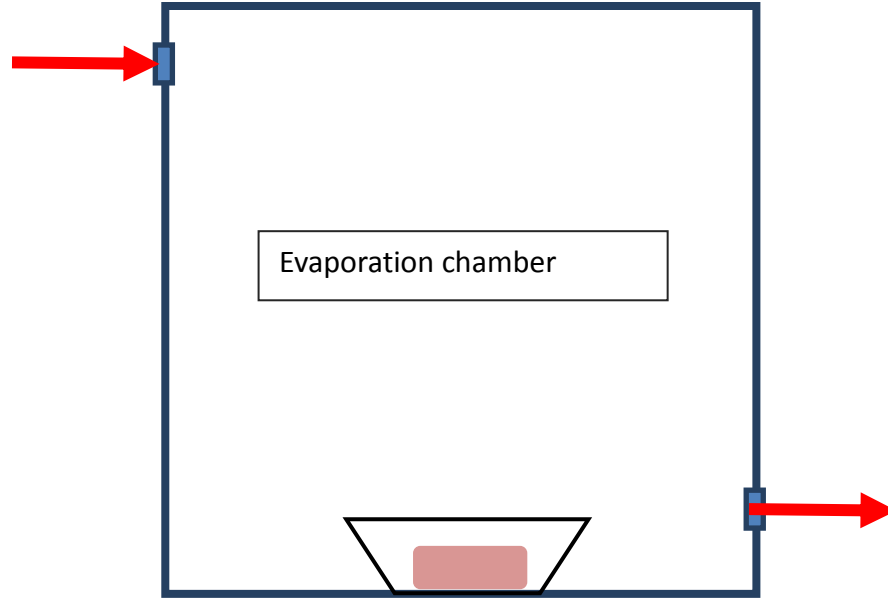


Figure 16: Diagram of a evaporation chamber

The mass balance on the evaporation chamber system (Figure 16) is described in equation 6 as:

$$Accumulation = Flow\ in - Flow\ out + Production + Consumption \quad Eq.6$$

First, we assume that the chamber is well mixed. This assumption is validated by comparing the mixing length of the LVP-VOCs and the chamber length.

$$L_{mix} = \sqrt{D^2 * t_{res}} \quad Eq. 7$$

L_{mix} : Mixing length (cm)

D: Diffusivity of LVP-VOC in air, in the magnitude of 10^{-5} m²/s

t_{res} : Residency time of LVP-VOC in the evaporation chamber, around 17 minutes in experiment

The diffusion length L_{mix} is found to be on the same order as the length scale of the chamber box which supports that diffusion itself is sufficient to mix the box and when combined with convective processes, one can assume the box is well mixed.

In this system, there is no flow in or consumption of LVP-VOC and the only production term is the evaporation of LVP-VOC. Therefore, mass balance of this system (Eq. 6) can be written as follows:

$$\frac{dc}{dt} * V = Eva - c_{out} * Q \quad Eq. 8$$

C: Concentration of gas phase LVP-VOC in chamber

V: Volume of the evaporation chamber

Eva: Evaporation rate of LVP-VOC

C_{out} : Concentration of LVP-VOC at the outlet. This is equal to c when chamber is well mixed.

Q: Volumetric flow rate at the outlet of the chamber.

The final concentration of LVP-VOC is measured when the concentration is stable ($d/dt = 0$) Therefore, the left side of the mass balance equation (Eq.8) above is zero yielding:

$$c * Q = Eva \quad \text{Eq. 9}$$

and

$$Eva = N * Area \quad \text{Eq. 10}$$

N: Mole flux of gas phase LVP-VOC during the evaporation

Area: Evaporation surface area of LVP-VOC

and

$$N = k * \Delta c \quad \text{Eq. 11}$$

k: Mass transfer coefficient, which is a function of the geometry of system and gas diffusivities in air.

Δc : Gas concentration difference between saturation concentration and measured concentration.

and

$$\Delta c = \frac{P^* - P^{meas}}{RT} \quad \text{for pure LVP-VOC; Eq. 12}$$

and

$$\Delta c = \frac{P^* - c(ppb) * P_{atm} / 10^9}{RT} \quad \text{for LVP-VOC in mixture; Eq. 13}$$

P^* : Partial pressure of LVP-VOC in the air above liquid surface

P^{meas} : Partial pressure of LVP-VOC in chamber air

P_{atm} : Pressure of air in evaporation chamber

c: Measured concentration of LVP-VOC in chamber

Δc also depends on the saturation pressure of LVP-VOC. The pressure and temperature are fixed for this system.

Unfortunately, the only unknown variable, k, is affected by mixing LVP-VOC into solution, which impacts the geometry of system.

It is unlikely that viscosity drives mass transfer limitation. For pure compounds, the viscosity of liquid does not matter. However, for a mixture, the ability of LVP-VOC to diffuse to surface could impact system. To investigate this, we use Stokes-Einstein relationship for diffusivity as:

$$D = \frac{k_B T}{6\pi\eta*d} \quad \text{Eq. 14}$$

k_B : Boltzmann constant, $1.38 * 10^{-23} \text{ m}^2 * \text{kg} * \text{s}^{-2} * \text{K}^{-1}$;

T: Temperature of the evaporation system, 298K;

η : Viscosity of liquid LVP-VOC;

d: Diffusive length.

Examples of evaporation time scale in the aerosol phase are provided in Figure 17 from Koop et al., 2011. It is noted that estimates provided in Figure 17 are for spherical particles with microscopic length dimensions (1 nm to 10 μm).

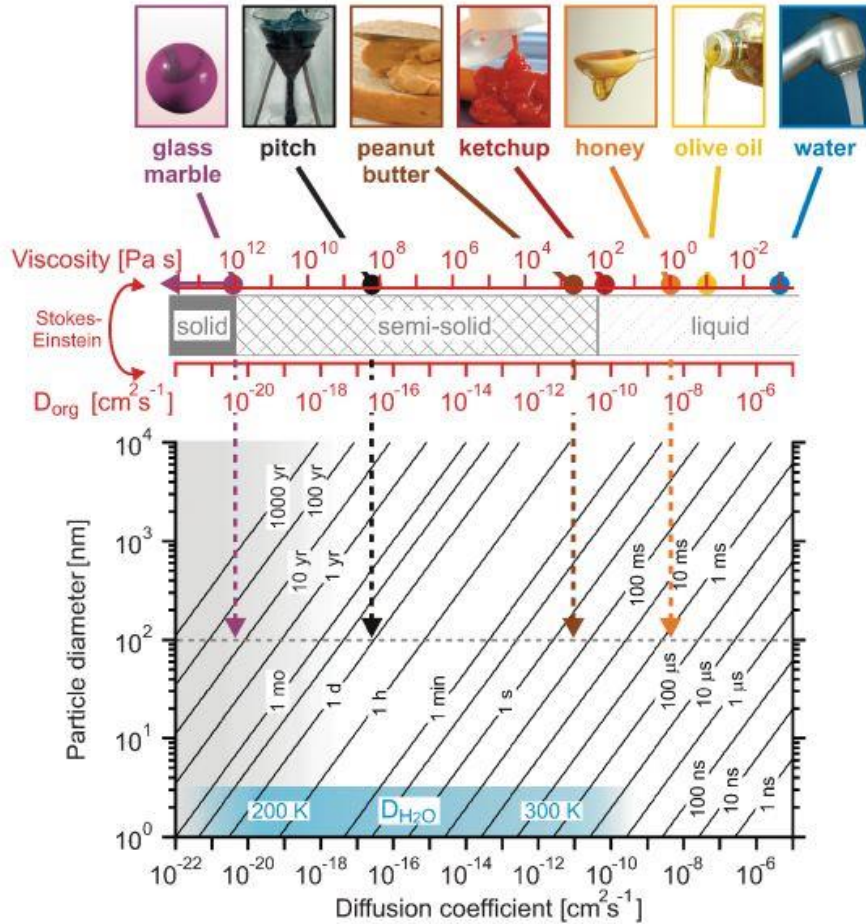


Figure 17: The co-relation of viscosity, diffusivity, mixing time and evaporation particle scale. (Koop et al. 2011)

Furthermore, the time constant for mixing is described by

$$\tau = \frac{L^2}{D} \quad \text{Eq. 15}$$

τ : Characteristic time of mass transfer

L : Relevant length in vertical direction.

D : Molecular diffusivity

The thickness of liquid LVP-VOC on aluminum dish was estimated as $L = 1$ mm. Further, we assume a diffusive length $d = 10$ μm, or one percent of L , to describe the replenishment of LVP-VOC to the surface for a slowly evaporating LVP-VOC. From the chart (Koop et al. 2011) above, if viscosity η is

less than 10 Pa*s, mixing time τ through the upper layer of the mixture would be less than 1 minute, which is considerably shorter than the time scale of the evaporation study (Table 7 lists diffusivity and viscosity for select substances). Consequently, viscosity may not significantly affect the mixing of LVP-VOC in evaporation chamber.

Table 7 : Viscosity and diffusivity of water, honey and propylene glycol at room condition (Koop et al. 2011)

	Water	Honey	Propylene Glycol
Diffusivity (cm ² /s)	2.4e ⁻¹	NA	1.06e ⁻¹
Viscosity (Pa*s)	8.9e ⁻⁴	6.3	4.2e ⁻²

Moreover, paint stripper gel is more viscous than caulk remover, while the evaporation of the same LVP-VOC from the two consumer products are similar, which also shows little effect from viscosity on LVP-VOC evaporation. The evaporation results of pure compound and the mixture can be looked at in two aspects: same volume of total material (similar geometry) or same amount of LVP-VOC (similar amount of LVP- VOC) (Figure 18). Same volume of material (pure compound or mixture) put into the chamber resulted in the equivalent evaporation surface area, while the other way led to the same amount of potential evaporating compound. It is noted that evaporation rates of consumer products are much lower than the time scale of the experiment; changes to the mole fraction of the LVP-VOC during the experiment are therefore negligible. Raoult's law is not applied to these systems based on the severe mass-transfer limitations noted above (e.g., Figure 15 and discussion thereof), which also masks the ability to estimate impacts of solution non-ideality in the consumer product mixtures (activity coefficient).

As shown in the graphs below, the pure compound evaporated more when same volume of material was put in chamber compared to the corresponding mixtures. Laundry detergent evaporated similarly with pure propylene glycol, while lotion evaporated far less than the other two. When the same amount of LVP-VOC (as part of the consumer product) were put in chamber, caulk remover and paint stripper had lower evaporation rates of DBE-5 than pure DBE-5, while the DEGBE evaporation rate from general purpose cleaner had comparable evaporation rate to the pure DEGBE. However, propylene glycol in the laundry detergent evaporated more quickly than did pure propylene glycol when the same volume of propylene glycol was present in the evaporation chamber.

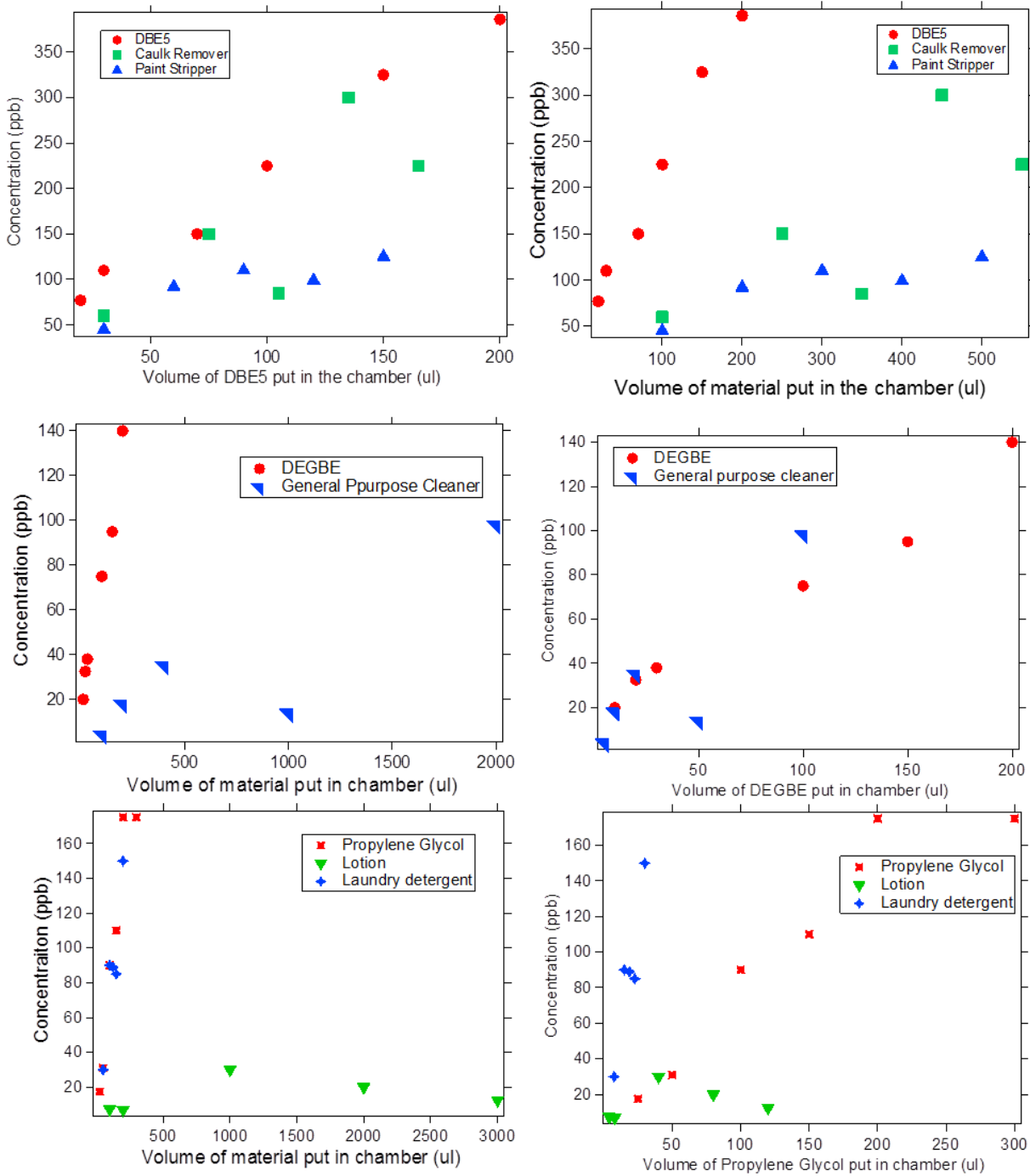


Figure 18: Evaporation results of pure LVP-VOC and its mixture

This work provides insight into governing parameters for pure compounds, but it was unable to provide enough information of impacts of mixtures given the combined thermodynamic and mass transfer impacts seen. Viscosity was ruled out as the driving parameter for differences in evaporation between

individual LVP-VOCs and LVP-VOCs within consumer products. Therefore, further investigation is required into how evaporation rates of individual LVP-VOCs present in consumer products differ from that observed from pure LVP-VOC.

c. Wall effects

A potentially significant parameter that must be accounted for is the role of the chamber walls in aerosol formation. The importance of characterizing and appropriately representing chamber effects in evaluations of mechanisms against chamber data has been recognized for some time in the context of gas-phase mechanism development (e.g., Carter et al., 1982; Jeffries et al., 1992), but to date it has received inadequate attention in evaluations of SOA models. We have observed, even in our remarkably clean chamber system, that some background aerosol formation occurs in the presence of only purified air (Carter et al., 2005a,b). Therefore, an important component of this project was to develop and evaluate a chamber effects model for background SOA formation in the UCR EPA chamber.

More recently, there have been several publications which have focused on losses of semi-volatile compounds to chamber surfaces leading to underprediction of SOA formation. Yeh and Ziemann at UCR (2014) monitored the decay of a suite of synthesized alkyl nitrates added to the chamber. They found that gas-to-wall partitioning increased with increasing carbon number and with proximity of the nitrooxy group to the terminal carbon. Krechmer and his coworkers at University of Colorado, Boulder (2016) studied the decay of semi-volatile species produced within the chamber. They reported time scales for reaching gas-wall partitioning equilibrium were 7-13 min for all compounds they measured. The Donahue group at CMU (2016) and the Seinfeld group at Caltech (2014) both use aerosol seeds to demonstrate importance of these losses, with the Caltech group reporting that increasing seed surface area increased SOA formation in select systems, while the CMU group monitored differential losses of select semi-volatiles coated onto seed particles. Therefore, semi-volatile wall losses were of concern for this study given the relatively low starting vapor pressure of the precursor LVP-VOCs studied in this work.

At the time of this report, another paper by Ng et al. at Georgia Tech (2016) was being released that suggests that semi-volatile wall losses may not be as great as originally suggested by Zhang et al., (2014) for many systems studied in environmental chambers due to relative time constants for condensation.

d. Chamber background

Another example of wall effects is the production of background aerosol during a pure air irradiation. A ten-hour pure air (with added NO_x) irradiation leads to production of several hundred particles per cubic centimeter of air with a mass of nearly one-tenth of a microgram per cubic centimeter. While this background is lower than found in most aerosol forming experiments conducted in the chamber, it still may play a non-negligible role in aerosol formation for experiments with low starting hydrocarbon concentrations. The addition of CO or NO_x to the system is found to suppress this background aerosol formation. This suggests that the background SOA formation is due to the presence of some precursor that reacts with OH radicals to form PM products, since both CO and NO_x suppress OH levels in this system. Examples of background PM data in the UCR EPA chamber are given by Carter et al (2005a, b).

e. LVP-VOC stability within the UCR environmental chamber

A LVP-VOC has a relative low vapor pressure indicating that it may be lost to the wall during an experiment leading to under estimation of SOA formation. We monitored the decay of several gas phase LVP-VOCs added to the chamber by SIFT-MS, which were labeled as stability runs. The goal of it was to test whether a LVP-VOC would stay in gas phase without going to the wall of the chamber during the experiment. Three stability runs were performed to correct for LVP-VOC vapor wall loss (Table 8).

Table 9 shows all the LVP-VOCs tested for stability in UCR Chamber as part of this project. We found that all LVP-VOCs maintained a constant concentration within measurement error during the stability test (Figure 19). (Stability data of n-Heptadecane could not be obtained due to instrumental error.) Therefore, wall loss of LVP-VOCs to the extremely hydrophobic Teflon chamber surface was considered negligible for the LVP-VOCs studied.

Table 8: Stability run

Run ID	LVP-VOCs tested
1939	n-Tridecane, n-Heptadecane
1984	Diethylene Glycol, Propylene Glycol, DEGEE, DEGBE, n-Tridecane, n-Heptadecane, DBE-5, benzyl alcohol
2022	DPGMEA, Glyceryl triacetate, Texanol

Table 9 : Tested LVP-VOCs

Compound	Can see on SIFT-MS	Injected into Chamber	Stable in Chamber	Successful MIR and SOA expt
Diethylene Glycol	✓	✓	✓	✓
Propylene Glycol	✓	✓	✓	✓
Diethylene Glycol Ethyl Ether	✓	✓	✓	✓
Diethylene Glycol Monobutyl Ether	✓	✓	✓	✓
n-Tridecane	✓	✓	✓	✓
n-Heptadecane	✓	✓	✓	✓
Dimethyl Glutarate	✓	✓	✓	✓
Benzyl Alcohol	✓	✓	✓	✓
Dipropylene Glycol Methyl Ether Acetate	✓	✓	✓	✓
Texanol	✓	✓	✓	✓
Glyceryl Triacetate	✓	✓	✓	✓

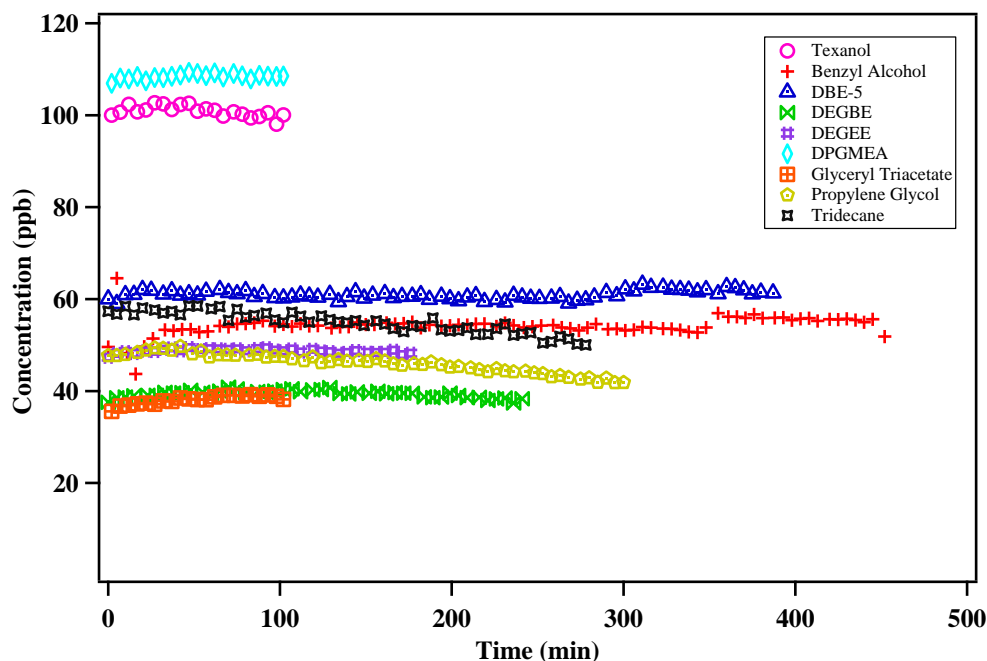


Figure 19: Stability test for LVP-VOCs in chamber

f. Particle wall loss correction

Loss of particles to the environmental chamber walls must also be accounted for. While there are a number of methods utilized to achieve this task, we chose to use a single first order wall loss factor or equation obtained from each experiment to correct for the deposition of particles on walls. Therefore, the same wall loss correction procedures described in detail in Cocker et al. (2001) were used for this study. Size dependent particle wall losses were not accounted for as characterization of such losses require additional experiments conducted on different days as the actual experiment. It has been our experience that variations in day-to-day particle wall losses change more significantly than any corrections made for particle size dependent wall loss.

g. Chamber characterization run

Well-characterized environmental chamber experiments are critical to the development of chemical models with predictive capability, particularly for processes whose chemical details are not well understood. They also provide important information on how best to model these processes, which in turn provides clues on the chemical reactions that occur under atmospheric conditions. It is critical to understand the impact of reactor walls on gas-phase reactivity and SOA formation, which could be assessed by conducting various types of characterization experiments. The chamber effects relevant to gas-phase mechanism evaluation that have been assessed and the types of experiments utilized for assessing them are summarized in Table 10.

The CO experiments were carried out to demonstrate NO_x offgasing as well. The CO- NO_x experiments were carried out to determine the strength of the HONO radical source. The clean air experiments were carried out to screen for background VOC effects with the NO_x offgasing. The m-xylene- NO experiments were carried out to test the repeatability of chamber experiments. Error in SOA formation is estimated from using the m-xylene control system as 6.56%, the root mean square deviation of aerosol yield divided by the measured average SOA yield. The root mean square deviation is measured

as the differences between predicted and observed values, calculated as $(\frac{\sum(Yield_{measured}-Yield_{predicted})^2}{N})$ where N is the number of samples (N=10).

Table 10: Summary of types of characterization experiments

Type	Run ID	Compounds Used
CO-Air	EPA1837	CO characterization
	EPA2112	
CO-NO _x	EPA1840	CO + NO
	EPA2111	
Air	EPA1838	Pure air irradiation
	EPA1845	
	EPA1854	
	EPA1855	
	EPA1874	
	EPA1896	
	EPA1905	
	EPA1957	
	EPA1960	
	EPA2009	
	EPA2010	
	EPA2068	
	EPA2076	
	EPA2108	
Xylene	EPA1841	m-xylene + NO
	EPA1843	
	EPA1930	
	EPA1933	
	EPA1950	
	EPA1975	
	EPA2053	
	EPA2066	
	EPA2077	
	EPA2079	
	EPA2109	
	EPA2113	
EPA2201		

h. Experimental types

This section introduces the experimental types carried out for this project as follows. LVP-VOC concentrations were selected to be sufficiently high for accurate quantitation and detection limits and were similar to concentrations commonly studied in the UCR environmental chamber in other ozone and SOA research programs. These concentrations are considerably higher (orders of magnitude) than would be expected to be present outdoors (~100 ppb vs < 1 ppb).

- LVP-VOC and 1 ppm H₂O₂ injected and mixed within chamber, followed by 6+ hours of UV irradiation. Simplest oxidation experiment to study SOA formation from LVP-VOC, no surrogate added. The photolysis of H₂O₂ increases both OH and HO₂ radical concentrations.
- LVP-VOC + NO_x + UV: Photooxidation system with individual LVP-VOC to study directly LVP-VOC oxidation and SOA formation.
- LVP-VOC + Surrogate + NO_x + UV: Photooxidation system where a surrogate mixture of reactive organic gases (ROG; originally developed by Carter et al. (1995)) was used to study the effects of individual compounds on overall ozone formation. The simplified ROG surrogate used for this work to mimic total atmospheric reactivity included seven representative compounds: n-butane, n-octane, ethene, propene, trans-2-butene, toluene, and m-xylene. Total surrogate concentrations used were 1.1 ppmC. The selected surrogate is the same as that used in many previous research programs at UC Riverside including those used to develop the MIR scales. The mixture provides a method to provide similar atmospheric reactivity conditions as what might be expected in outdoor Southern California air. Experiments with surrogate are listed in Table 11 as Surr. MOIR is defined as maximum ozone incremental reactivity.
- LVP-VOC + Surrogate + NO_x + H₂O₂ + UV: Introduction of a test compound into the surrogate mixture can lead to competition for the hydroxyl radical. Experiments were conducted with 1 ppm H₂O₂ to reduce the impact of hydroxyl radical loss. Total surrogate concentrations used were 1.1 ppmC. Experiments with surrogate are listed in Table 11 as MOIR/2. The photolysis of H₂O₂ increases both OH and HO₂ radical concentrations.
- Surrogate control experiments: Performed in parallel (as control) for surrogate containing experiments described immediately above. Experiments conducted by injecting surrogate mixture, NO_x, H₂O₂ (as needed) into the chamber, followed by side to side mixing so that all chemical concentrations are identical in both chambers prior to injection of desired LVP-VOC to one side.
- Seeded: These experiments were conducted to evaluate the impact of preexisting surfaces for semi-volatile oxidation products to condense onto. The use of seed is expected to minimize chamber wall loss of semi-volatile compounds by providing additional surfaces for condensation to occur. It is expected that increases in SOA formation in the presence of seed would indicate that semi-volatile wall losses of gas-phase vapors are significantly influencing SOA formation.

Table 11 summarizes the experiments performed and analyzed as part of this program. This includes Run ID, brief description of experiment, amount of LVP-VOC, NO, NO₂ and H₂O₂ injected, total irradiation time, final ozone, PM volume, average density, and mass concentration of PM produced.

Table 11 : EPA run table for LVP-VOCs

Run ID	Compound	Target LVP-VOC (ppb) ⁺	Initial NO (ppb)	Initial NO ₂ (ppb)	Initial H ₂ O ₂ (ppm)	Photo oxidation Time (mins)	Final O ₃ (ppb)	Final PM (µm ³ /cm ³)	Average Density (g/cm ³)	Final PM* (µg/m ³)
EPA1850(A)	Surr	-	10.0	5.0	-	315	115.9	0.5	1.8	0.9
EPA1850(B)	Surr	-	10.0	5.0	-	315	112.6	0.5	1.8	0.9
EPA1851(A)	Surr+Propylene glycol	40.0	14.9	8.0	-	420	194.4	5.8	1.9	11.0
EPA1851(B)	Surr		15.0	8.2	-	420	168.2	1.5	1.5	2.3
EPA1877(A)	Surr+Propylene Glycol	40.0	19.5	8.9	-	526	182.5	2.4	1.5	3.6
EPA1877(B)	Surr		19.5	8.9	-	526	171.4	1.8	1.5	2.7
EPA1882(A)	Surr+Propylene Glycol	40.0	34.1	19.8	-	530	267.1	3.2	1.5	4.8
EPA1882(B)	Surr		34.5	19.8	-	530	263.2	3.1	1.5	4.7
EPA1883(A)	Surr+Diethylene Glycol	80.0	22.6	11.0	-	204	201.3	2.2	1.5	3.3
EPA1883(B)	Surr		23.2	11.3		204	155.5	0.1	1.5	0.2
EPA1886(A)	Surr+Diethylene Glycol Ethyl Ether (DEGEE)	40.0	26.0	10.4	-	540	221.7	15.1	1.5	22.7
EPA1886(B)	Surr		26.0	10.0	-	540	200.7	1.3	1.5	2.0
EPA1887(A)	Surr+Diethylene Glycol	80.0	20.6	9.4	-	484	205.2	1.7	1.5	2.6
EPA1887(B)	Surr		21.0	9.4		484	176.5	0.4	1.5	0.6
EPA1888(A)	Surr+Propylene Glycol	80.0	23.6	9.7	-	413	200.6	0.1	1.6	0.2
EPA1888(B)	Surr		23.3	10.1		413	175.5	0.4	1.5	0.6
EPA1891(A)	Surr+Diethylene Glycol Monobutyl Ether (butoxyethoxyethanol)	40.0	20.2	10.2	-	480	177.8	32.5	1.5	48.8
EPA1891(B)	Surr		20.5	10.4		480	179.4	1.8	1.5	2.7
EPA1892(A)	Surr+n-Tridecane	40.0	20.1	9.9	-	570	160.0	11.1	1.3	14.4
EPA1892(B)	Surr		19.8	10.6		570	184.0	1.9	1.5	2.9
EPA1893(A)	Surr+Triethanolamine	40	21.9	6.2	-	447	165.4	1.9	1.5	2.9
EPA1893(B)	Surr	-	21.7	6.8	-	447	166.4	1.2	1.5	1.8
EPA1894(A)	Surr	-	20.2	9.5	-	420	182.8	1.5	1.5	2.3
EPA1894(B)	Surr	-	20.2	9.3		420	182.8	1.4	1.5	2.1
EPA1908	LVP-VOC injection test	-	-	-	-	-	-	-	-	-
EPA1910(A)	Surr+n-Heptadecane	40.0	23.0	10.8	-	480	172.3	104.6	1.0	104.6
EPA1910(B)	Surr	-	24.0	10.4	-	480	190.1	2.77	1.5	4.2
EPA1911(A)	Surr+Dimethyl Glutarate (DBE-5)	160.0	18.0	13.4	-	505	178.7	7.1	1.4	9.9
EPA1911(B)	Surr	-	18.7	12.5	-	505	180.7	3.1	1.5	4.7
EPA1912(A)	S+Triethanolamine	40.0	20.9	14.9	-	421	154.4	101	1.4	141.4
Run ID	Compound	Target LVP-VOC	Initial NO (ppb)	Initial NO ₂ (ppb)	Initial H ₂ O ₂ (ppm)	Photo oxidation Time	Final O ₃ (ppb)	Final PM (µm ³ /cm ³)	Average Density (g/cm ³)	Final PM* (µg/m ³)

		(ppb)				(mins)				
EPA1912(B)	Surr	-	21.5	9.1	-	421	174.6	2.2	1.5	3.3
EPA1913	LVP-VOC injection test	-	-	-	-	-	167.4	-	-	-
EPA1914(A)	Surr+Methyl palmitate	40.0	21.0	6.9	-	454	149.8	185.8	1.1	204.4
EPA1914(B)	Surr		19.4	8.4		454	167.4	6.4	1.5	9.6
EPA1922(A)	Surr + DEGEE	40.0	19.7	11.6	-	460	186.8	21.1	1.3	27.4
EPA1922(B)	Surr	-	19.8	11.4	-	-	163.4	3.3	1.5	5.0
EPA1923(B)	NO + DEGEE	40.0	20.5	-	-	610	130.2	8.8	1.5	13.2
EPA1925(B)	NO + DEGBE	40.0	22.0	-	-	530	70.5	9	1.6	14.4
EPA1926(A)	NO + DEGBE	80.0	22.4	-	-	580	73.1	5.6	1.4	7.8
* EPA1926 (B)	1,2-Dimethoxyetane+ NO	160	22.7	-	-	580	162.2	-	1.4	-
EPA1974(A)	NO + DEGEE	80	22.5	4.6	-	385	105.9	-	1.4	-
*EPA1974(B)	NO + DEGDME	80	22.5	3.6	-	385	48.1	-	1.4	-
EPA1984	LVP-VOC +benzyl alcohol Stability test	-	-	-	-	-	-	-	-	-
EPA1985(A)	NO + DEGEE	80.0	23.5	-	-	486	76.4	2.01	1.4	2.8
EPA1986(A)	NO + DEGBE	40.0	27.5	-	-	465	22.5	1.55	1.4	2.2
EPA1986(B)	DEGEE+ H ₂ O ₂	40.0	-	-	1	465	23.2	30.9	1.3	40.2
EPA1987(A)	Surr+ benzyl alcohol	80.0	20.3	10.9	-	480	144.5	54.9	1.4	76.9
EPA1987(B)	Surr	-	20.2	11.0	-	480	182.6	1.2	1.5	1.8
EPA1988(A)	Surr+ H ₂ O ₂ + tridecane	40.0	17.8	12.7	1	493	163.2	58.7	1.4	82.2
EPA1988(B)	Surr+ H ₂ O ₂	-	17.9	12.6	1	493	183.4	10.1	1.5	15.2
EPA1991(A)	H ₂ O ₂ + DEGEE	40.0	-	-	1	403	23.9	30.9	1.4	43.3
EPA1993(A)	NO + DEGEE	40.0	25.0	-	-	525	86.8	2.94	1.6	4.7
EPA1999(A)	H ₂ O ₂ + DEGBE	40.0	-	-	1	472	21.8	110.5	1.3	143.7
EPA2006(A)	Surr+ H ₂ O ₂ + Benzyl Alcohol	80.0	20.1	8.3	1	380	134.9	109.2	1.4	152.9
EPA2006(B)	Surr+ H ₂ O ₂		19.9	8.6	1	380	178.1	8.8	1.5	13.2
*EPA2007(A)	EGDBE + H ₂ O ₂	80.0	-	-	1	515	29.8	7.1	1.4	9.9
*EPA2007(B)	MEMP + H ₂ O ₂	80.0	-	-	1	515	22.2	2.3	1.5	3.5
EPA2022(A)	LVP-VOC Stability Test	-	-	-	-	-	-	-	-	-
EPA2023(A)	Surr+ DPGMEA	40.0	21.5	9.5	-	478	185.1	4.3	1.4	6.0
EPA2023(B)	Surr	-	21.6	8.7	-	478	181.3	1.3	1.5	2.0
EPA2024(A)	Surr+ Texanol	80.0	17.6	10.5	-	472	163.5	0.8	1.4	1.1
EPA2024(B)	Surr	-	17.8	10.2	-	472	167.7	0.7	1.5	1.1
EPA2025(A)	S+ Glyceryl triacetate	80.0	20.4	9.1	-	425	169.6	0.5	1.4	0.7
EPA2025(B)	Surr	-	21.2	8.4	-	425	168.3	0.5	1.5	0.8
EPA2026(A)	Half Surrogate + H ₂ O ₂ + DBE-5	160.0	17.6	8.5	1	413	162.0	7.3	1.4	10.2
EPA2026(B)	Half Surrogate+ H ₂ O ₂	-	17.8	8.4	1	413	165.6	12.6	1.5	18.9
Run ID	Compound	Target LVP-VOC	Initial NO (ppb)	Initial NO ₂ (ppb)	Initial H ₂ O ₂ (ppm)	Photo oxidation Time	Final O ₃ (ppb)	Final PM (µm ³ /cm ³)	Average Density (g/cm ³)	Final PM* (µg/m ³)

		(ppb)				(mins)				
EPA2027(A)	Surr+ H ₂ O ₂ + DBE-5	160.0	20.4	10.9	1	418	182.0	5.1	1.5	7.7
EPA2027(B)	Surr	-	20.4	10.1	1	418	184.0	9.1	1.5	13.7
EPA2028(A)	Surr+ H ₂ O ₂ + Propylene Glycol	80.0	21.3	11.2	1	380	190.5	3.7	1.5	5.6
EPA2028(B)	Surr+ H ₂ O ₂	-	21.5	11.3	1	380	187.7	6.5	1.5	9.8
EPA2029(A)	Surr+ H ₂ O ₂ + DEGEE	40.0	21.9	9.5	1	422	193.1	24.9	1.4	34.9
EPA2029(B)	Surr+ H ₂ O ₂	-	21.9	9.4	1	422	187.3	7.0	1.5	10.5
EPA2030(A)	Surr+ H ₂ O ₂ + DEGBE	40.0	18.9	9.7	1	450	179.9	70.4	1.3	91.5
EPA2030(B)	Surr+ H ₂ O ₂	-	18.8	9.6	1	450	179.0	8.0	1.5	12.0
EPA2033(A)	H ₂ O ₂ + DEGEE + seed	20.0	-	-	1	259	23.7	14.2	1.6	22.7
EPA2033(B)	H ₂ O ₂ + DEGEE	30	-	-	1	259	21.3	15.2	1.6	24.3
EPA2034(A)	H ₂ O ₂ + DEGEE + seed	40.0	-	-	1	350	23.0	16.2	1.5	24.3
EPA2034(B)	H ₂ O ₂ + DEGEE	40.0	-	-	1	350	30.3	17.2	1.5	25.8
EPA2035(A)	H ₂ O ₂ + DEGBE + seed(A)	40.0	-	-	1	288	15.0	18.2	1.5	27.3
EPA2035(B)	H ₂ O ₂ + DEGBE	40.0	-	-	1	288	24.7	19.2	1.5	28.8
EPA2036(B)	H ₂ O ₂ + DEGEE	<40	-	-	1	368	9.3	6.1	1.5	9.2
EPA2041(A)	H ₂ O ₂ + DEGEE + seed	40.0	-	-	1	277	16.6	9.2	1.6	14.7
EPA2041(B)	H ₂ O ₂ + DEGEE + seed	40.0	-	-	1	277	15.6	7.7	1.6	12.4
EPA2042(A)	H ₂ O ₂ + n- Tridecane + seed	40.0	-	-	1	280	9.3	2.6	1.4	3.6
EPA2042(B)	H ₂ O ₂ + n- Tridecane	40.0	-	-	1	280	5.3	2.6	1.4	3.6
*EPA2048(A)	DEGDME+ H ₂ O ₂	80.0	-	-	1	504	27.8	0.1	1.4	0.1
EPA2048(B)	DEGBE+NO	40.0	20.0	-	-	504	71.3	0.01	1.4	0.0
EPA2051(A)	DEGBE+NO	80.0	40.0	-	-	450	31.2	79.2	1.4	110.9
*EPA2051(B)	DPGBE+ H ₂ O ₂	80.0	-	-	1	450	10.2	-	1.4	-
EPA2055(A)	DPGBE+NO	40.0	20.0	-	-	360	18.5	-	1.4	-
*EPA2055(B)	DEGME+ H ₂ O ₂	80.0	-	-	1	360	12.7	-	1.4	-
EPA2056(A)	DEGBE+NO	160.0	10.0	-	-	363	30.6	-	1.4	-
EPA2056(B)	DEGEE+NO	160.0	10.0	-	-	552	80.9	-	1.4	-
EPA2058(A)	DEGEE+ H ₂ O ₂	80.0	-	-	1	392	18.6	19.3	1.4	27.0
EPA2058(B)	DEGEE+ H ₂ O ₂ +NO	80.0	10.0	-	1	392	134.5	31.2	1.4	43.7
EPA2059(A)	DEGEE+ H ₂ O ₂ +NO	80.0	20.0	-	1	275	231.0	28.7	1.4	40.2
EPA2059(B)	DEGEE+ H ₂ O ₂ +NO	80.0	40.0	-	1	275	310.4	20.1	1.4	28.1
EPA2063(A)	DEGBE+ H ₂ O ₂	80.0	20.0	-	1	285	189.4	122.1	1.3	158.7
EPA2063(B)	DEGBE+ H ₂ O ₂ +NO	80.0	-	-	1	452	11.2	122.4	1.4	171.4
EPA2093(A)	Surr+ Caulk Remover Mixture	160.0	16.2	7.6	-	479	167.0	1.8	1.4	2.5
EPA2093(B)	Surr	-	16.3	7.2	-	479	163.1	2.0	1.5	3.0
EPA2094(A)	Surr+ Paint Stripper Mixture	160.0	17.1	9.6	-	509	158.8	21.0	1.4	29.4
Run ID	Compound	Target LVP- VOC	Initial NO (ppb)	Initial NO ₂ (ppb)	Initial H ₂ O ₂ (ppm)	Photo oxidation Time	Final O ₃ (ppb)	Final PM (µm ³ /cm ³)	Average Density (g/cm ³)	Final PM* (µg/m ³)

		(ppb)				(mins)				
EPA2094(B)	Surr	-	16.6	8.3	-	509	168.8	1.1	1.5	1.7
EPA2095(A)	Surr+ General Purpose Spray Cleaner Mixture	40.0	15.1	8.5	-	488	161.8	44	1.4	61.6
EPA2095(B)	Surr	-	15.2	8.2	-	488	153.0	1.2	1.5	1.8
EPA2096(A)	DBE-5 + H ₂ O ₂ + seed	160.0	-	-	2	472	15.6	24.2	1.1	26.6
EPA2096(B)	DBE-5 + H ₂ O ₂	160.0	-	-	2	472	16.1	25.2	1.4	35.3
EPA2097(A)	Glyceryl Triacetate + H ₂ O ₂ + seed	80.0	-	-	1	360	14.2	26.2	1.4	36.7
EPA2097(B)	Glyceryl Triacetate + H ₂ O ₂	80.0	-	-	1	360	12.9	27.2	1.4	38.1
EPA2098(A)	Surr+ Caulk Remover Mixture w/out water added	160.0	15.5	5.9	-	465	153.3	1.3	1.4	1.8
EPA2098(B)	Surr only	-	16.0	5.9	-	465	153.0	0.6	1.5	0.9
EPA2099(A)	DBE-5 + H ₂ O ₂ + seed	160.0	-	-	1	362	11.6	2.3	1.5	3.5
EPA2099(B)	DBE-5 + H ₂ O ₂ + seed	160.0	-	-	1	362	9.0	2.7	1.5	4.1
EPA2100(A)	DPGMEA + H ₂ O ₂ + seed	40.0	-	-	1	360	9.2	5.9	1.4	8.3
EPA2100(B)	DPGMEA + H ₂ O ₂	40.0	-	-	1	360	6.7	0.03	1.4	0.0
EPA2101(A)	H ₂ O ₂ + DBE-5+ NO + seed	160.0	24.4	-	1	419	216.6	3.4	1.3	4.4
EPA2101(B)	H ₂ O ₂ + DBE-5+ NO	160.0	24.4	-	1	419	221.9	0.8	1.3	1.1
EPA2102(A)	Glyceryl triacetate + H ₂ O ₂ + NO + seed	80.0	25.0	-	1	465	204.2	7.8	1.4	10.9
EPA2102(B)	Glyceryl triacetate + H ₂ O ₂ + NO	80.0	25.0	-	1	465	222.7	2.1	1.4	2.9
EPA2103(A)	DPGMEA + H ₂ O ₂ + NO + seed	40.0	25.0	-	1	373	217.7	6	1.4	8.6
EPA2103(B)	DPGMEA + H ₂ O ₂ + NO	40.0	25.0	-	1	373	218.2	0.6	1.4	0.8
EPA2104(A)	Surr+ heptadecane+ H ₂ O ₂	40.0	15.8	8.1	1	426	160.2	8.0	1.5	12.0
EPA2104(B)	Surr+ H ₂ O ₂	-	4.2	16.4	1	426	148.2	71.0	1.5	106.5
*EPA2123(A)	1,3-Diethoxy-2-propanol+ H ₂ O ₂	40.0	-	-	1	310	11.6	20.5	1.4	28.7
*EPA2123(B)	1,3-Diethoxy-2-propanol + NO	40.0	20.0	-	-	310	8.7	0	1.4	0.0
*EPA2124(A)	3,3-Diethoxy-1-propanol+ H ₂ O ₂	80.0	-	-	1	400	11.6	29.5	1.4	41.3
*EPA2124(B)	3,3-Diethoxy-1-propanol+ NO	80.0	20.0	-	-	400	49.9	0	1.4	0.0
*EPA2152(A)	DPGBE+H ₂ O ₂	160.0	-	-	1	360	11.0	7.6	1.4	10.6
*EPA2152(B)	DPGBE+NO	160.0	20.0	-	-	360	9.3	5.1	1.4	7.1
*EPA2154(A)	EDGEE+H ₂ O ₂	160.0	-	-	1	473	17.3	8.9	1.4	12.5
*EPA2154(B)	EDGEE+NO	160.0	20.0	-	-	473	29.3	0	1.4	0.0
EPA2172(A)	Surr+n-Heptadecane	40.0	16.3	8.1	-	358	130.3	12.3	1.4	17.2
EPA2172(B)	Surr	-	13.3	7.5	-	358	136.1	0.3	1.5	0.5
EPA2173(A)	Surr+ n-Heptadecane+ H ₂ O ₂	80.0	12.2	8.8	1	326	143.0	40.9	1.1	45.0
Run ID	Compound	Target LVP-	Initial NO	Initial NO ₂	Initial H ₂ O ₂	Photo oxidation	Final O ₃	Final PM (µm ³ /cm ³)	Average Density	Final PM* (µg/m ³)

		VOC (ppb)	(ppb)	(ppb)	(ppm)	Time (mins)	(ppb)		(g/cm ³)	
EPA2173(B)	Surr+ H ₂ O ₂	-	12.8	7.6	1	326	143.1	2.3	1.5	3.5
EPA2174(A)	Surr+ H ₂ O ₂ + DPGMEA	40.0	11.8	6.9	1	398	130.4	74.8	1.1	82.3
EPA2174(B)	Surr+ H ₂ O ₂	-	11.8	7.2	1	398	144.6	8.7	1.5	13.1
EPA2175(A)	Surr+laundry detergent	-	16.8	9.0	-	339	183.7	38.4	1.4	53.8
EPA2175(B)	Surr	-	22.9	10.3	-	339	82.0	3.3	1.5	5.0
EPA2176(A)	Surr+laundry detergent+ H ₂ O ₂	-	12.0	10.9	1	328	147.7	153.9	1.4	215.5
EPA2176(B)	Surr+ H ₂ O ₂	-	12.9	10.3	1	328	174.7	5.3	1.5	8.0
EPA2177(A)	DPGMEA + H ₂ O ₂ + NO + seed	40.0	24.4	-	1	304	183.0	21.4	1.1	23.5
EPA2177(B)	DPGMEA + H ₂ O ₂ + NO	40.0	24.4	-	1	304	198.7	7.1	1.4	9.9
EPA2178(A)	Glyceryl triacetate + H ₂ O ₂ + NO + seed	88.7	23.5	-	1	319	165.8	18.3	1.2	21.9
EPA2178(B)	Glyceryl triacetate + H ₂ O ₂ + NO	88.7	23.5	-	1	319	187.7	10.3	1.4	14.4
EPA2179(A)	DBE-5 + H ₂ O ₂ + NO + seed	160.0	23.6	-	1	371	165.8	39.0	1.2	46.8
EPA2179(B)	DBE-5 + H ₂ O ₂ + seed	160.0	23.6	-	1	371	189.2	12.4	1.4	17.4
EPA2180(A)	Surr+ Conosol C- 200	156.4	15.8	9.4	-	369	132.0	26.5	1.2	31.8
EPA2180(B)	Surr	-	15.5	10.3	-	369	139.0	1.1	1.5	1.7
EPA2181(A)	Surr+ Conosol C- 200_new	156.4	16.7	8.9	1	325	105.5	60.3	1.2	72.4
EPA2181(B)	Surr	-	15.7	10.3	1	325	135.4	0.5	1.5	0.8
EPA2182(A)	Conosol C-70 + H ₂ O ₂	156.4	-	-	1	408	30.5	23.0	1.2	27.6
EPA2182(B)	H ₂ O ₂	-	-	-	1	408	23.2	0.3	1.4	0.4
EPA2183(A)	Conosol C-400 + H ₂ O ₂	156.4	-	-	1	339	20.0	34.3	1.1	37.7
EPA2183(B)	H ₂ O ₂	-	-	-	1	339	8.1	29.0	1.4	40.6
EPA2184(A)	Conosol C-200 + H ₂ O ₂	156.4	-	-	1	346	15.0	51.3	1.1	56.4
EPA2184(B)	C16 + H ₂ O ₂	40.5	-	-	1	346	8.0	58.8	1.4	82.3
EPA2185(A)	Surr+ Conosol C- 200+ H ₂ O ₂	156.4	13.2	8.9	1	374	148.3	72.2	1.2	86.6
EPA2185(B)	Surr+ H ₂ O ₂	-	13.2	9.0	1	374	161.8	20.5	1.5	30.8
EPA2186(A)	Surr+ Conosol C- 200+ H ₂ O ₂	156.4	13.5	13.0	1	329	133.1	183.7	1.2	220.4
EPA2186(B)	Surr+ H ₂ O ₂	-	14.0	11.9	1	329	175.1	28.2	1.5	42.3
EPA2189(A)	Surr+ Isopar M + H ₂ O ₂	158.9	15.8	9.0	1	307	140.0	42.6	1.5	63.9
EPA2189(B)	Surr+ H ₂ O ₂	-	15.6	8.3	1	307	153.0	5.4	1.5	8.1
EPA2190(A)	Surr+ Isopar M + H ₂ O ₂	158.9	13.2	8.3	1	351	130.0	105.4	1.2	126.5
EPA2190(B)	Surr+ H ₂ O ₂	-	13.1	8.8	1	351	150.3	5.2	1.5	7.8
EPA2191(A)	Surr+Isopar M	158.9	14.3	8.3	-	367	124.0	21.7	1.2	26.0
EPA2191(B)	Surr	-	14.3	8.6	-	367	135.9	1.2	1.5	1.8
EPA2192(A)	Surr+Isopar M	158.9	14.3	7.9	-	366	116.5	22.9	1.2	27.5
EPA2192(B)	Surr	-	13.9	7.9	-	366	132.8	1.0	1.5	1.5
Run ID	Compound	Target LVP-	Initial NO	Initial NO ₂	Initial H ₂ O ₂	Photo oxidation	Final O ₃	Final PM (µm ³ /cm ³)	Average Density	Final PM* (µg/m ³)

		VOC (ppb)	(ppb)	(ppb)	(ppm)	Time (mins)	(ppb)		(g/cm ³)	
EPA2193(A)	Surr+ Hand Lotion	-	12.7	7.4	-	325	160.2	1.1	1.3	1.4
EPA2193(B)	Surr	-	12.7	7.9	-	325	123.0	0.6	1.5	0.9
EPA2194(A)	Surr+ Hand Lotion	-	12.6	8.4	-	293	137.5	14.1	1.2	16.9
EPA2194(B)	Surr	-	12.8	8.8	-	293	123.1	0.2	1.5	0.3
EPA2195(A)	Surr+ Hand Lotion + H ₂ O ₂	-	14.5	10.9	1	242	185.5	3.0	1.4	4.2
EPA2195(B)	Surr+ H ₂ O ₂	-	14.6	11.0	1	242	152.0	4.9	1.5	7.4
EPA2196(A)	Surr+ Hand Lotion + H ₂ O ₂	-	15.9	8.6	1	380	179.6	5.9	1.4	8.3
EPA2196(B)	Surr+ H ₂ O ₂	-	15.7	8.5	1	380	154.8	4.7	1.5	7.1
EPA2225(A)	Surr+ Aromatic 200 + H ₂ O ₂	-	11.0	8.0	1	357	73.9	445.7	1.4	624.0
EPA2225(B)	Surr+ H ₂ O ₂	-	12.1	8.4	1	357	124.9	2.5	1.5	3.8
EPA2226(A)	Surr+ Aromatic 200 + H ₂ O ₂	-	11.4	6.7	1	390	73.3	506.2	1.3	658.1
EPA2226(B)	+ H ₂ O ₂	-	11.7	6.8	1	390	112.1	5.5	1.4	7.7
EPA2227(A)	Surr+ Aromatic 200	-	13.7	6.3	-	392	96.0	70.6	1.4	98.8
EPA2227(B)	Surr	-	13.3	6.8	-	392	109.0	0.3	1.5	0.5
EPA2228(A)	Surr+ Aromatic 200	-	13.5	6.5	-	339	99.8	62.5	1.4	87.5
EPA2228(B)	Surr	-	13.5	6.6	-	339	114.8	0.1	1.5	0.2
EPA2243(A)	Surr+ heptadecane + H ₂ O ₂	40.0	18.0	12.7	1	360	-	102.5	-	-

Assumed density of 1.5 g cm⁻³ for surrogate only and surrogate with H₂O₂ experiments (usually East reactor or side B) based on previous experimental results (EPA1894). Assume the same density as the density of side A for experiments without APM-SMPS data.

Surr: Surrogate MOIR/2

Half surrogate: 0.55 ppmC surrogate

*: chemical compounds were included beyond compounds listed in Table 9 to study structural impact of glycol ether on SOA formation.

+: Target concentrations provided. Typically, actual concentrations in these chamber systems are within 5% of target concentration.

A: West reactor

B: East reactor

2. Individual LVP-VOC experiments

a. Ozone experimental results

Figure 20 presents the results of ozone formation from individual LVP-VOCs with surrogate. The formed ozone concentration ranged from 145 to 222 ppb. DEGEE, DPGMEA, Diethylene Glycol, Glycerol Triacetate, and Propylene Glycol show enhanced O₃ formation, while TEA and DEGBE were similar to the surrogate only O₃ formation, and the presence of n-Tridecane, n-Hexadecane, Benzyl Alcohol, and Texanol reduced the O₃ formed from the surrogate mixture. Excellent experimental repeatability for ozone formation (174.5 +/-8.7 ppb) from surrogate experiments (only surrogate and NO_x, no test compound) was observed during the course of these experiments (Figure 21).

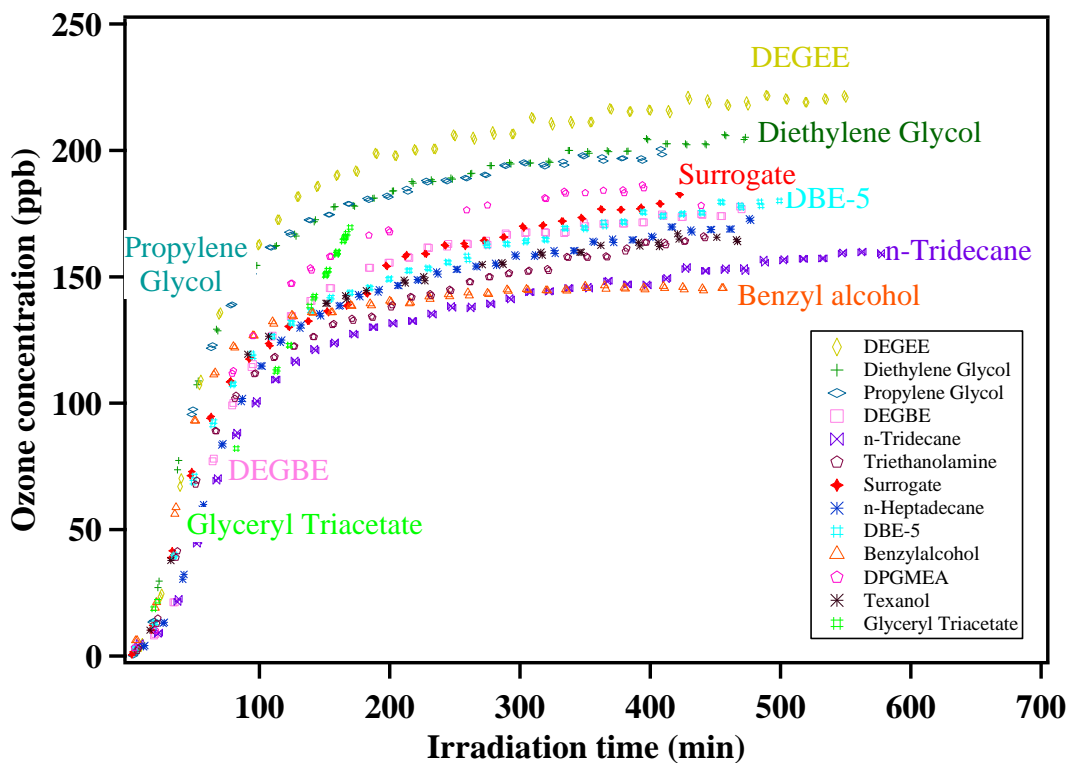


Figure 20: Ozone formation from individual LVP-VOCs with surrogate

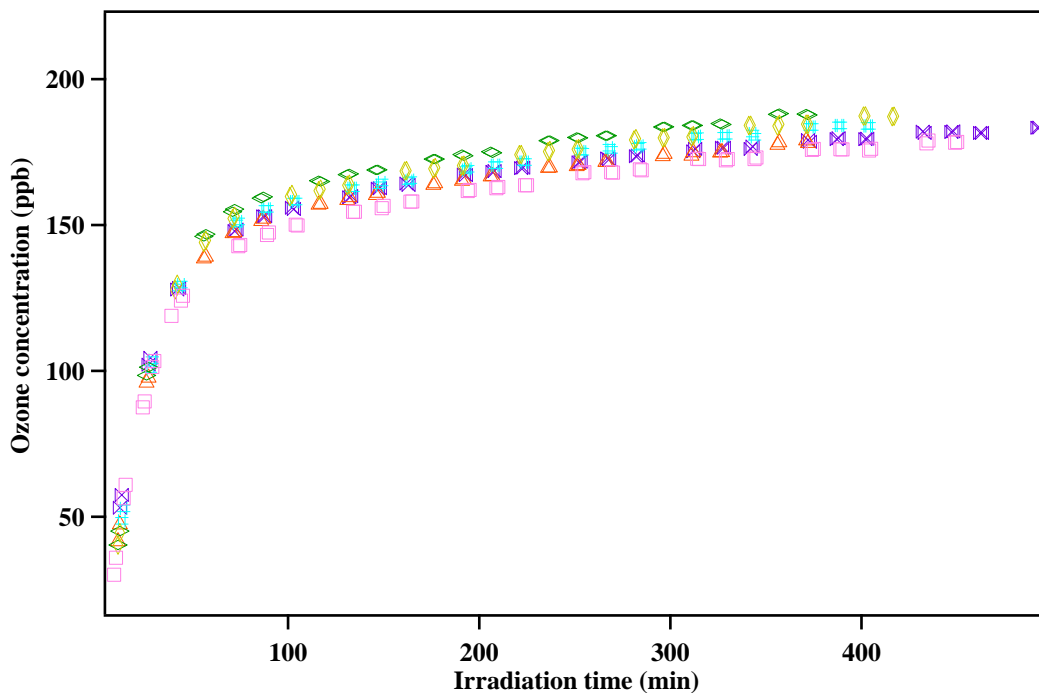


Figure 21: Ozone repeatability observed for repeat experiments within this work.

It is very important to note that a decrease (or increase) in ozone formed with the addition of the LVP-VOC does not necessarily indicate that the LVP-VOC will suppress (or enhance) ozone formation in the atmosphere—only that it is negatively (or positively) impacting the specific surrogate mixture ozone formation. This may be attributed to larger changes in radical concentrations, NO_x loadings, etc. than expected to occur within the more complex ambient atmosphere with its more significant reservoir. For example, addition of select LVP-VOCs reduces the overall hydroxyl concentrations available to oxidize both the LVP-VOC and the ozone forming surrogate hydrocarbons relative to the amount of oxidation and ozone that forms in the surrogate photooxidation alone. An additional series of experiments with enhanced hydroxyl radical concentration was performed to exercise the performance of the model and offset losses in hydroxyl reactivity in the mixture due to the addition of the LVP-VOC. Repeat surrogate runs with added H_2O_2 also showed excellent repeatability (180.2 ± 6.2 ppb) with slightly enhanced ozone formation. Figure 22 below plots the ozone formation for eight LVP-VOCs within the surrogate mixture with enhanced hydroxyl radical concentration (added H_2O_2). The formed ozone concentration ranged from 135 to 193 ppb. DEGEE, DBE-5, and Propylene Glycol enhanced O_3 formation at elevated OH concentration. Direct comparisons of ozone formation for select LVP-VOCs are also shown in Figure 23.

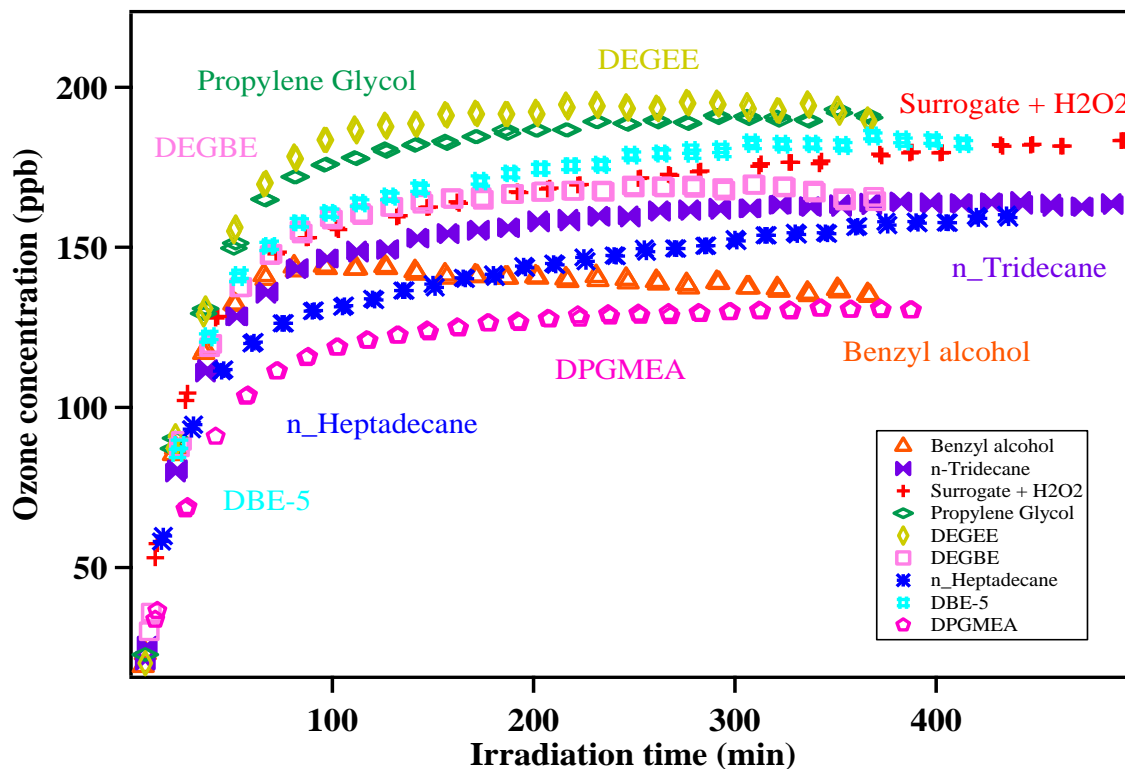


Figure 22: Ozone formation from individual LVP-VOCs with surrogate and H_2O_2

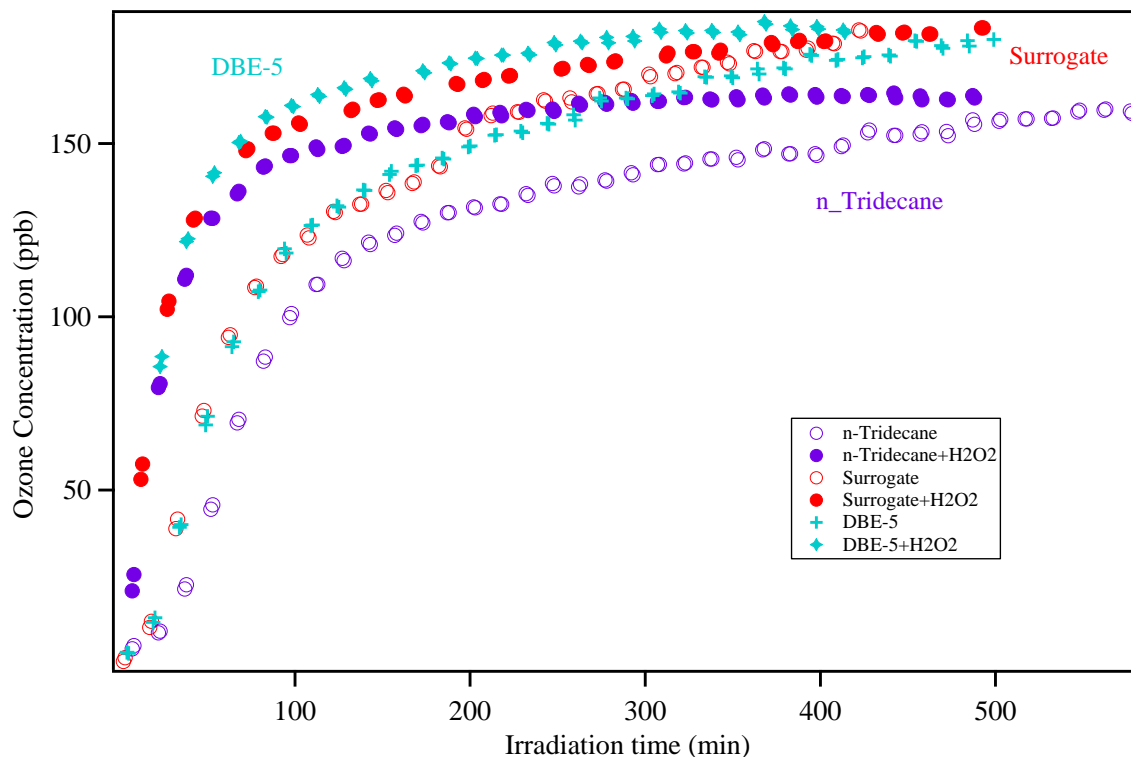


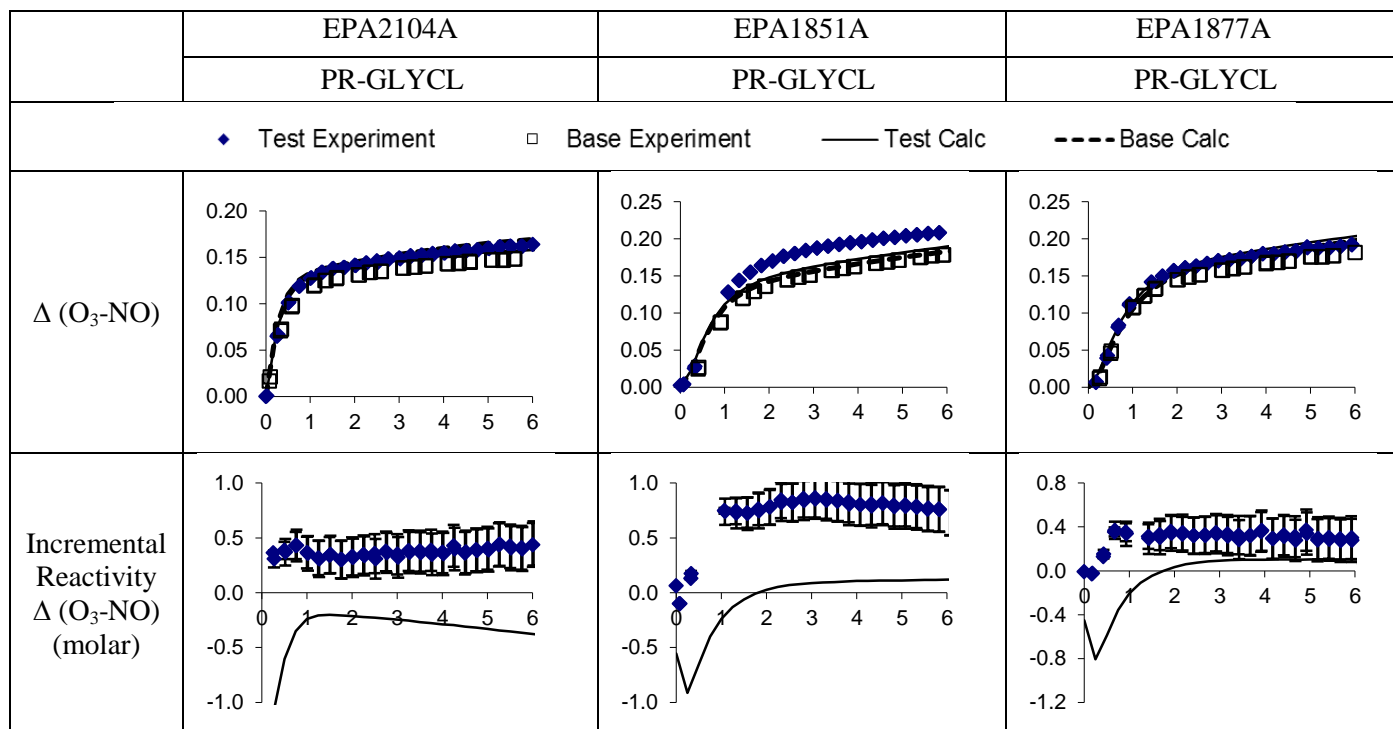
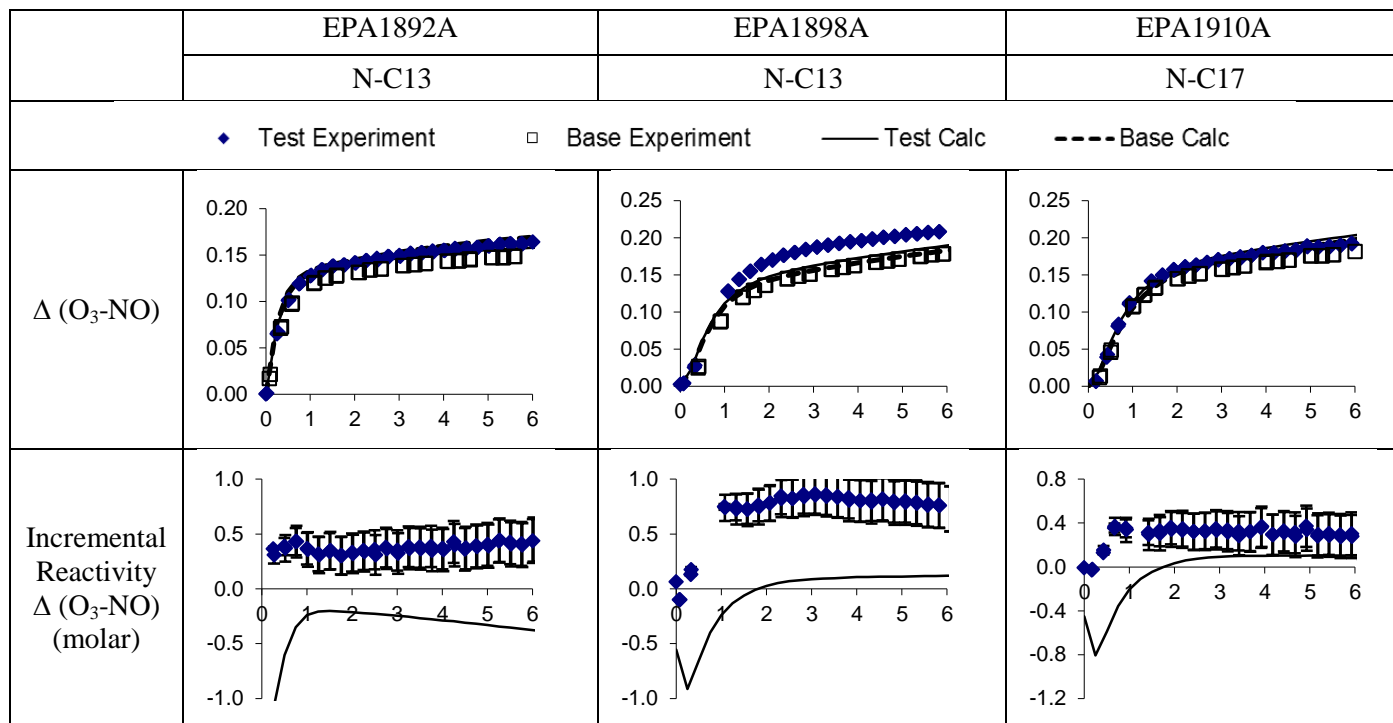
Figure 23: Typical ozone formation comparison between runs with or without H₂O₂

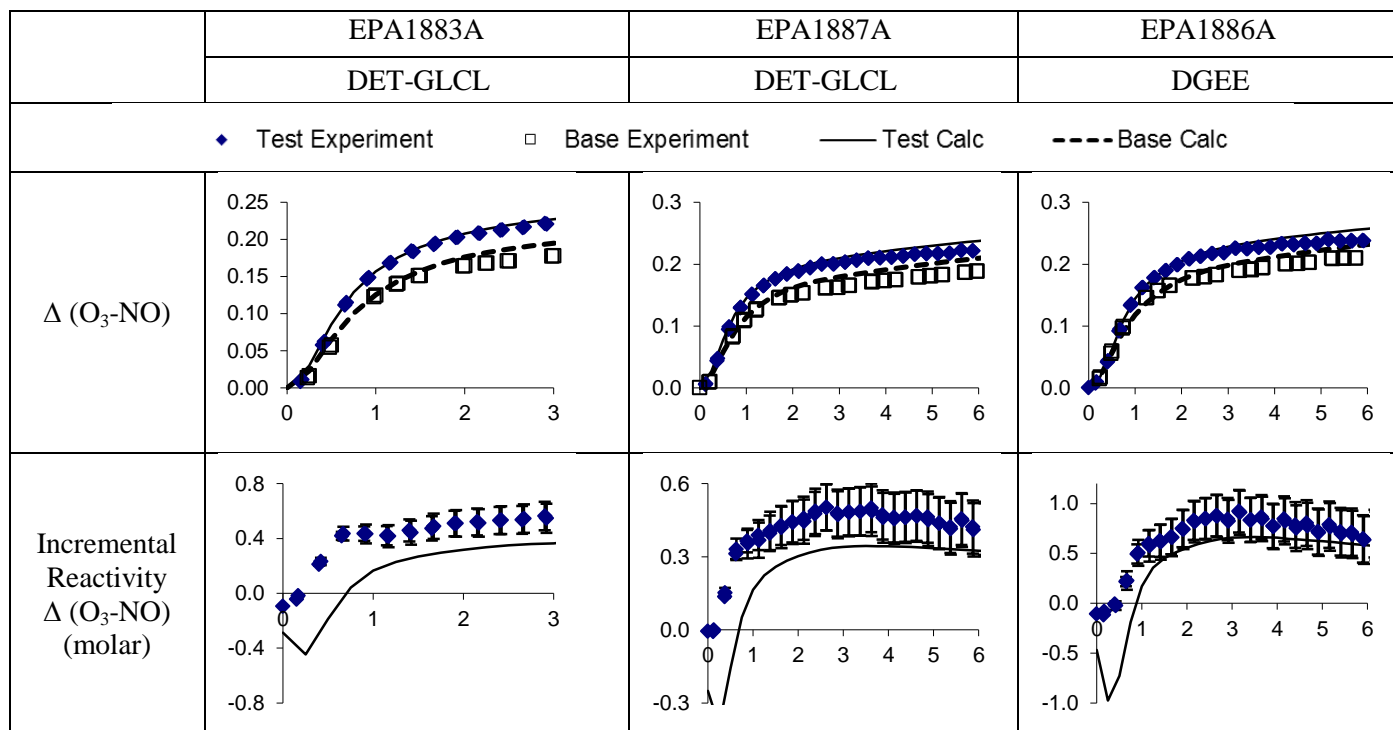
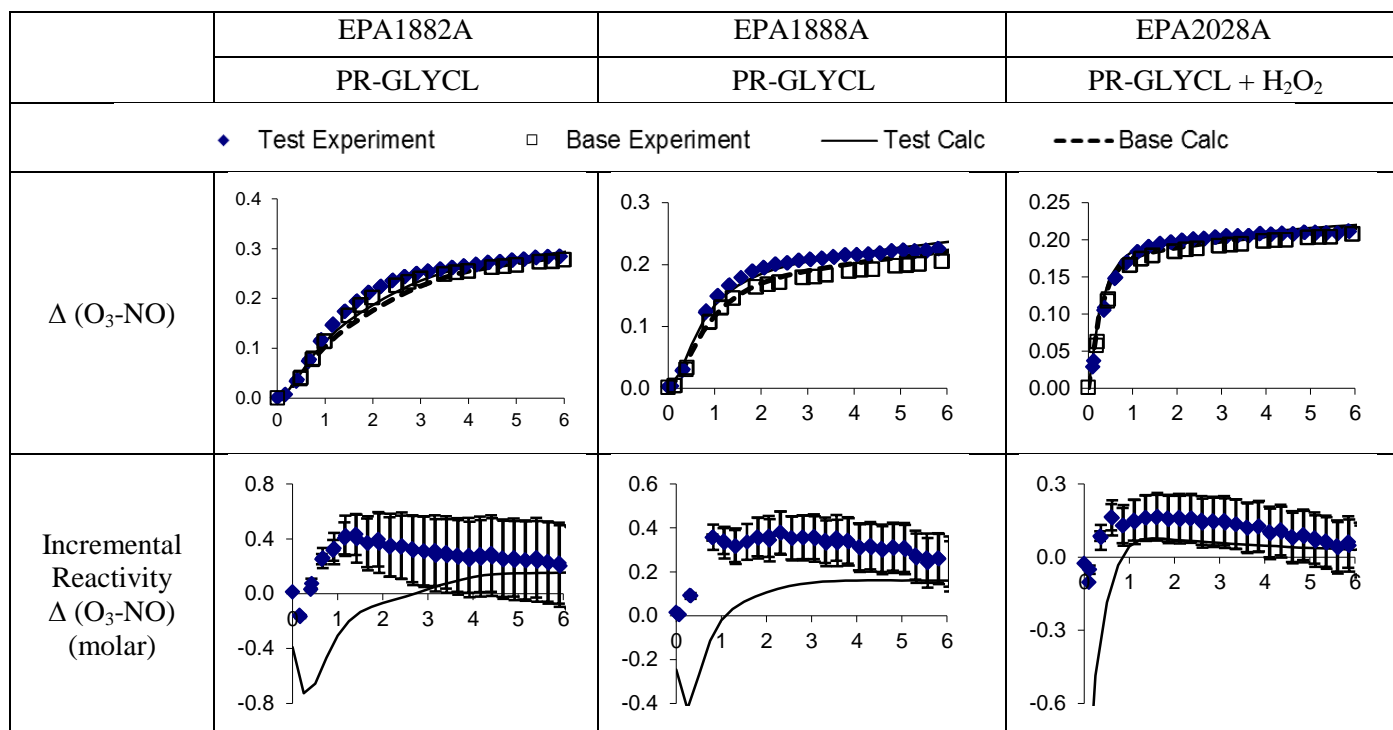
b. Ozone modeling results

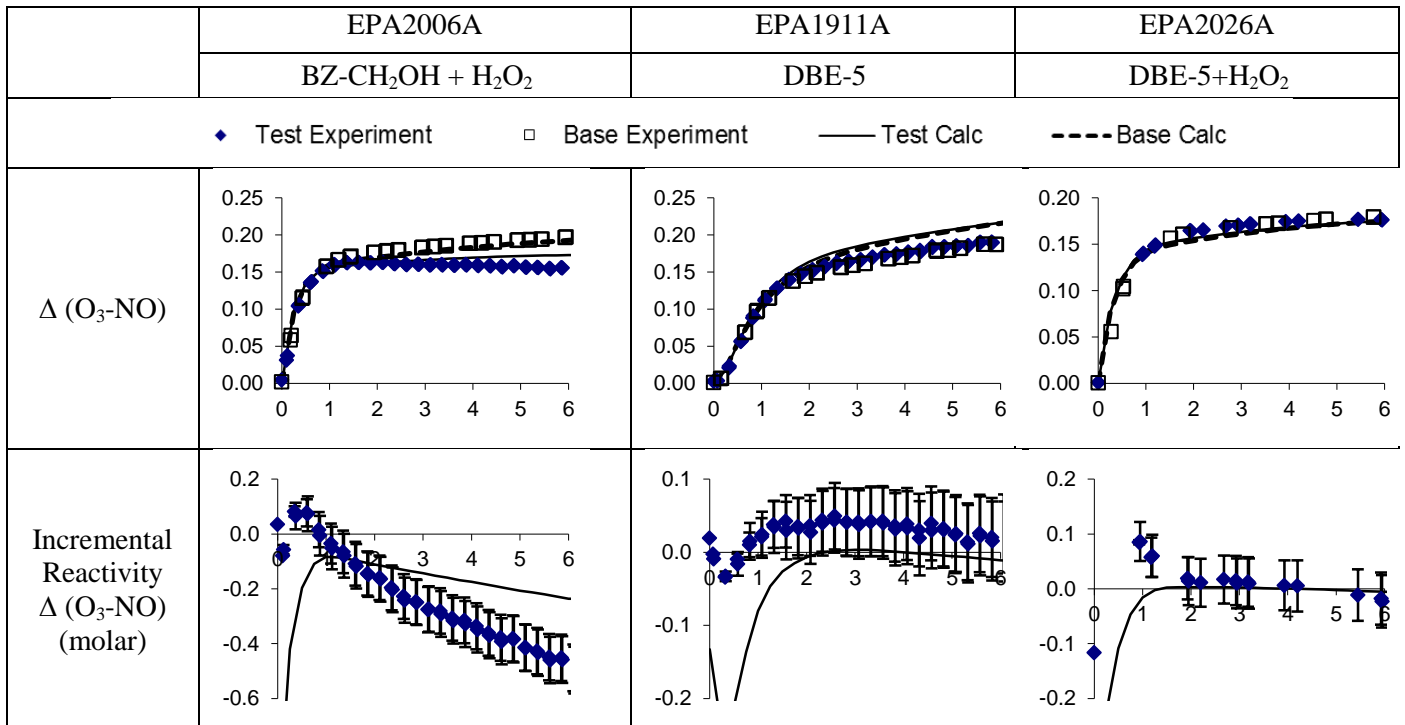
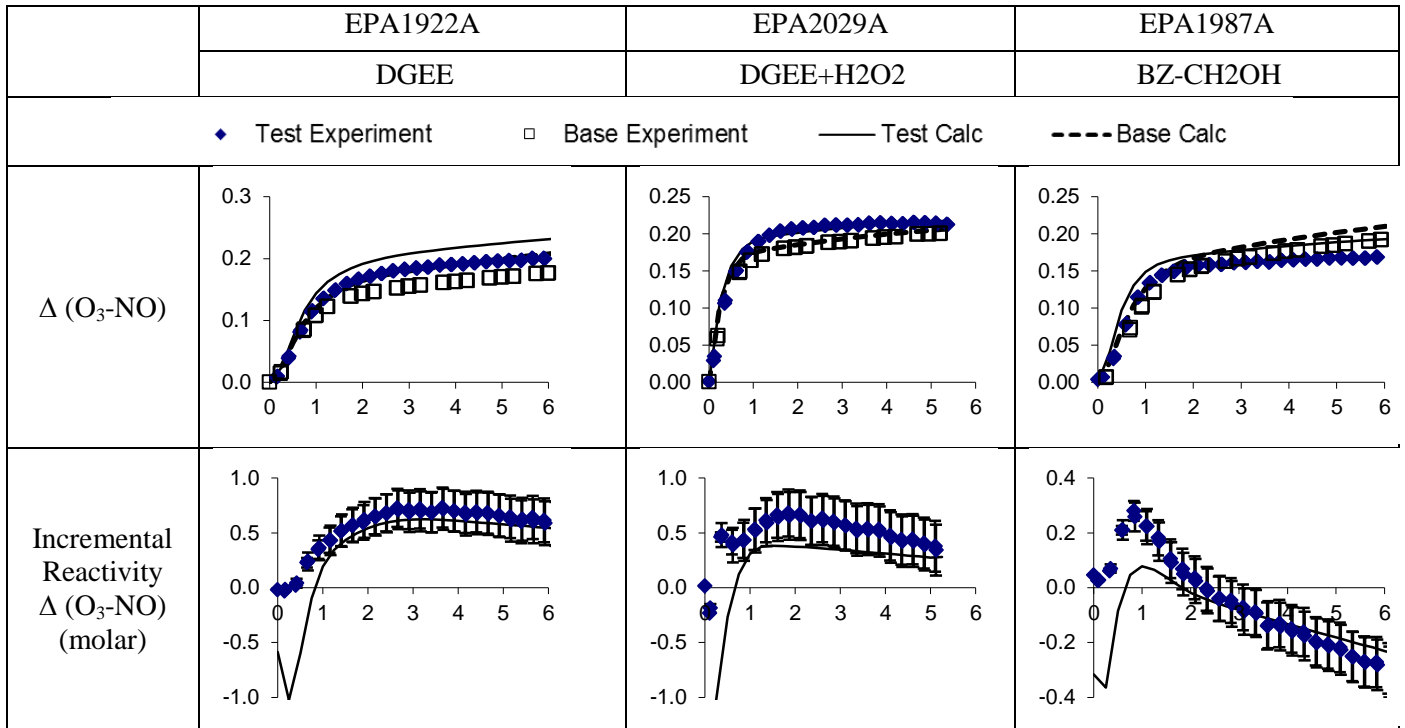
The SAPRC-2011 mechanism was used to predict O₃ formation within the environmental chamber studies conducted and to evaluate the ability of current models to accurately predict observed ozone formation for the experiments conducted. Model inputs include chamber photolysis rate (k_1), chamber wall effects (e.g., HONO offgasing), and starting VOC and NO_x concentrations. Significant measured experimental deviation from expected (predicted) ozone would indicate a need to revisit the chemical mechanisms currently used to predict atmospheric impacts of LVP-VOCs previously studied (e.g., MIRs). OH concentration for this work is estimated from measurements of m-xylene decay. The SAPRC-11 mechanism used in this work includes the rate constant and reactions updates based on current data, the SAPRC-07 chemical mechanism and chamber evaluations using more recent data (Carter and Heo, 2013; Carter, 2010). Figure 24 presents the summary of O₃ prediction results for LVP-VOCs by the SAPRC-11 model. The upper figures compare calculated and measured ozone results (O₃-NO) while the lower figures show differences in the predicted incremental reactivity for the individual LVP-VOC. The dashed line shows the base calculation. The empty square represents the base experiment. The blue diamond indicates test experiment. The solid line expresses test calculations. Generally, excellent agreement is observed between the LVP-VOC experiments within this work and that predicted by the model providing confidence in the gas-phase reactivity data previously obtained and currently used for these compounds. However, some of this excellent agreement is attributed to the fact that the OH concentrations were adjusted to fit measured m-xylene decay rates within SAPRC-11 rather than in previous model iterations where the hydroxyl radical concentrations were estimated independently.

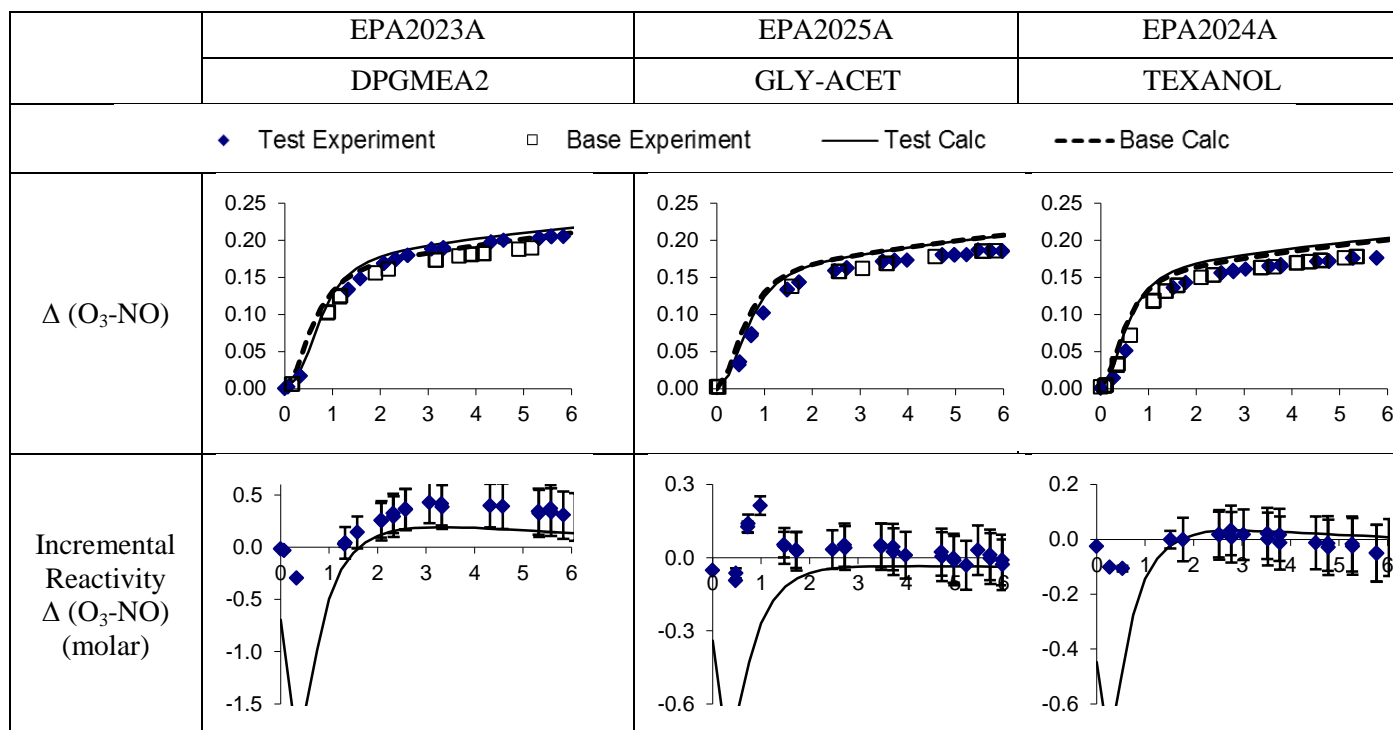
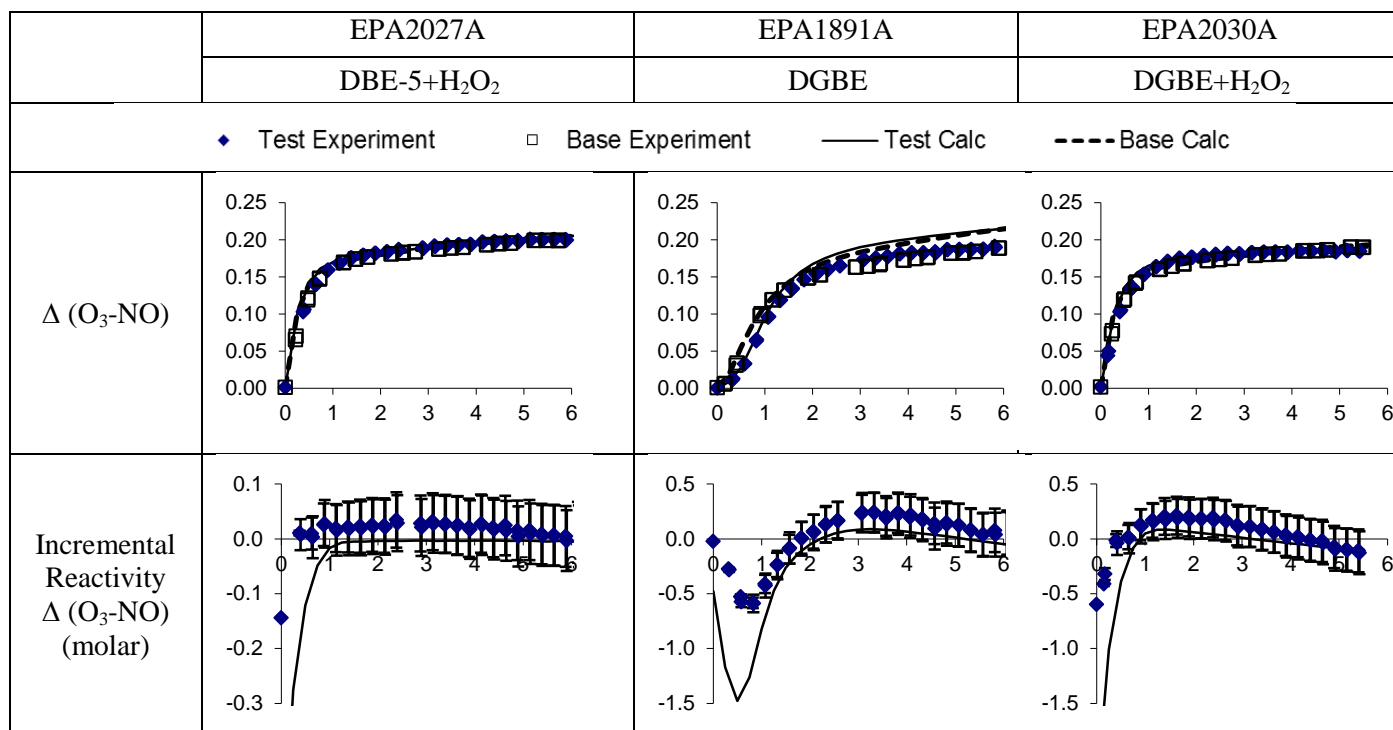
Note that less ozone was formed when some compounds were added to the surrogates, consistent with model predictions that account for the decreased availability of hydroxyl radical due to consumption of hydroxyl radicals by select LVP-VOCs. This has been observed and discussed previously (Carter, 2011) is attributed to the fact that many compounds, including most LVP-VOCs, tend to inhibit OH radical levels due to their reactions. Even addition of the 1 ppm H₂O₂ did not sufficiently enhance OH production to offset consumption by the LVP-VOCs. Although their reactions form radicals that convert NO to NO₂ and form O₃, the reduced OH levels tend to cause less O₃ formation from the reactions of the VOCs in the base case surrogate, and if the reduction is large enough and the experiment is sensitive enough to this reduction then less net O₃ formation will occur when the added LVP-VOC is present. The sensitivity of the experiment to reduced radical levels depends on the conditions of the experiment, and calculations indicate that most of our experiments are more sensitive to reduced radical levels than is the case for atmospheric conditions where the relative abundance of the LVP-VOC to other VOCs participating in the reaction is lower. (Carter, 2011). Under low NO_x conditions the added VOCs will also remove more NO_x from the system than would be the case if it were not present, which would also cause lower O₃ if the compound is present if the experiment is sensitive enough to NO_x conditions and the amount of NO_x reduced by the VOC's reactions is large enough. A challenge with environmental chambers is that, unlike atmospheric conditions, they have a contained chemical system without continuous inputs of other chemicals (such as NO_x). Generalization of the environmental chamber results requires accurate chemical mechanisms that can account for the wide range of atmospheric reactive conditions encountered. Data obtained for reactive conditions (Initial VOC:NO_x with surrogate, see Table 11) in this study is consistent with previous modeling work.

Although the experiments measure the effects of the test compounds or mixtures on ozone formation under the conditions of the experiments, because of different sensitivities to effects on radical levels and other factors, the effects on ozone in the experiments is not exactly the same as their effects on ozone in the atmosphere. The experiments are used to test the ability of the models to predict the effects of the compounds on ozone formation, and if they can simulate the effects in well controlled experiments then we can have more confidence in the model's predictions of ozone effects in the atmosphere. The models are then used to predict the effects of the compounds on atmospheric ozone as measured by the MIR or other reactivity scales (Carter, 1994). The MIR values for the compounds studied are given by Carter (2010), and the MIRs for the mixtures can be calculated from those given by Carter (2010) for the volatile and reactive constituents. MIR values for the LVP-VOCs studied in this work range from 0.42 (n-heptadecane) to 5.11 (benzyl alcohol) with an average MIR of 1.86. MIR values range from ~0.49-1.15 for C₃₊ straight chain alkanes, from ~0.4-1.5 for branched alkanes, from ~0.5-1.7 for cycloalkanes, from 1.3-15 for alkenes, and 0.7-12 for monocyclic aromatics.









	EPA1914A	EPA1912A	EPA2093A
--	----------	----------	----------

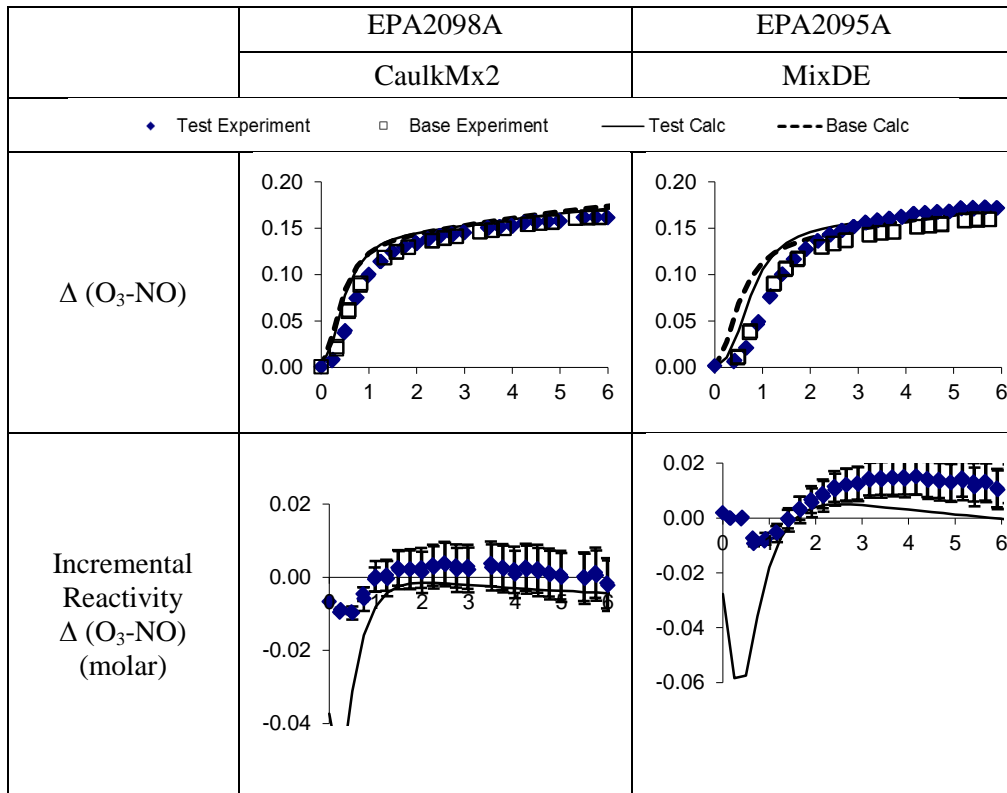
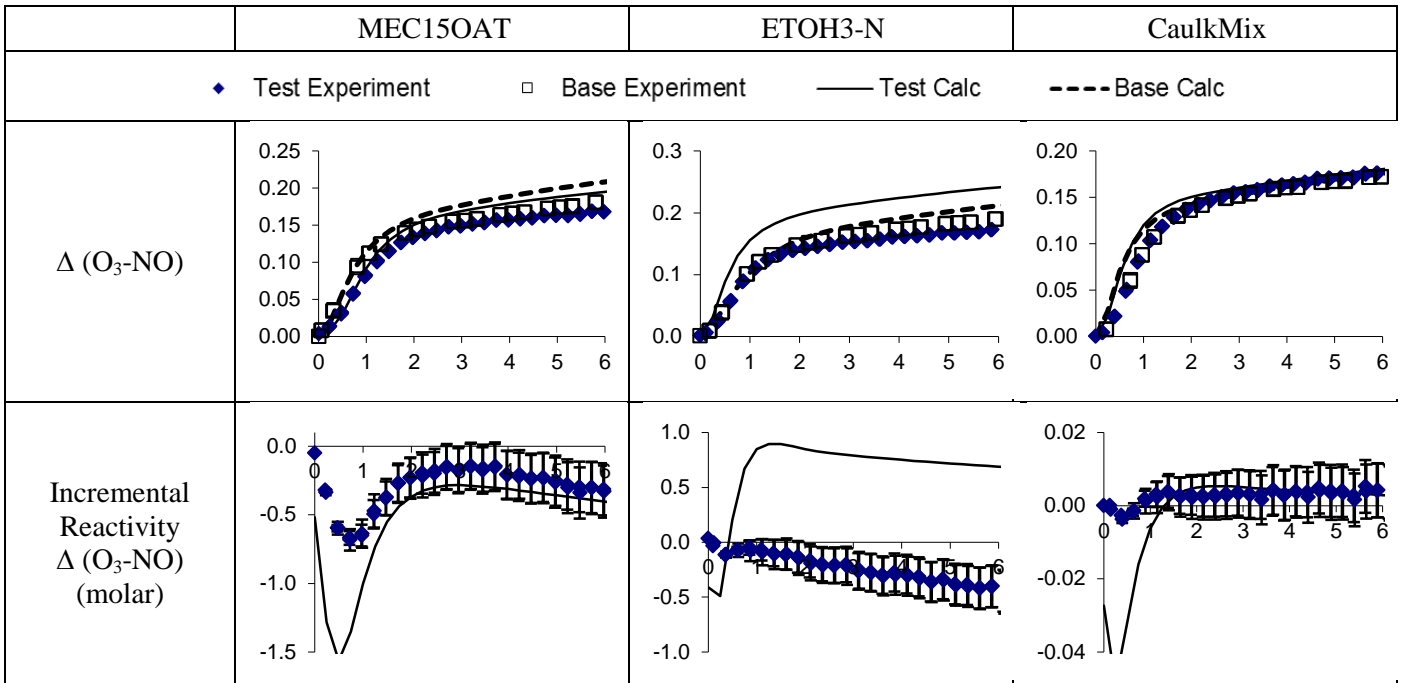


Figure 24: The summary of O_3 prediction results during experiment (elapsed time in hour) for LVP-VOCs by the SAPRC-11 model.

c. SOA results

Secondary organic aerosol is ubiquitous in the atmosphere formed from oxidation of VOCs leading to the formation of lower vapor pressure oxidation products that subsequently condense onto existing aerosol. SOA formation is typically studied in environmental chambers by injecting known concentrations of precursors and then observing the SOA formation as the precursor is oxidized. The current environmental chamber is ideally suited (Carter, 2005) for the study of SOA due to the excellent control of environmental parameters (e.g., temperature), excellent run-to-run reproducibility, and the design of the chamber (e.g., positive pressure control, chamber surrounded by purified air) that enables the study of SOA formation nearer to atmospheric conditions (lower concentrations of aerosol precursors).

This work utilizes initial precursor concentrations of LVP-VOC in the range of 40 to 160 ppb. As aerosol formation is a function of organic aerosol concentration (see discussion that follows on yield curves), the representativeness of the experiment is related to the final organic aerosol formed during a given experiment. Typically, ambient fine particle organic aerosol concentrations tend to be less than $10 \mu\text{g m}^{-3}$. Detailed SOA formation experiments require multiple experiments at varying concentrations to elicit detailed aerosol yield curves (see yield curve description below) or VBS data sets (see Section D). Rather than invest in obtaining full data sets necessary for yield curve determinations for very few LVP-VOCs, it was determined in discussions with the program advisory committee to measure SOA formation for a number of LVP-VOC precursors (described in Ozone section above). Therefore, the SOA formation observed is used as guidance as to the extent of SOA formation that might be expected from a variety of SOA precursors. Experiments were conducted while simulating typical California atmospheric reactive conditions (in the presence of surrogate and NO_x). Relative amounts of SOA formation from the LVP-VOC precursors provides a strong indication of which LVP-VOC precursors are important (or unimportant) SOA producers warranting further investigation.

Figure 25 presents SOA formation ($\mu\text{m}^3 \text{cm}^{-3}$ refers to aerosol volume concentration; when multiplied by aerosol density (g cm^{-3}) the units convert to mass concentration ($\mu\text{g m}^{-3}$)) from individual LVP-VOCs when oxidized in the presence of the surrogate, NO_x and UV. n-Heptadecane, DEGBE, and Benzyl Alcohol have the most aerosol formation (on the order seen from similar concentrations of precursor aromatic compounds) while DEGEE, DBE-5, and n-Tridecane show relatively more moderate aerosol formation. These series of experiments were performed following similar methods (test compound plus surrogate mixture) used to evaluate ozone formation.

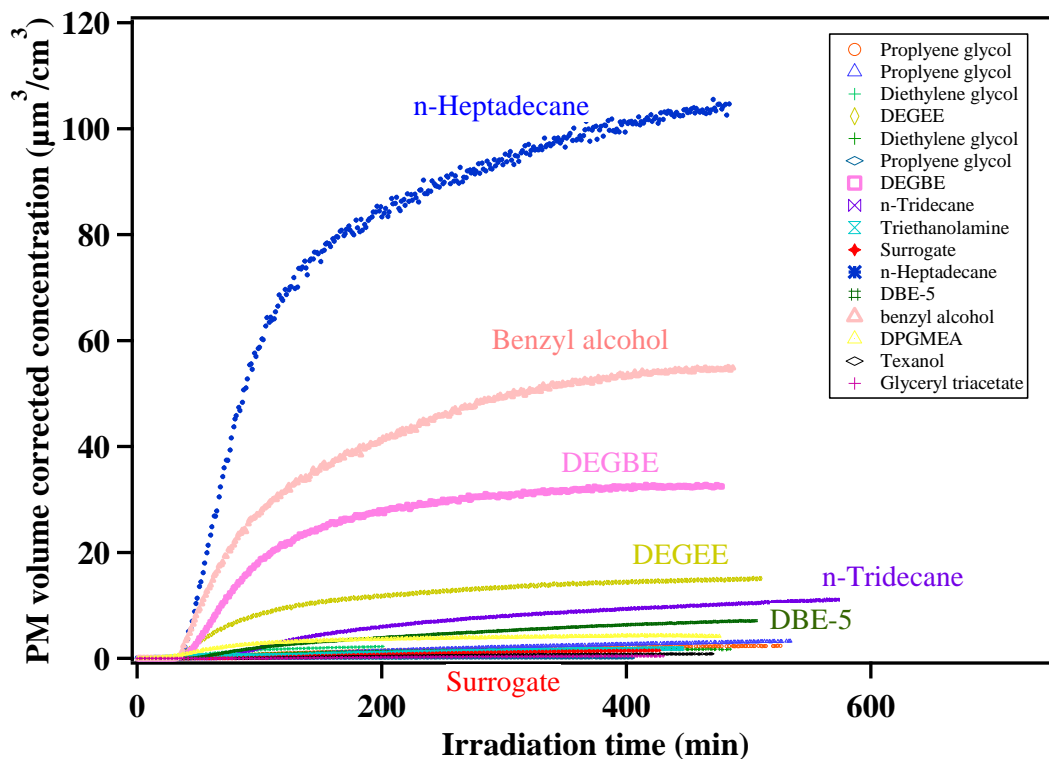


Figure 25: SOA formation from individual LVP-VOCs with surrogate

SOA formation from the surrogate only experiments were very low ($1.25 \pm 0.8 \mu\text{g m}^{-3}$) so no correction for baseline SOA formation in these experiments is performed. Figure 26 and 27 show repeat SOA formation observed for the surrogate only and surrogate with H_2O_2 experiments, respectively.

As noted in Section III-2a, a series of experiments were conducted with enhanced reactivity by increasing H_2O_2 . This allows for greater consumption of the initial LVP-VOC by offsetting losses in reactivity due to hydroxyl radical consumption. Figure 27 illustrates the SOA formation for the surrogate plus H_2O_2 experiments. The baseline surrogate SOA formation rises to $6.33 \pm 3.13 \mu\text{g/m}^3$ for surrogate experiments with enhanced H_2O_2 .

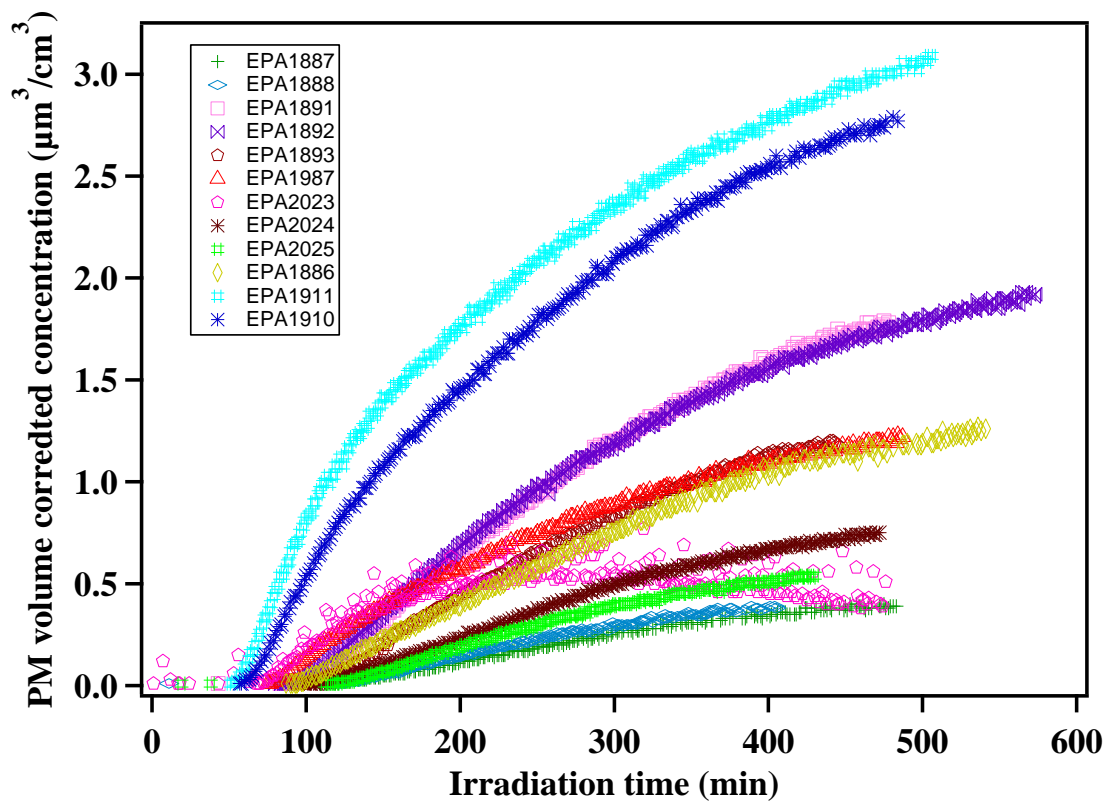


Figure 26: SOA formation in surrogate only experiments

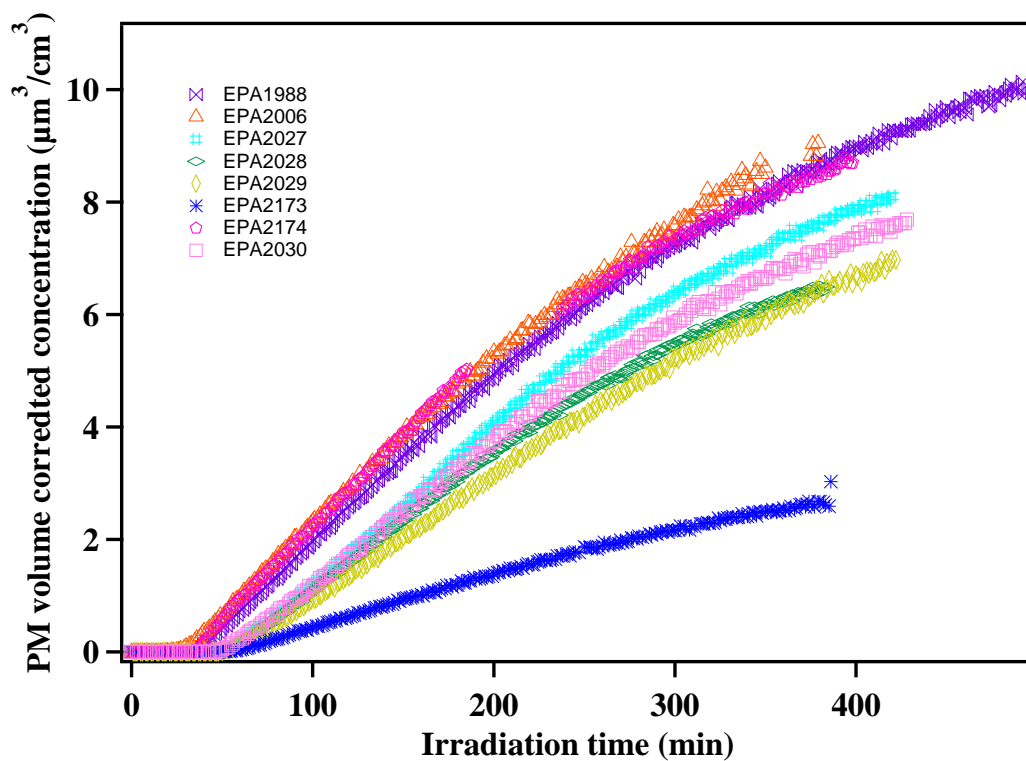


Figure 27: SOA formation from repeat surrogate experiments with H_2O_2 .

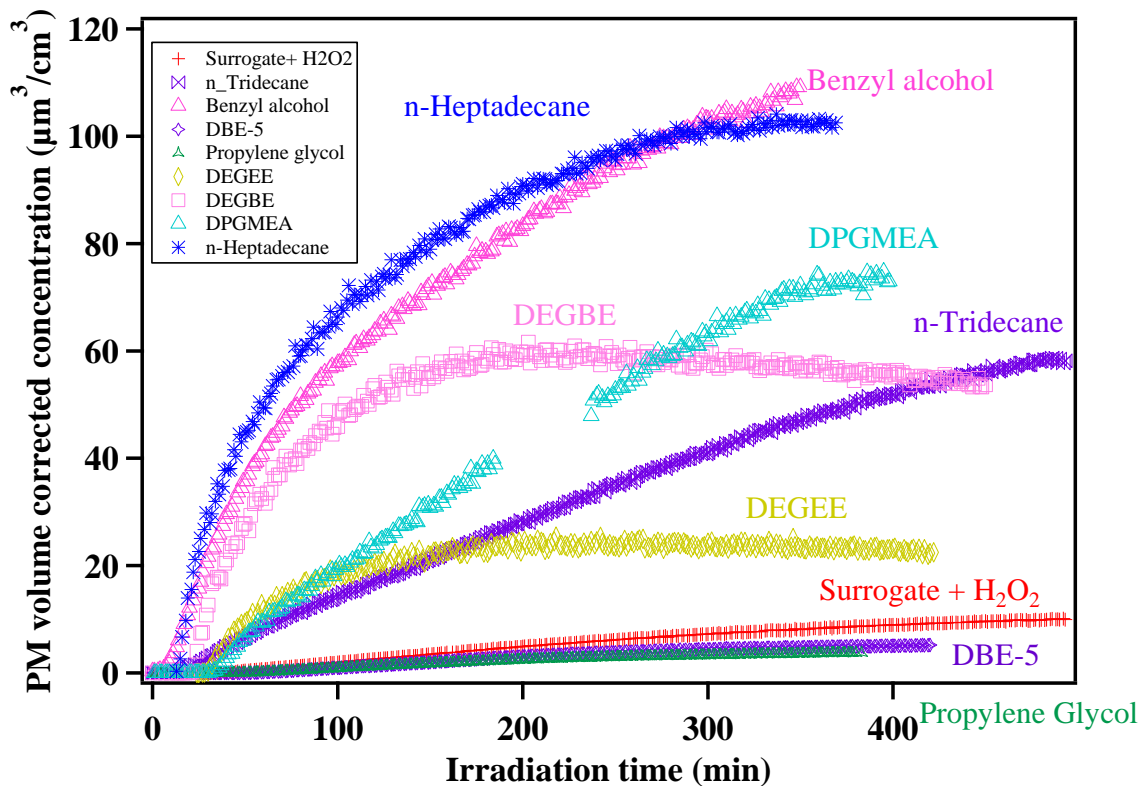


Figure 28: SOA formation from individual LVP-VOCs with surrogate and H_2O_2

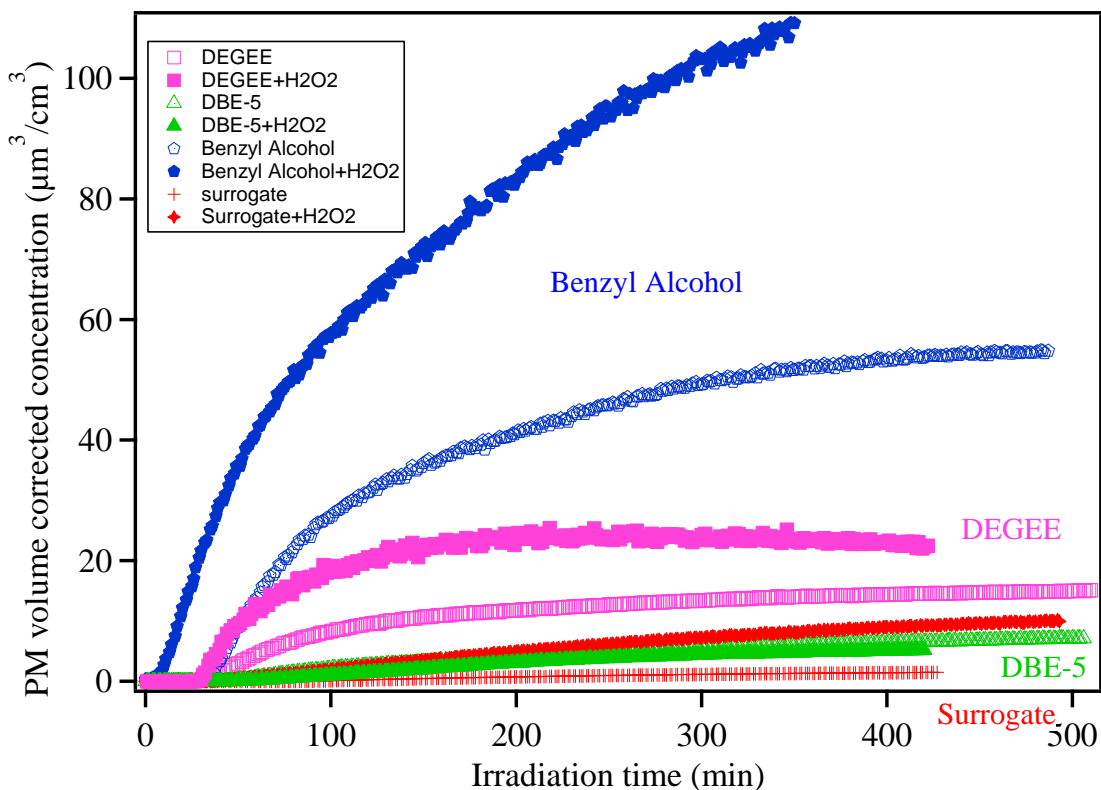


Figure 29: Comparison of SOA formation with and without H_2O_2 for select LVP-VOCs.

Figure 28 illustrates the results of SOA formation from individual LVP-VOCs with surrogate, NO_x, UV and H₂O₂. Figure 29 illustrates the SOA formation for select LVP-VOCs with and without H₂O₂.

More aerosols formed after injecting H₂O₂ for all LVP-VOCs that formed measurable SOA. DEGBE, benzyl alcohol, and n-Tridecane show significant aerosol formation. DEGEE shows moderate aerosol formation. SOA yields from LVP-VOC photooxidation with surrogate range from <0.01% (negligible) to 121% (Table 12). SOA yields from LVP-VOCs photooxidation with surrogate and H₂O₂ range from 8.8% to 152% (Table 12).

Greater SOA yields are expected in experiments that consume greater amounts of hydrocarbon due to the non-linear response of aerosol formation to hydrocarbon consumed—increased suspended organic mass provides a larger reservoir for condensing semi-volatile species to reside. This is seen best in the classic aerosol yield curve (Figure 30). SOA formation from DBE-5 and propylene glycol was negligible for both systems.

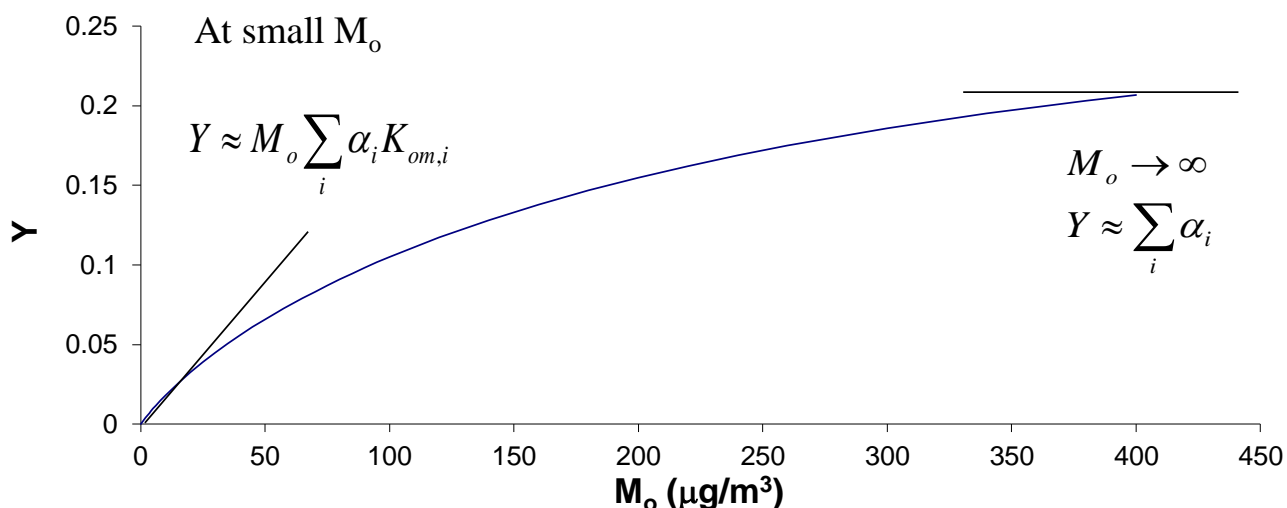


Figure 30: Typical yield curve showing changes in aerosol formation as a function of M_o (Aerosol mass).

Yield is defined in the following equation:

$$Y = \sum_i Y_i = M_o \sum_i \frac{\alpha_i K_{om,i}}{1 + K_{om,i} M_o} \quad \text{Eq.16}$$

Y : Yield

M_o : Amount of aerosol produced

$K_{om,i}$: Partitioning coefficient of compound i

α_i : Mass-based stoichiometric coefficient of compound i

Oxidation products, produced from the atmospheric oxidation of an ROG, can be semivolatile and partition themselves into an absorbing organic aerosol (M_o) phase at concentrations below their saturation concentrations. The partitioning of each semivolatile oxidation product is described by a partitioning coefficient ($K_{om,i}$). SOA yields for an individual ROG are not uniquely valued, but rather are a function of the available absorbing organic aerosol concentration.

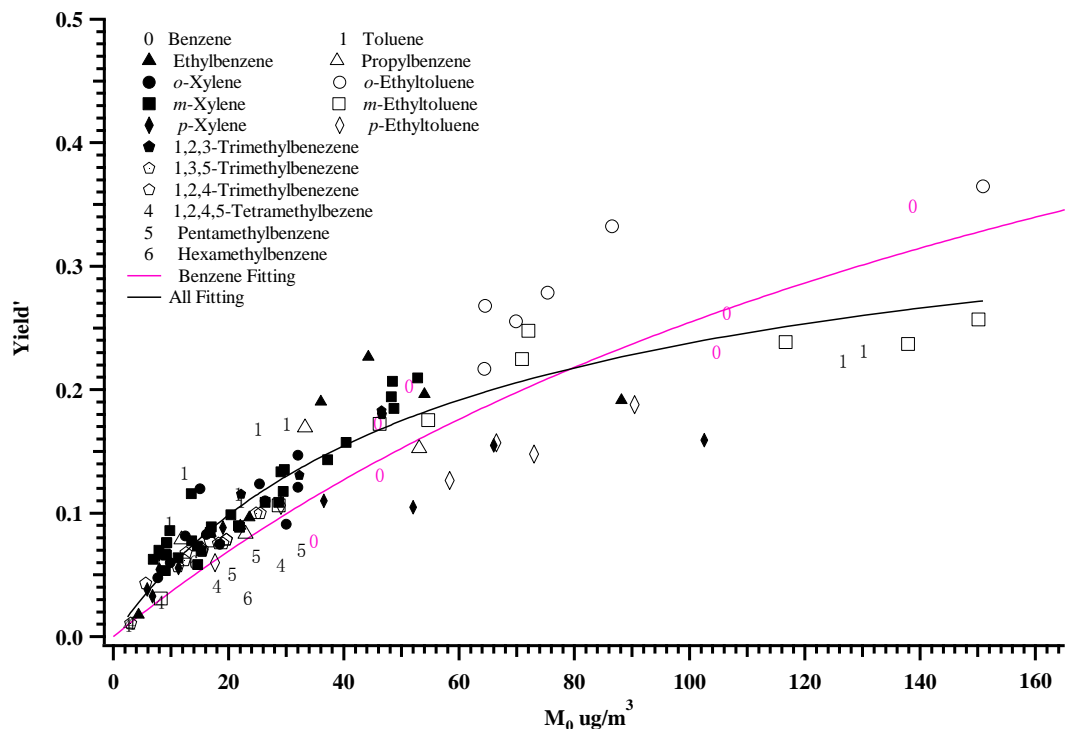


Figure 31: Yield curves for C6-C9 aromatics

Aerosol yield is typically reported as the mass fraction of aerosol formed compared to hydrocarbon consumed ($Y = \Delta M_0 / \Delta \text{HC}$). Figure 31 shows that the yields for typical aromatics are between 0.01 and 0.4, which is shown as a comparative. These aromatics formed moderate amount of aerosol. Individual aerosol yield experiments are insufficient to fit empirical two-product models or VBS sets. However, the values still provide insight into those LVP-VOCs that are most likely to contribute to SOA formation. While the initial hypothesis was that LVP-VOCs would form significant SOA, only propylene glycol, DEGBE, *n*-tricane, *n*-heptadecane, and benzyl alcohol have yields greater than or equal to 0.1 without added H_2O_2 and only *n*-heptadecane and benzyl alcohol have very high yields relative to common VOC precursors. (Odum et al. 1996) Addition of H_2O_2 to the chamber experiments (see ozone section) adds DBE-5 and DEGBE to the list of SOA precursors with measurable SOA formation. Therefore, as hydroxyl radical levels are maintained during the experiment, greater SOA formation from the LVP-VOC precursor is observed.

Table 12: Yield for individual LVP-VOC runs

Type	Run ID	Compound**	Δ HC ($\mu\text{g}/\text{m}^3$)	Δ M ($\mu\text{g}/\text{m}^3$)	Yield (GC)
LVP-VOC + surrogate + NO _x	EPA1877(A)	Surr + Propylene glycol	28.01	3.67	0.131
	EPA1882(A)	Surr + Propylene glycol	21.47	4.77	0.222
	EPA1883(A)	Surr + Diethylene glycol	211.19	3.39	0.016
	EPA1886(A)	Surr + DEGEE	355.02	22.95	0.065
	EPA1887(A)	Surr + Diethylene glycol	430.85	2.58	0.0060
	EPA1888(A)	Surr + Propylene glycol	93.37	0.16	0.00168
	EPA1891(A)	Surr + DEGBE	314.70	47.78	0.152
	EPA1892(A)	Surr + n-Tridecane	146.28	14.69	0.100
	EPA1893(A)	Surr + Triethanolamine	-	2.86	-
	EPA1910(A)	Surr + n-Heptadecane	85.56	103.34	1.21
	EPA1911(A)	Surr + DBE-5	286.92	9.73	0.0339
	EPA1987(A)	Surr + Benzyl alcohol	176.91	82.91	0.469
Surrogate only	EPA1894(A)	Surr	0	0	N/A
Surrogate + H ₂ O ₂ only	EPA1988(B)	Surr + H ₂ O ₂	0	0	N/A
LVP-VOC + surrogate + H ₂ O ₂ + NO _x	EPA1988(A)	Surr + H ₂ O ₂ + n-Tridecane	369.47	71.57	0.194
	EPA2006(A)	Surr + H ₂ O ₂ + Benzyl Alcohol	300.74	163.74	0.544
	EPA2023(A)	Surr + DPGMEA	323.66	5.96	0.0184
	EPA2024(A)	Surr + Texanol	176.94	1.12	0.00635
	EPA2025(A)	Surr + Glyceryl triacetate	66.40	0.63	0.00956*
	EPA2027(A)	Surr + H ₂ O ₂ + DBE-5	6.55	7.56	1.15
	EPA2028(A)	Surr + H ₂ O ₂ + Propylene Glycol	62.25	5.45	0.0876
	EPA2029(A)	Surr + H ₂ O ₂ + DEGEE	246.93	34.79	0.141
	EPA2030(A)	Surr + H ₂ O ₂ + DEGBE	136.68	90.82	0.664
	EPA2173(A)	Surr + H ₂ O ₂ + n-Heptadecane	-	40.72	-
	EPA2174(A)	Surr + H ₂ O ₂ + DPGMEA	-	74.45	-

- Surr: surrogate
- -: No GC or SYFT data
- *: Yield calculated using data obtained from SYFT
- **: All surrogate experiments also contain NO_x

A quick summary of the changes in O₃ and aerosol formation changes for the surrogate mixture with the addition of the individual LVP-VOC are shown in Table 13.

Table 13: Ozone and SOA formation relative to surrogate runs for individual LVP-VOC runs

Run ID	Compound	O ₃	ΔM
EPA1877(A)	S + Propylene glycol	I	I
EPA1882(A)	S + Propylene glycol	I	I
EPA1883(A)	S + Diethylene glycol	I	I
EPA1886(A)	S + DEGEE	I	I
EPA1887(A)	S + Diethylene glycol	I	I
EPA1888(A)	S + Propylene glycol	I	D
EPA1891(A)	S + DEGBE	D	I
EPA1892(A)	S + n-Tridecane	D	I
EPA1893(A)	S + Triethanolamine	D	I
EPA1910(A)	S + n-Heptadecane	I	D
EPA1911(A)	S + DBE-5	Same	I
EPA1987(A)	S + Benzyl alcohol	D	I
EPA1988(A)	S + H ₂ O ₂ + n-Tridecane	D	I
EPA2006(A)	S + H ₂ O ₂ + Benzyl Alcohol	D	I
EPA2023(A)	S + DPGMEA	I	I
EPA2024(A)	S + Texanol	D	I
EPA2025(A)	S + Glyceryl triacetate	I	D
EPA2027(A)	S + H ₂ O ₂ + DBE-5	D	I
EPA2028(A)	S + H ₂ O ₂ + Propylene Glycol	I	D
EPA2029(A)	S + H ₂ O ₂ + DEGEE	I	I
EPA2030(A)	S + H ₂ O ₂ + DEGBE	I	I
EPA2173(A)	S + H ₂ O ₂ + n-Heptadecane	D	I
EPA2174(A)	S + H ₂ O ₂ + DPGMEA	D	I

- I: Increase
- D: Decrease

d. Seeded experiment-vapor wall loss effects

Previous studies by other groups demonstrate that losses of SOA-forming vapors to chamber walls during photooxidation experiments can lead to substantial and systematic underestimation of SOA (Section II-2a)). Therefore, several experiments were conducted with seed particles present to study vapor wall loss effects for LVP-VOCs. Ammonium sulfate seeds were added to the chamber until the number concentration exceeded $1 \times 10^4 \text{ cm}^{-3}$. Figure 32 shows the seeded experiments results. Table 14 summarizes all seeded experiments. The presence of seed does not appreciably affect aerosol formation from DEGEE, DEGBE, and n-tridecane, which means the vapor wall loss in the environmental chamber, even for these LVP-VOC precursors, is negligible. However, for glyceryl triacetate, DBE-5, and DPGMEA, SOA formation appears to be higher in the presence of the seed indicating that vapor wall loss of lower volatility oxidation products is occurring thereby lowering the SOA formation. These

compounds (with or without seed) are not the major SOA forming species observed in the current study. For these species the particle numbers formed in the chamber are much lower (typically $\ll 1000 \text{ cm}^{-3}$ particle number concentrations compared with $> 10000 \text{ cm}^{-3}$ in non-seed experiments not perturbed by aerosol seeding).

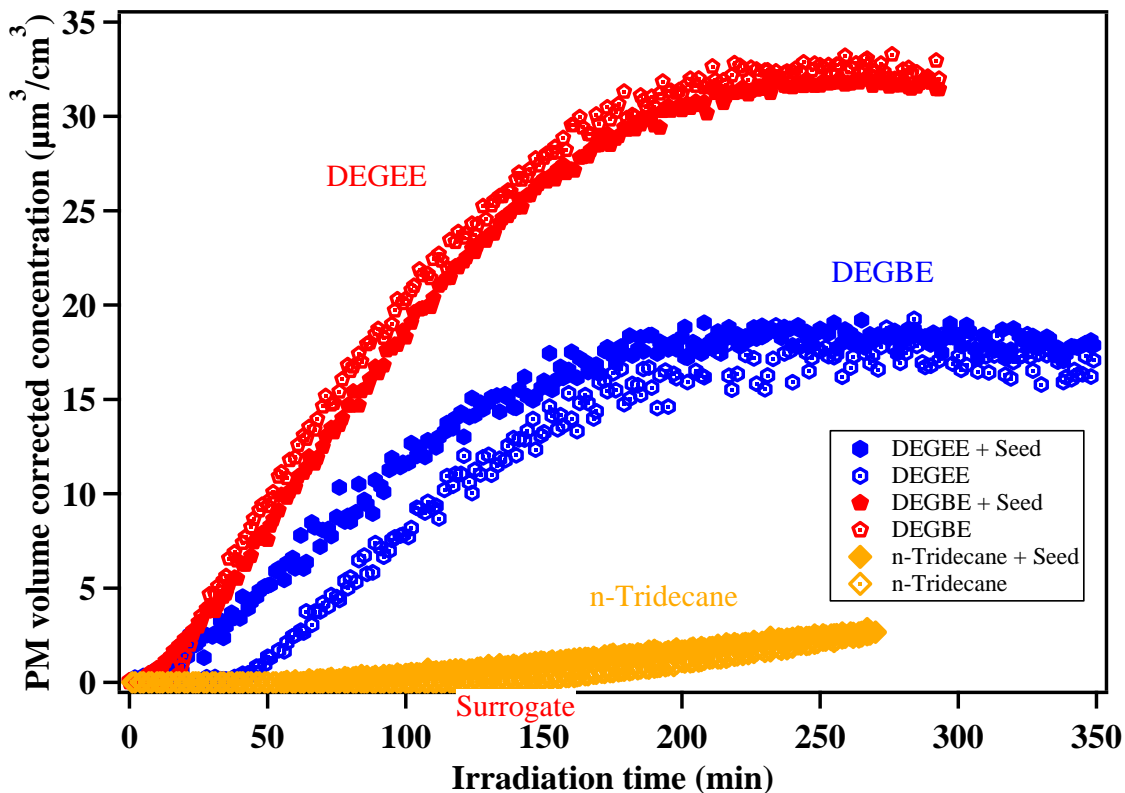


Figure 32: Vapor Wall Loss Effects – Seeded Experiments

Table 14: Yield for individual LVP-VOC runs with seed

Run ID	Compound	Δ HC ($\mu\text{g}/\text{m}^3$)	Δ M ($\mu\text{g}/\text{m}^3$)	Yield (G)
EPA2033(A)	H ₂ O ₂ + DEGEE + seed	89.4	22.7	0.25
EPA2033(B)	H ₂ O ₂ + DEGEE	102.1	24.3	0.23
EPA2034(A)	H ₂ O ₂ + DEGEE + seed	93.3	24.3	0.27
EPA2034(B)	H ₂ O ₂ + DEGEE	93.3 ^{&}	25.8	0.28
EPA2035(A)	H ₂ O ₂ + DEGBE + seed	24.6	27.3	1.11
EPA2035(B)	H ₂ O ₂ + DEGBE	-	28.8	-
EPA2036(B)	H ₂ O ₂ + DEGEE	83.6	24.9	0.30
EPA2041(A)	H ₂ O ₂ + DEGEE + seed	-	14.7 ⁺	-
EPA2041(B)	H ₂ O ₂ + DEGEE + seed	-	12.4 ⁺	-
EPA2042(A)	H ₂ O ₂ + Tridecane + seed	141.0	3.6	0.03
EPA2042(B)	H ₂ O ₂ + Tridecane	144.9	3.6	0.03
EPA2097(A)	Glyceryl Triacetate + H ₂ O ₂ + seed	28.7 [*]	12.2	0.43 [*]
EPA2097(B)	Glyceryl Triacetate + H ₂ O ₂	-	0.3	-
EPA2099(A)	DBE-5 + H ₂ O ₂ + seed	149.2 [*]	3.5	0.02 [*]
EPA2099(B)	DBE-5 + H ₂ O ₂ + seed	-	1.1	-
EPA2100(A)	DPGMEA + H ₂ O ₂ + seed	132.5 [*]	8.4	0.06 [*]
EPA2100(B)	DPGMEA + H ₂ O ₂	-	0	-
EPA2101(A)	H ₂ O ₂ + DBE-5+ NO + seed	75.3	4.3	0.06
EPA2101(B)	H ₂ O ₂ + DBE-5+ NO	-	1.0	-
EPA2102(A)	Glyceryl triacetate + H ₂ O ₂ + NO + seed	64.8 [*]	15.1	0.23 [*]
EPA2102(B)	Glyceryl triacetate + H ₂ O ₂ + NO	-	2.9	-
EPA2103(A)	DPGMEA + H ₂ O ₂ + NO + seed	17.9	7.7	0.43
EPA2103(B)	DPGMEA + H ₂ O ₂ + NO	-	0.8	-
EPA2177(A)	DPGMEA + H ₂ O ₂ + NO + seed	13.1 [*]	23.5	1.79 [*]
EPA2177(B)	DPGMEA + H ₂ O ₂ + NO	-	9.9	-
EPA2178(A)	Glyceryl triacetate + H ₂ O ₂ + NO + seed	-	21.9	-
EPA2178(B)	Glyceryl triacetate + H ₂ O ₂ + NO	-	14.4	-
EPA2179(A)	DBE-5 + H ₂ O ₂ + NO + seed	- ^{+,++}	46.8	-
EPA2179(B)	DBE-5 + H ₂ O ₂ + seed	- ^{+,++}	17.4	-

*: Yield and hydrocarbon decay calculated using data obtained from SYFT

-: No experimental data

&: Value used data from side A (west chamber) due to GC error

+: GC data poor, possible low injection

++: Four times more DBE-5 injected than in EPA2101 and EPA2099

e. In depth glycol ether study

A large amount of SOA is formed from glycol ethers (DEGEE and DEGBE) with surrogate (Figure 25) compared to all the other LVP-VOCs studied. The impact of molecular structure on SOA formation from glycol ethers was further investigated. We studied the photooxidation of a series of ethers (with and without -OH, with methyl group hindrance on -OH and with -OH at different location) under H₂O₂

conditions. And we found that SOA formation from the photooxidation of selected ethers (Figure 33) is associated with the presence and location of $-OH$. The molecular structure of ethers determines the branching ratio among carbonyl formation, cyclization and fragmentation. Cyclization is considered a critical SOA formation mechanism during the oxidation of glycol ethers under ambient conditions. The presence and location of $-OH$ in the carbon bond of ethers determine the occurrence of the cyclization mechanism during ether oxidation. Ethers with $-(OCH_2CH_2)_2-OH$ structure is found to readily form cyclization products and is evaluated as a dominating SOA precursor among all ethers. This suggests that DEGEE and DEGBE are the two most important ethers studied that could contribute to SOA formation under atmospheric conditions. It is noted that the SOA fractional yields of ether depend on the amount of ether precursor reacted.

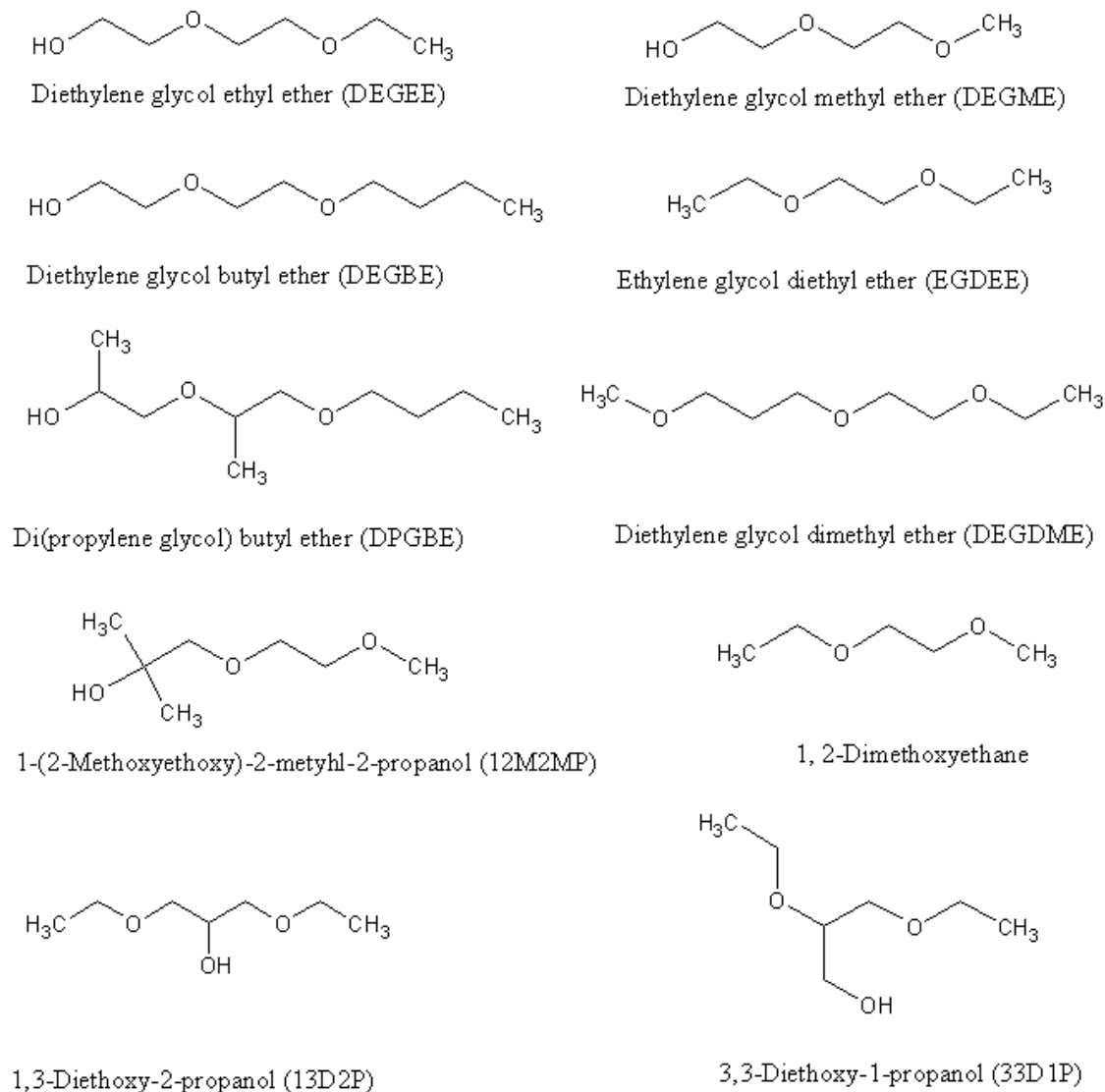


Figure 33: Molecular structure of ethers investigated

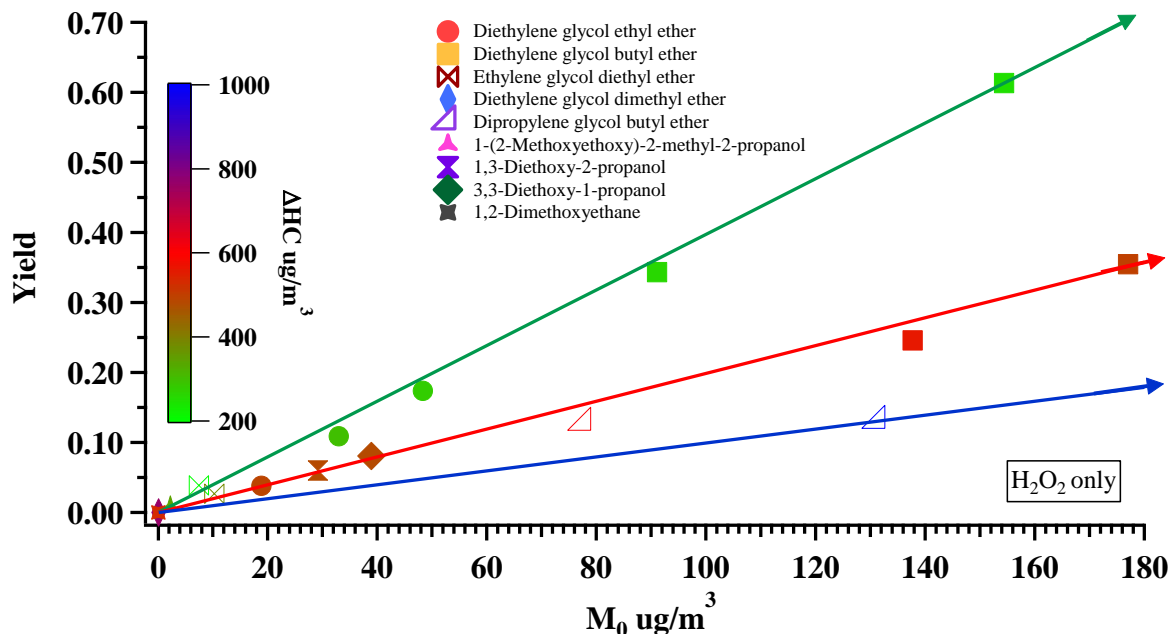


Figure 34: SOA yield from glycol ethers and related ethers in absence of NO_x. (Colored by the amount of ether (precursor) reacted to aid in visual comparison of which ethers on a per ether reacted basis is producing the greatest relative amount of SOA)

f. Individual LVP-VOC with NO and UV only

A subset of experiments was performed evaluating SOA formation and chemical composition (see Section III-6) where only the LVP-VOC and NO were present during UV irradiation. These experiments were designed to provide SOA formation and chemical composition data without the presence of other VOCs in the surrogate. These tests provide the simplest evaluation of SOA formation from individual LVP-VOCs performed following classical SOA environmental chamber procedures. Aerosol evolution for each of these experiments is provided in Figure 35. Without the presence of the surrogate mixture the atmospheric reactions did not proceed as far as seen in earlier experiments. This is due to the general lack of hydroxyl radical evolution/generation of the LVP-VOC itself. Further, progression of the experiment to a point where NO consumption is complete allowing for evolution of peroxy and hydroperoxy radicals is stunted with respect to experiments where the surrogate mixture simulates atmospheric reactivity. Therefore, only by the end of the experiment are conditions favoring SOA formation in the LVP-VOC/NO_x only experiment reached. Hence, measurable aerosol formation is only starting to commence and accelerate in the relative absence of NO at the end of the experiment. This is achieved much earlier with surrogate mixture present as shown earlier in the report (e.g., section a above). Further, due to the lower reactivity without the surrogate mixture, the amount precursor LVP-VOC consumed for the current LVP-VOC/NO_x experiments is less. The reactive conditions present for SOA formation under ambient conditions are expected to be much more similar to those when the surrogate was present.

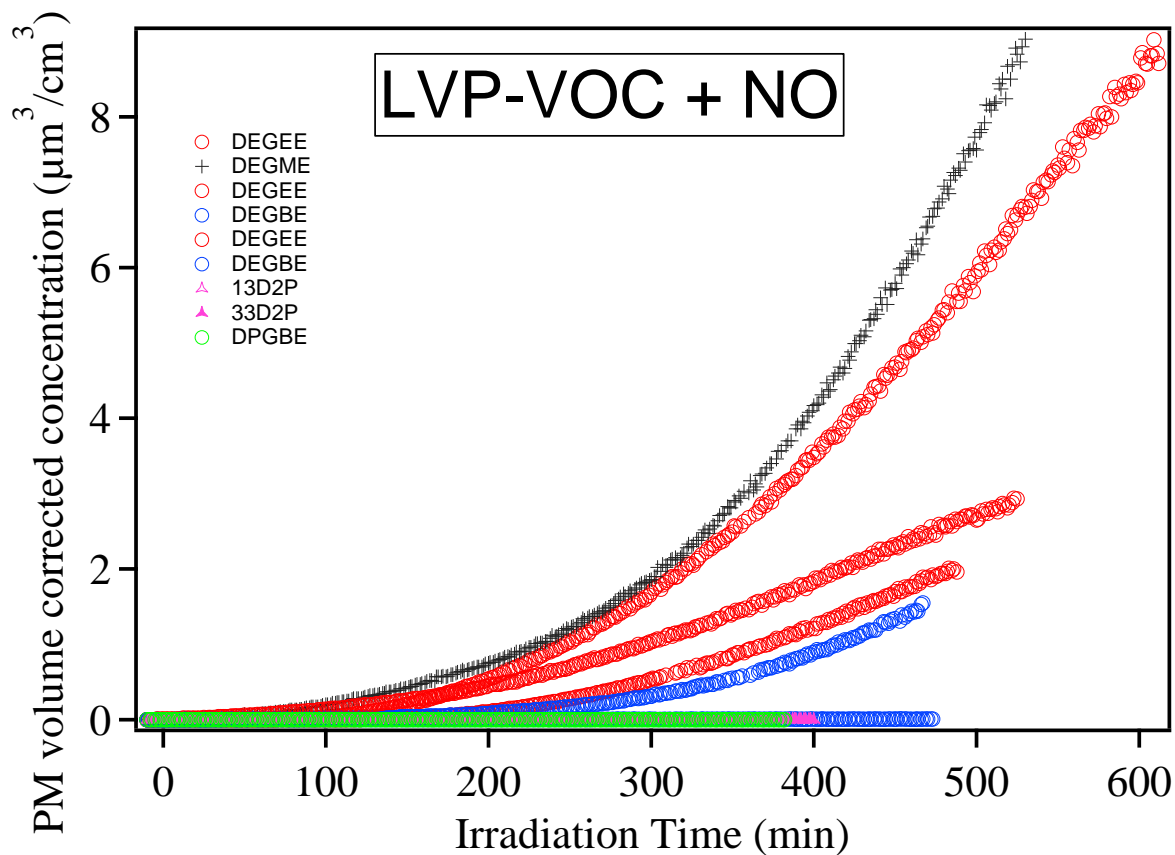


Figure 35: SOA formation from individual LVP-VOCs with NO

g. Individual LVP-VOC with H₂O₂ only

Additional environmental chamber experiments were performed on select LVP-VOC compounds to identify SOA chemical composition (see Section III-6) with only the hydroxyl radical present for oxidation of the single LVP-VOC. These experiments provide the cleanest signal of SOA formed from LVP-VOCs due to hydroxyl radical oxidation pathways. Figure 36 below summarizes the evolution of SOA for select LVP-VOCs in this study.

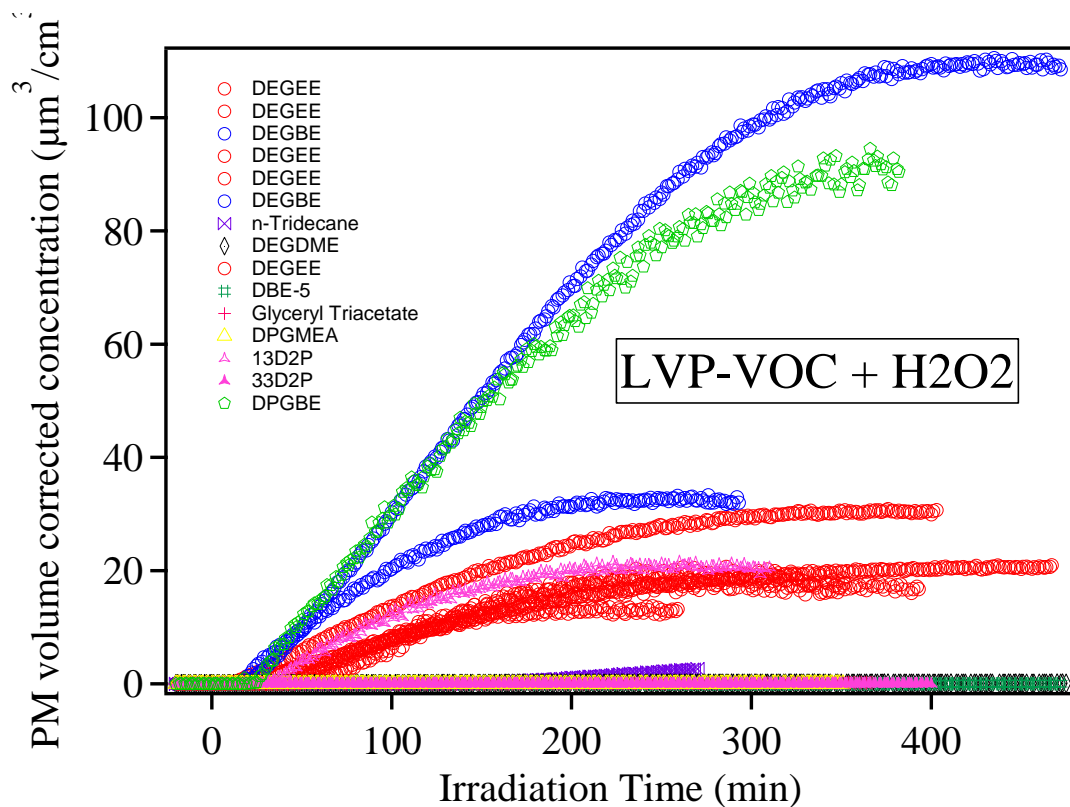


Figure 36: SOA formation from individual LVP-VOCs with H₂O₂

A comparison of the SOA formation from a select LVP-VOC (DEGEE) for the variety of SOA experiments discussed is provided in Figure 37. SOA formation was the highest for conditions that favored greater consumption of the LVP-VOC and enhanced the general rate of reactions that occurred. Therefore, the experiment where the surrogate mixture providing a baseline reactivity in the system with enhanced hydroxyl radical (H₂O₂ added) had the greatest SOA formation followed by the experiment with only enhanced hydroxyl radical and then the reaction with only the surrogate baseline reactivity without the hydroxyl radical enhancement. Experiments where the DEGEE had to provide its own reactivity without hydroxyl radical enhancements had considerably less SOA formation. SOA from surrogate mixtures with and without enhanced hydroxyl radical are shown for background comparison.

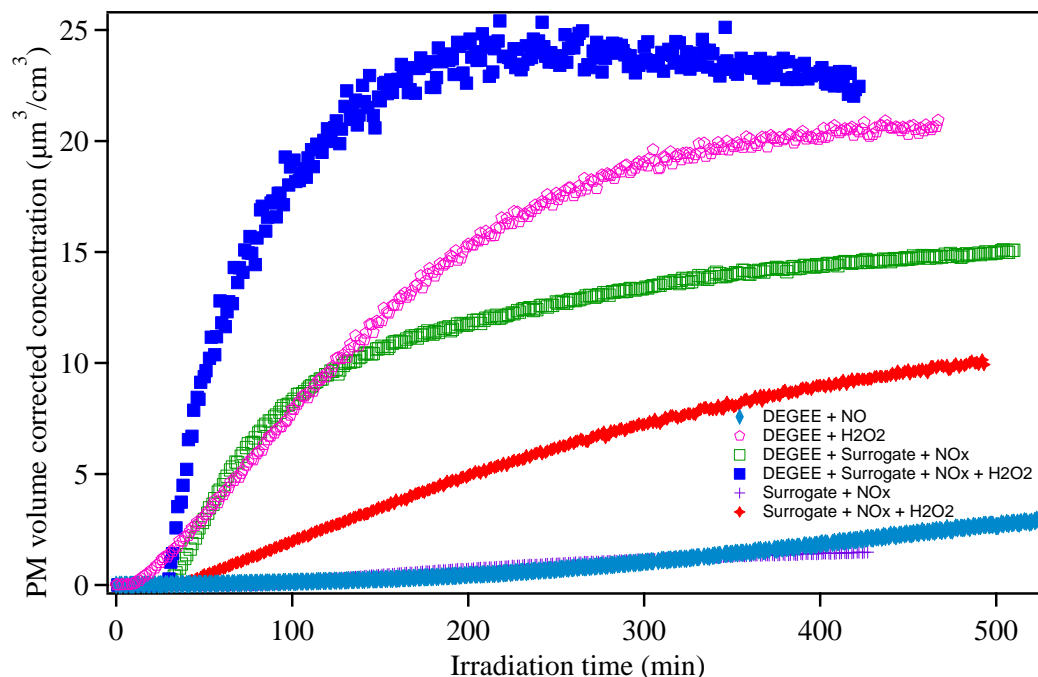


Figure 37: Comparison of SOA formation from DEGREE at different conditions

3. Consumer products

a. Ozone results

The five mixtures intended to mimic consumer products containing LVP-VOCs studied in the volatility experiment were also evaluated for ozone and SOA formation. Each product was injected as the mixture/consumer product and allowed to evaporate under a stream of nitrogen in gentle heat. Simulated products included paint stripper, caulk remover, laundry detergent, hand lotion, and general purpose spray cleaner. Caulk remover was investigated with and without water added to the caulk remover. Each consumer product was introduced to the surrogate mixture with ozone formation from each consumer product shown (Figure 38). Only the laundry detergent (contains 15% propylene glycol) measurably influenced ozone formation with the laundry detergent increasing ozone formation. These trends are consistent with the impacts of the LVP-VOCs investigated as propylene glycol (major LVP-VOC component) also enhanced ozone formation in the surrogate mixture. Insufficient chemical reactivity information is available for the components of the complete laundry detergent simulant (Pareth 25-9 and fatty coconut oil) to model completely the ozone formation of the laundry detergent plus surrogate mixture. Propylene glycol (laundry detergent component) in the individual experiments also forced ozone formation in the surrogate mixture upward, while DBE-5 and DEGBE (components of other consumer products studied) had little impact as individual LVP-VOCs on ozone formation. Ozone formation from caulk remover with water formed a little bit more ozone than that without water. The water is not expected to have a significant effect on the gas-phase oxidation chemistry as the water will dissociate from the LVP-VOCs in caulk remover upon evaporation in to the chamber. The total water added to the chamber is only sufficient to raise relative humidity (RH) by 0.007%, which is not expected to have any impact on ozone formation. The small difference in ozone is attributed to the slightly different (~10%) amounts of NO_x present in the two experiments due to experiment to experiment variation in NO_x injections.

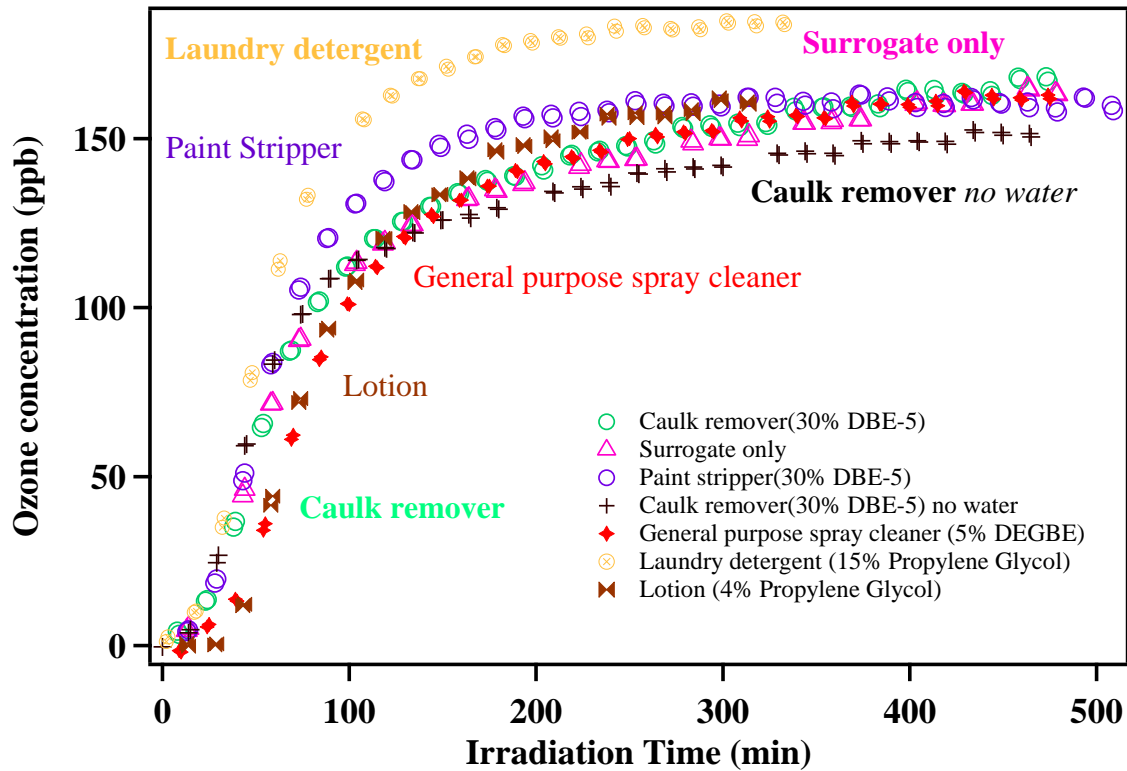


Figure 38: Ozone formation trends for each consumer product injected into surrogate mixture.

Select consumer products were also evaluated for ozone formation with increased H_2O_2 (Figure 39). Hand lotion was found to elevate ozone produced by the surrogate mixture while laundry detergent was found to have little effect with added H_2O_2 . It is important to note that the hand lotion and laundry detergent were extremely difficult to inject into the chamber due to their overall low volatility, which may have impacted some of the results for ozone formation from those consumer products as not all of the consumer product may have reached the environmental chamber. When deviations from the ozone formation of the surrogate were observed, the increase is consistent with that seen individually for propylene glycol.

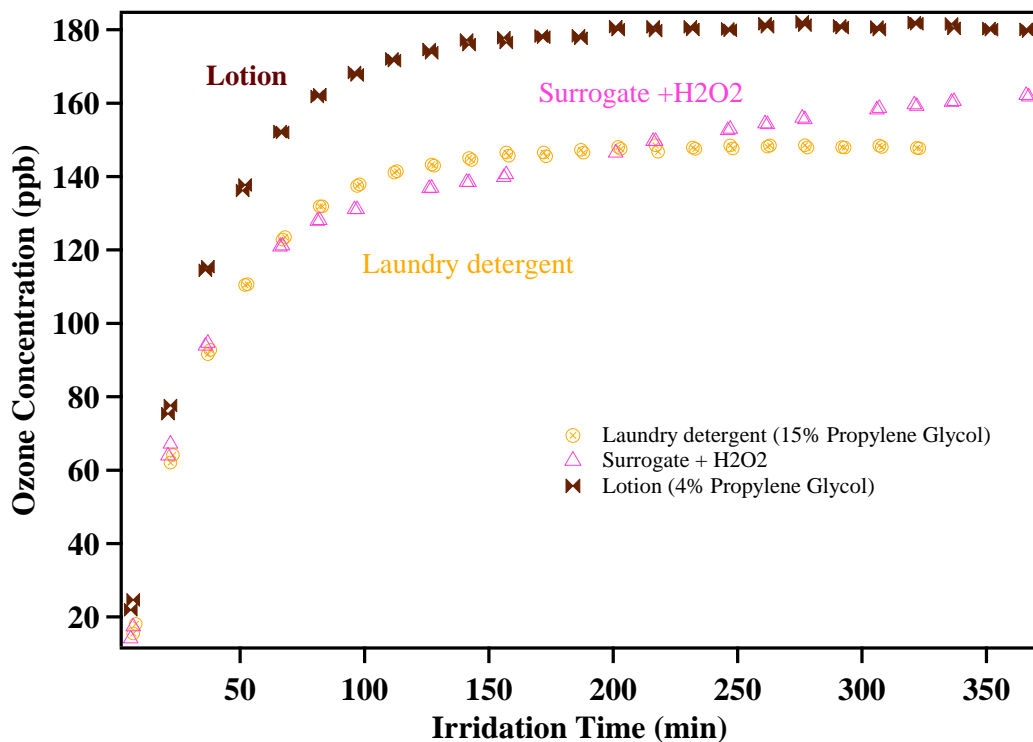


Figure 39: Ozone formation from consumer products in surrogate mixture with enhanced H₂O₂.

b. SOA results

The particle formation for the consumer products was also investigated within the environmental chamber (Figure 40). Laundry detergent, spray cleaner, and paint stripper (from most to least) each formed appreciable amounts of SOA compared to the surrogate while the hand lotion and caulk remover (with or without water) formed minimal amounts of SOA compared to the surrogate only experiments. SOA formation exceeded that of the individual LVP-VOC (Figure 25) indicating that there were other SOA forming components of these three consumer products in addition to the LVP-VOC precursors investigated in this work. In particular, the laundry detergent main LVP-VOC component was propylene glycol, which was observed individually to have little SOA formation.

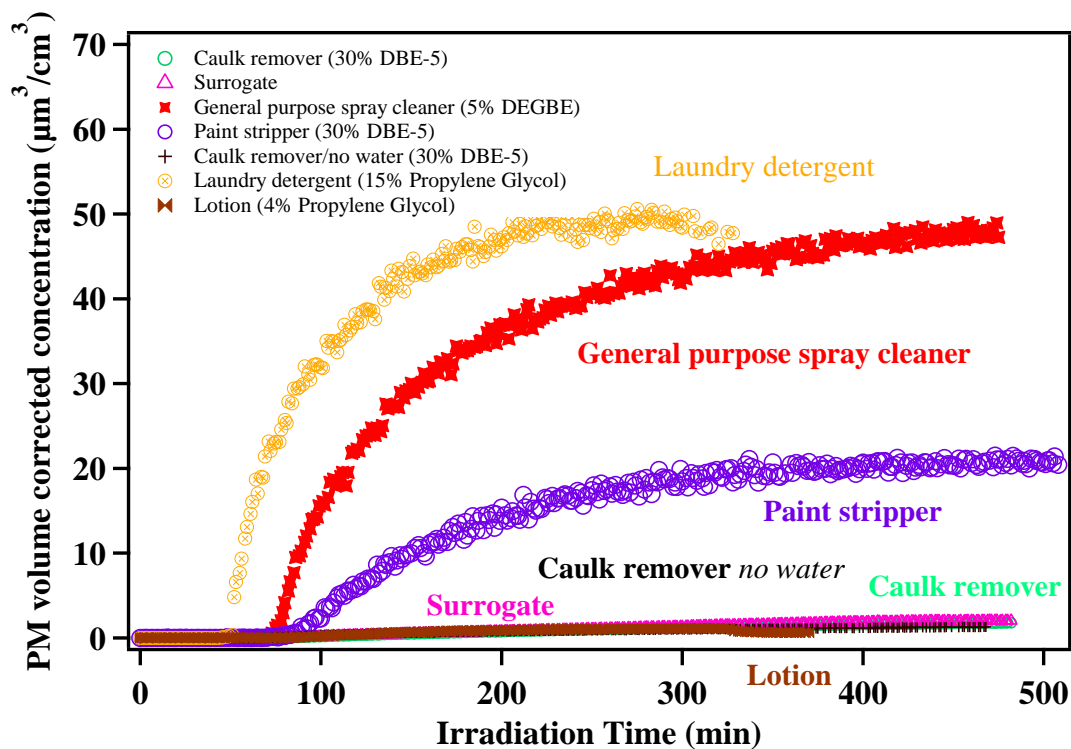


Figure 40: Aerosol volume formation for consumer products corrected for wall loss.

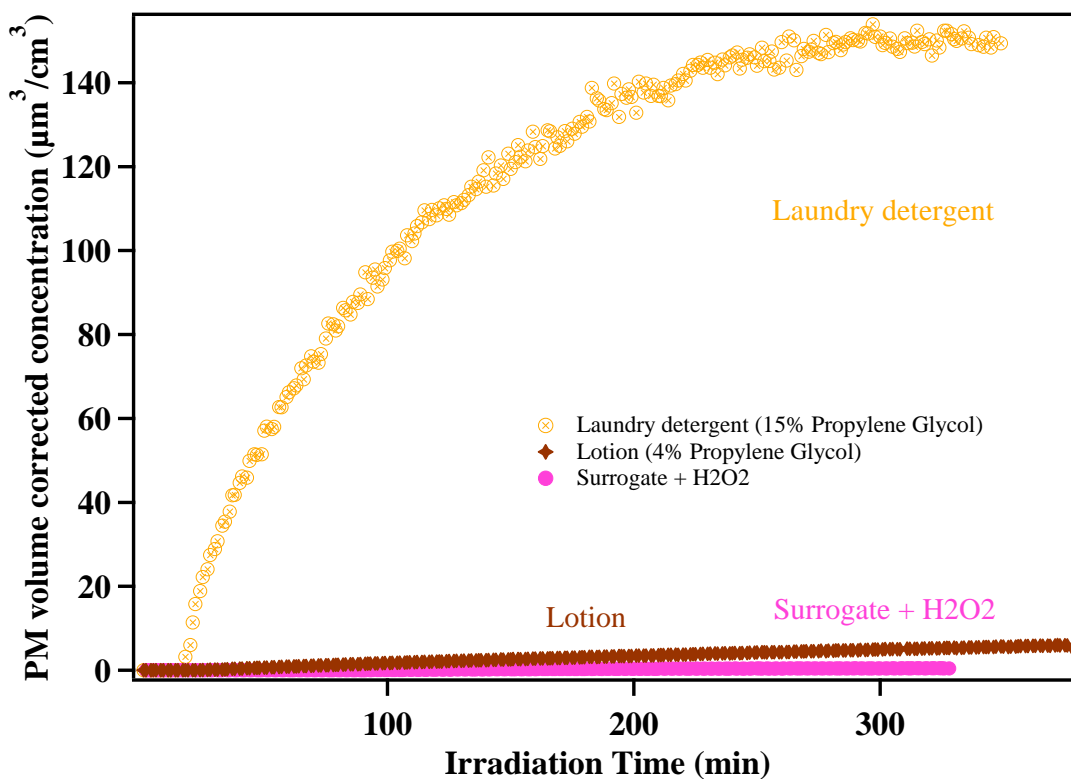


Figure 41: PM volume formation from consumer products in surrogate mixture with H_2O_2 added.

Two consumer products (laundry detergent and caulk remover) were studied in the presence of the surrogate mixture with enhanced H_2O_2 (Figure 41). The hand lotion still produced little SOA while the laundry detergent SOA formation was enhanced. The SOA enhancement for laundry detergent is consistent with enhancements seen for individual LVP-VOCs in Section III-3c above (however, SOA formation much greater than anticipated from propylene glycol). As stated in Section III-4a, the hand lotion was difficult to inject, which may have led to lower SOA formation than expected from the mixture.

Finally, Figure 42 shows the reproducibility of the consumer product experiments for ozone and PM along with comparisons of ozone and SOA formation with and without added H_2O_2 .

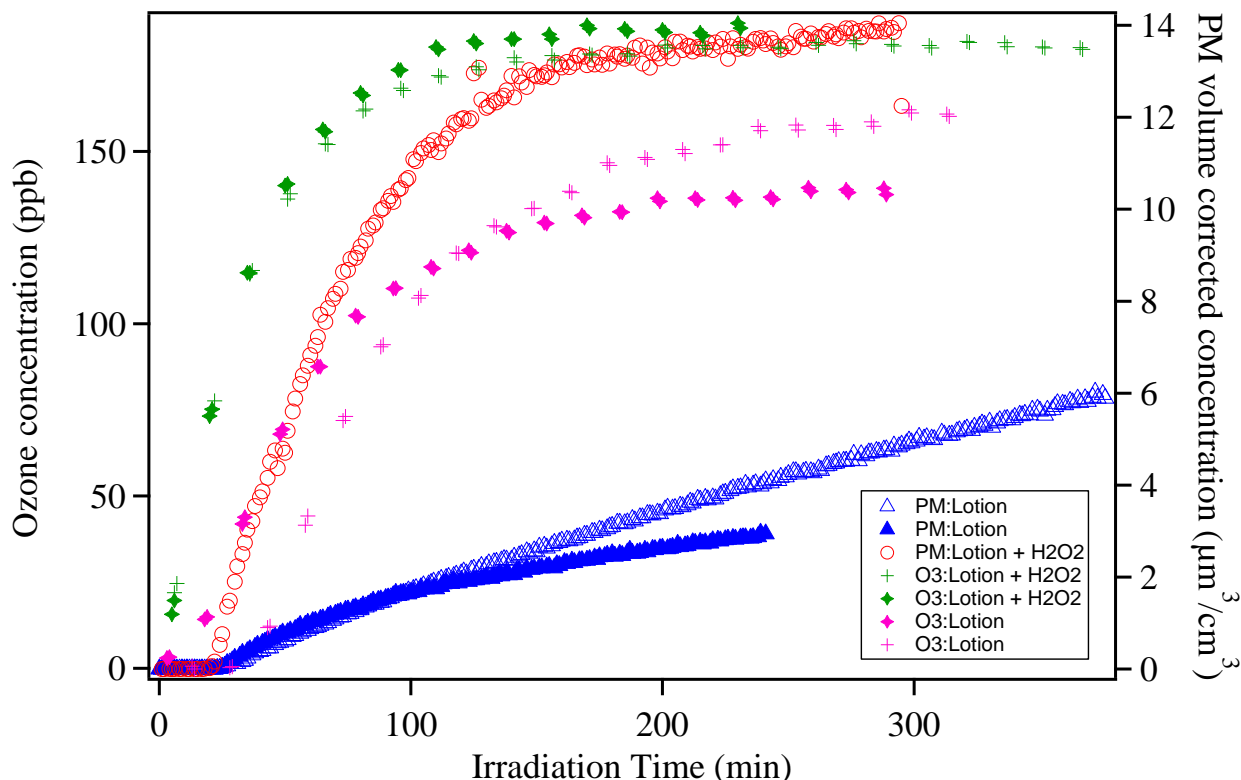


Figure 42: Ozone and aerosol formation from repeat experiments of hand lotion with and without added H_2O_2 .

c. Comparison with single compounds

Figure 43 compares the SOA formation between single LVP-VOCs and mixtures. General purpose spray cleaner contains DEGBE and more aerosols were formed in the general spray cleaner mixture than by DEGBE alone. Similarly, the laundry detergent mixture formed more aerosol than its LVP-VOC, propylene glycol. Both paint stripper and caulk remover contain DBE-5. However, DBE-5 aerosol behaved differently in the two different product mixtures. Paint stripper formed more aerosol than DBE-5 while caulk remover formed fewer aerosols than DBE-5. Clearly, the presence of chemicals other than the LVP-VOC in the consumer product also influences the reactivity and aerosol formation routes. For instance, the paint stripper contains 5% d-limonene, a known reactive compound individually capable of forming significant amounts of SOA (and ozone), which is expected to have an additive effect on the SOA formed from the individual LVP-VOC. The additive effect includes both increased reactivity of the LVP-VOC (more is consumed) as well as the additional SOA produced by the d-limonene itself. This

further leads to greater SOA formation as more SOA present increases the expected SOA yield of the compound through increased sorptive partitioning (see yield discussions above). Conversely, other ingredients in the caulk remover may be acting as a hydroxyl radical scavenger reducing the extent of LVP-VOC oxidation and thus SOA formation from the caulk remover compared to the individual compound itself.

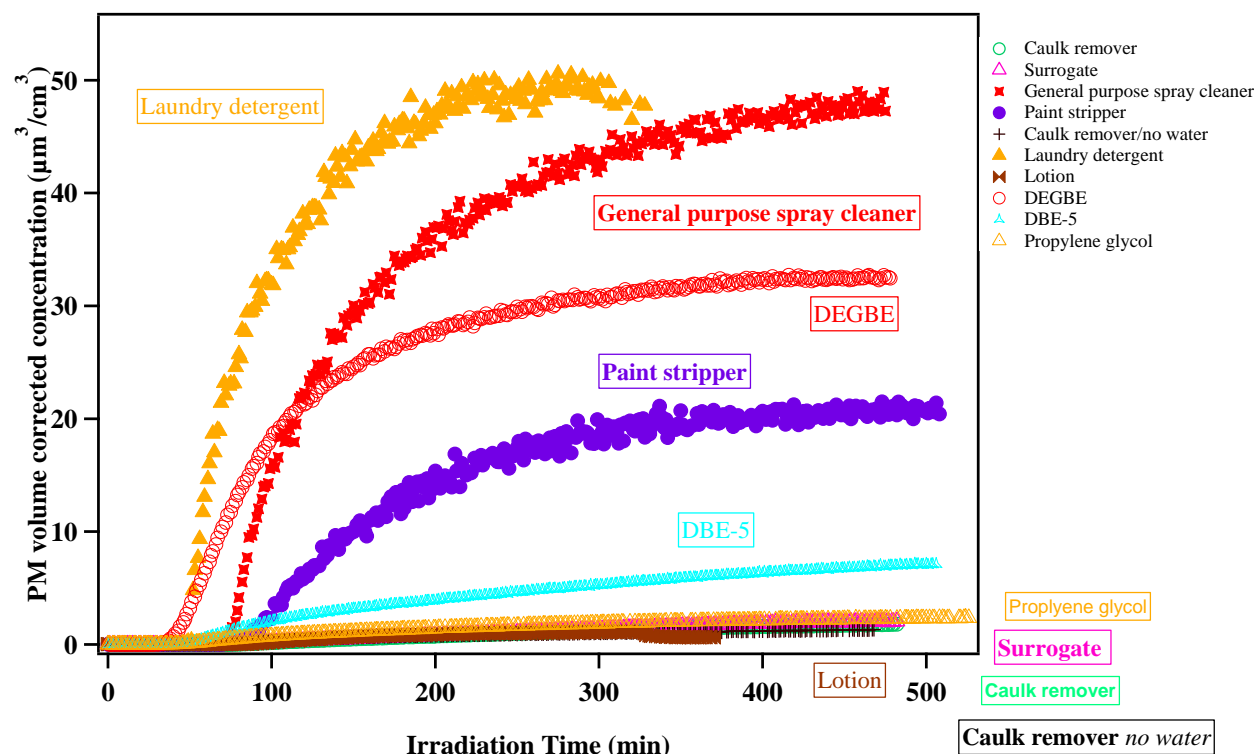


Figure 43: Comparison of SOA formation from single LVP-VOCs with that from mixtures in the presence of surrogate

4. Hydrocarbon solvent mixtures

a. Ozone formation

Three hydrocarbon solvents were identified by ARB staff for further evaluation of their ozone and SOA forming potentials. These were selected to replace glyceryl triacetate, methyl palmitate, and triethanol amine which were removed due to the extremely low evaporation rates observed for these three LVP-VOCs. The three hydrocarbon solvents selected were Isopar M (low-aromatic mixture of alkanes, iso-alkanes, and cycloalkanes), Conosol 200 (low-aromatic mixture of cycloparaffinic and isoparaffinic hydrocarbons), and Aromatic 200 (predominantly aromatic compounds, b.p. 230°C). C-200* refers to a custom mixture of C-70* and C-400* blended to create C-200* with appropriate viscosity and was used prior to obtaining C-200 (labelled in report as C-200**) from a major vendor. Ozone formation was suppressed by both Isopar M and Conosol 200 hydrocarbon solvents (as expected) due to the ability of the solvent mixture to reduce the reactivity by scavenging hydroxyl radicals (as expected from alkanes, e.g., see n-tridecane and n-heptadecane in this study) and therefore the ozone formation of the surrogate mixture (Figure 44). The Aromatic 200 ozone formation is not shown due to significant interference of the UV absorption of Aromatic 200 with that for ozone within the ozone analyzer. Variability between C-

200* and C-200** is attributed to variability in the composition due to the blending of C-70 and C-400 performed to simulate C-200 (C-200*) versus C-200 obtained directly from the manufacturer (C-200**).

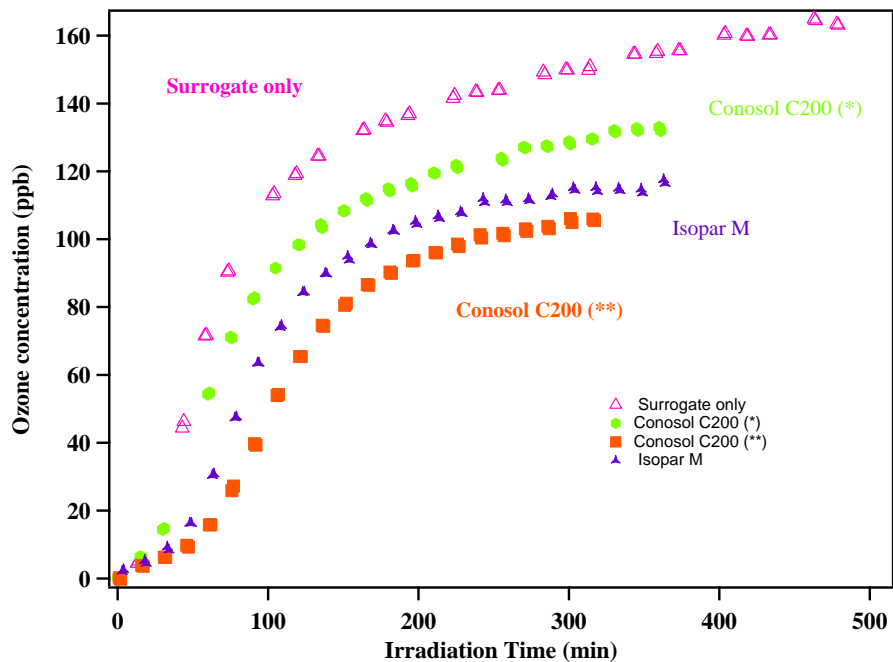


Figure 44: Ozone formation for solvent mixtures. Two Conosol C200 mixtures were investigated for ozone formation (local vendor (*) and large vendor (**)). Aromatic-200 is not shown due to interferences of the Aromatic 200 with the UV absorption of the ozone analyzer.

Similar to the individual LVP-VOCs, additional surrogate experiments were performed with added H_2O_2 to enhance the OH reactivity of the system and offset some of the losses of OH to the solvent mixtures. The ozone formation for these experiments is shown in Figure 45. Increases in ozone were observed with injection of H_2O_2 over injection without H_2O_2 . Differences between observed ozone for these experiments were also reduced over those without injected H_2O_2 .

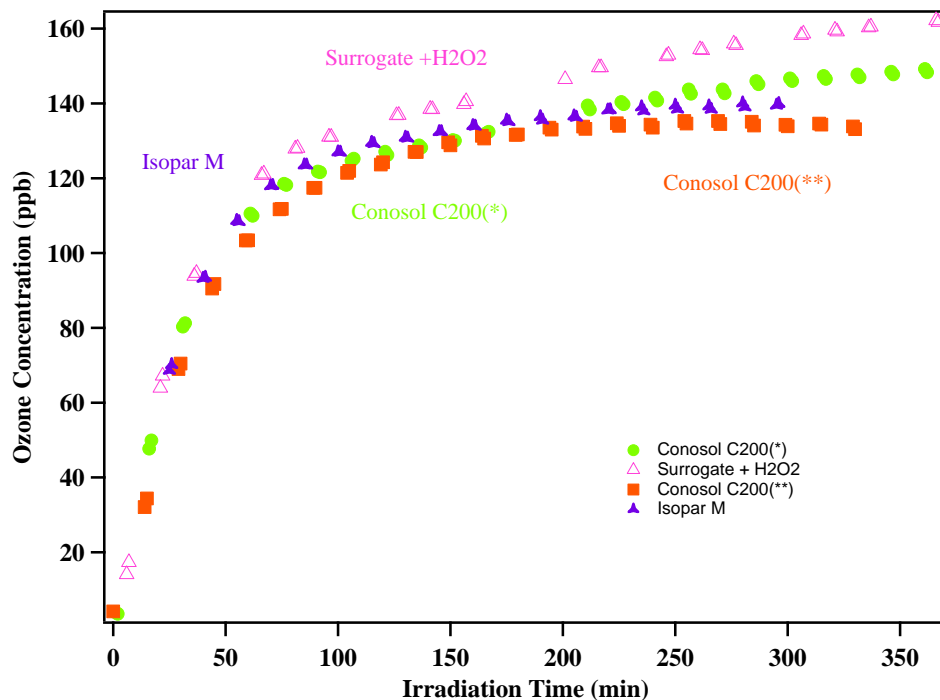


Figure 45: Ozone formation from surrogate with hydrocarbon solvent mixtures and H₂O₂ added.

b. SOA formation

The SOA formation from each hydrocarbon solvent mixture in the presence of the surrogate is provided in Figure 46. Significant aerosol formation is observed for all three solvent mixtures with Aromatic 200 greater than Conosol 200 which was greater than Isopar M. Aerosol yields are not provided as an accurate assessment of the hydrocarbon consumed for the mixtures is not available. Similar experiments with large alkanes n-C13 and n-C17 are seen to bracket the aerosol formation of the Conosol 200 and Isopar M and are provided as reference points. Differences in SOA formation between C-200* (blended from C-70 and C-400) and C-200** (obtained directly as C-200 from manufacturer) is attributed to compositional differences between the two blends.

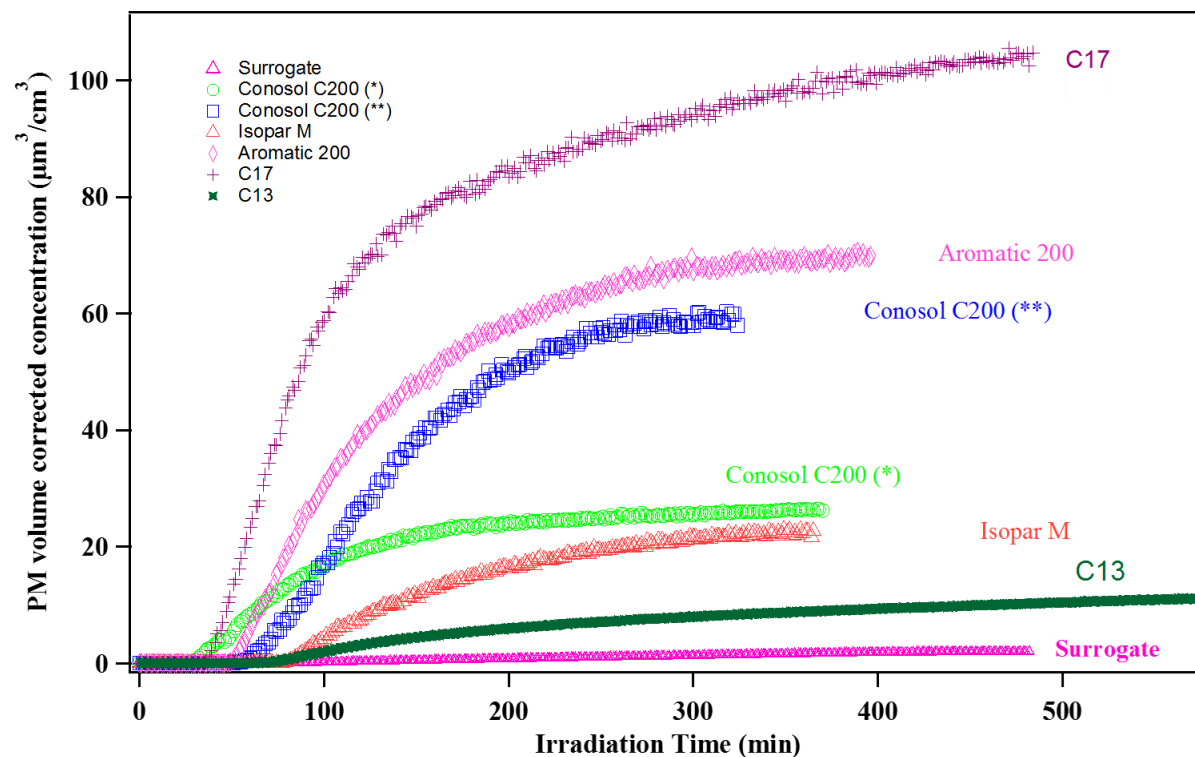


Figure 46: PM volume formation corrected for wall loss for solvent mixtures added to surrogate mixture

These experiments were then repeated with enhanced H_2O_2 (Figure 47). As seen for individual LVP-VOCs, the enhanced H_2O_2 increased the amount of aerosol formed, likely due to a combination of increased kinetics, increased radical oxidant concentrations, and the added increase in PM due to the fact that more PM was available to condense upon due to the first two reasons. The aerosol formation from the surrogate mixture itself is seen to be minimal compared to the aerosol production from the solvent mixtures. No aerosol yield information is calculated due to the absence of accurate measurements of total solvent consumption in the chamber experiments. However, even without hydrocarbon decay data, the aerosol formation on the order of $400 \mu m^3 cm^{-3}$ is far greater than the aerosol formation expected from pure monoaromatic (C6-C9) compounds (benzene, toluene, xylenes, trimethylbenzenes, ethyltoluenes, etc.). Monoaromatics are generally observed to have higher aerosol yields than for similarly sized alkanes due to the ring structure providing either stable aromaticity to retain ring structure and reduce fragmentation during oxidation or far greater sites for functionalization due to their highly unsaturated nature when the ring opens during oxidation. Individual n-heptadecane and n-tricane runs (with surrogate and H_2O_2) are also included in Figure 47 for comparison to the large alkane solvent mixtures Isopar M and Conosol 200.

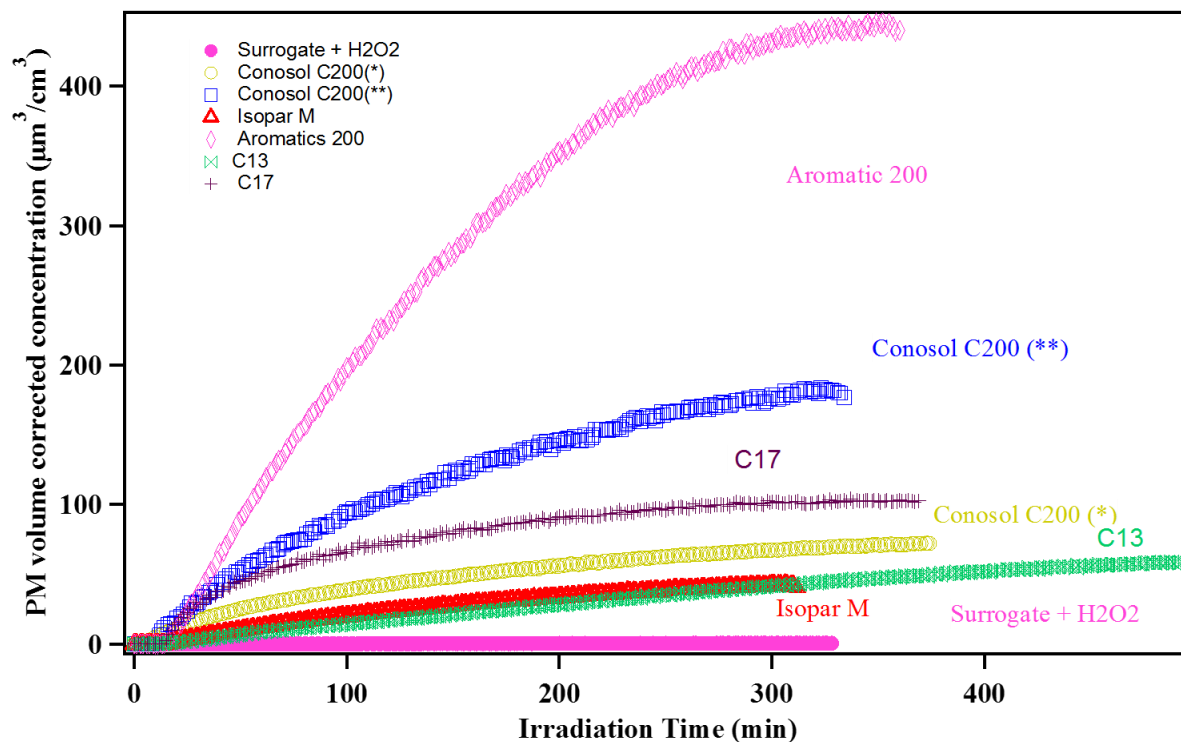


Figure 47: Aerosol formation for hydrocarbon solvent mixtures added to surrogate mixture with enhanced H_2O_2 .

c. Hydrocarbon solvent mixture experimental repeatability

The repeatability of the chamber experiments and hydrocarbon solvent mixtures was also explored. Two Aromatic 200 experiments are provided in Figure 48 below showing excellent reproducibility of the aerosol produced in the presence of the surrogate mixture with and without added H_2O_2 . Ozone and SOA formation from repeat experiments of Isopar M plus surrogate with and without H_2O_2 are shown in Figure 49. Ozone reactivity is seen to be quite similar even after addition of H_2O_2 to enhance hydroxyl reactivity while the aerosol forming potential of Isopar M increases nearly 10-fold. This is attributed to increased availability of hydroxyl radicals overcoming losses of hydroxyl radicals to the alkanes present in the Isopar M mixture. These results are very similar to those observed earlier for n-heptadecane and are significant in the fact that alkanes are generally not associated with significant SOA formation.

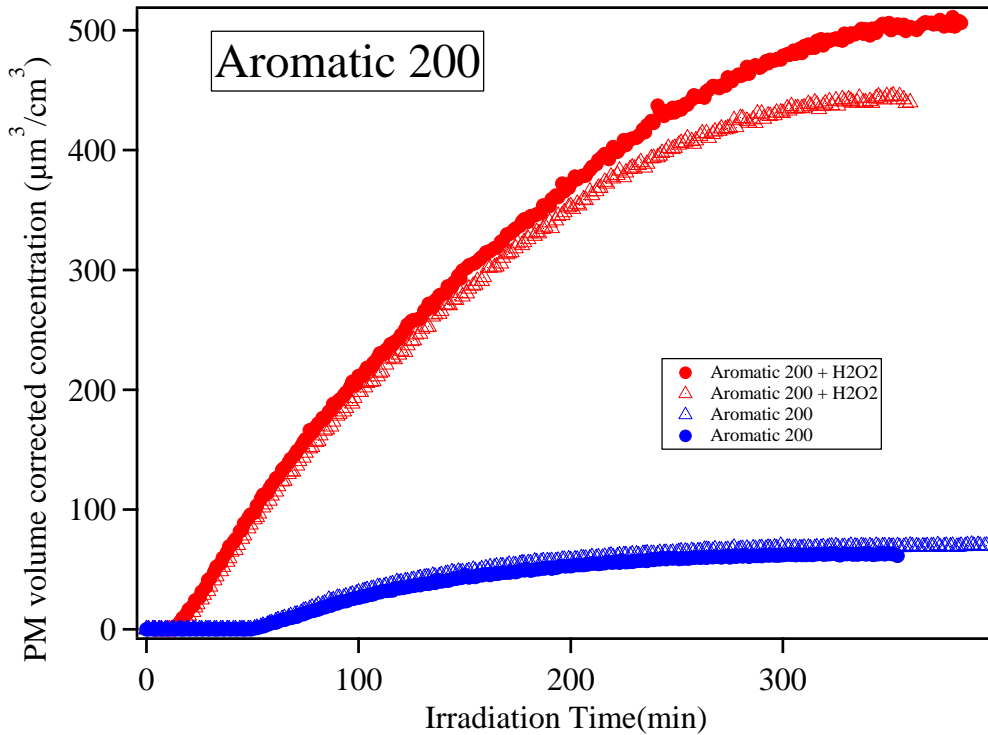


Figure 48: SOA formation from repeat Aromatic 200 solvent mixtures. Ozone is not shown as the aromatic content of the aromatic 200 interfered with the UV absorption of the ozone analyzer due to the conjugate double bonds.

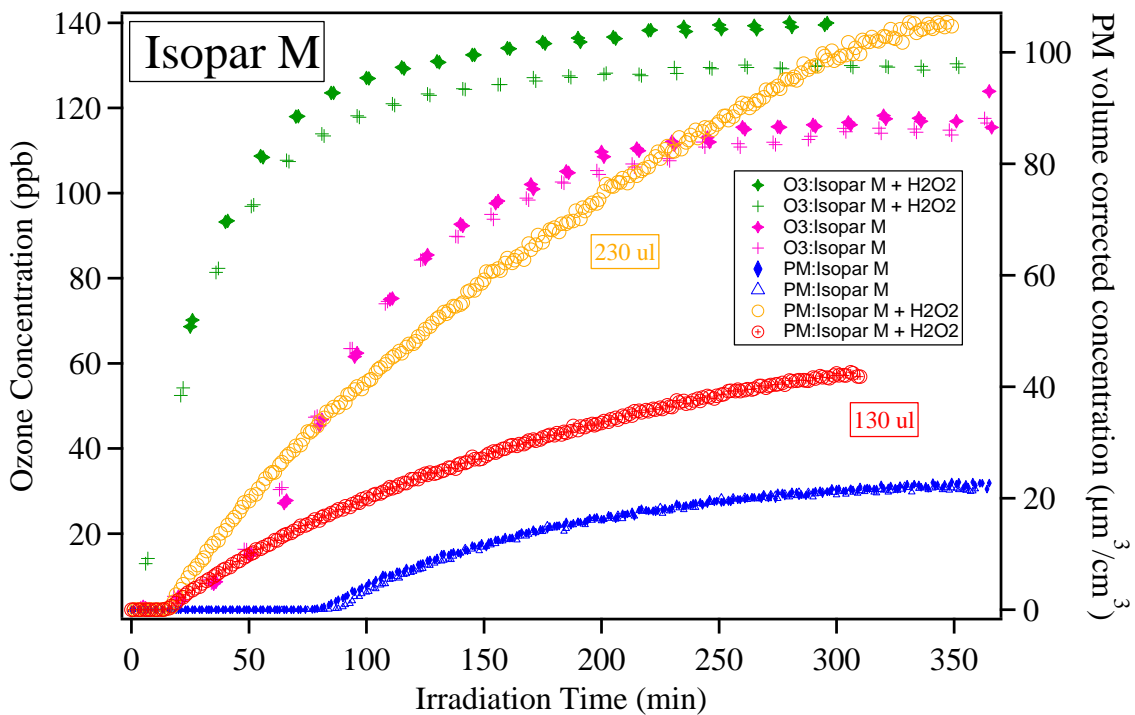


Figure 49: Ozone and SOA formation from repeat experiments of Isopar M plus surrogate with and without H₂O₂.

5. Overall ozone and SOA formation comparison

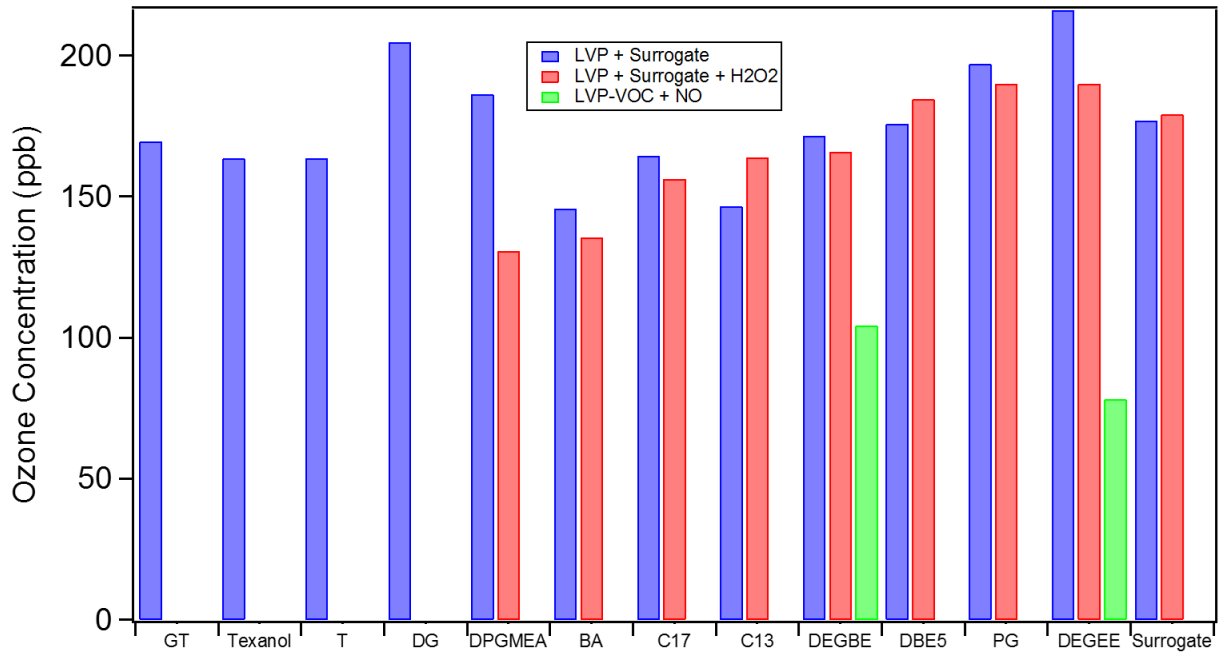
Figure 50 compares ozone formation from individual LVP-VOCs under different scenarios. The last column shows the ozone formation from surrogate only and surrogate with H₂O₂ experiments. Compared with surrogate only results, ozone formation was enhanced for DEGEE, Propylene Glycol, Diethylene Glycol, and DPGMEA. DBE-5 formed similar amount of ozone as the surrogate did. Compared with surrogate with H₂O₂ only results, ozone formation was enhanced for DEGEE, Propylene Glycol, and DBE-5. Figure 50 also illustrates that far more ozone was formed by adding surrogate than that formed by LVP-VOC plus NO only experiments. Glycerol triacetate did not form any additional observable ozone for the surrogate NO_x experiment; ozone formation from glycerol triacetate was not explored with enhanced H₂O₂ or without surrogate.

Figure 51 compares ozone formation from consumer products and hydrocarbon solvents under different scenarios. The last column shows the ozone formation from surrogate only and surrogate with H₂O₂ experiments. More ozone was formed from laundry detergent and caulk remover with water than that formed from surrogate only experiment. General purpose cleaner formed similar amount of ozone as the surrogate only experiment did.

As mentioned before, addition of select LVP-VOCs reduces the overall hydroxyl concentrations available to oxidize both the LVP-VOC and the ozone forming surrogate hydrocarbons relative to the amount of oxidation and ozone that forms in the surrogate photooxidation alone. An additional series of experiments with enhanced hydroxyl radical concentration was performed to offset losses in hydroxyl reactivity in the mixture due to the addition of the LVP-VOC. However, ozone formation was either enhanced or suppressed for both individual LVP-VOC and mixture experiments.

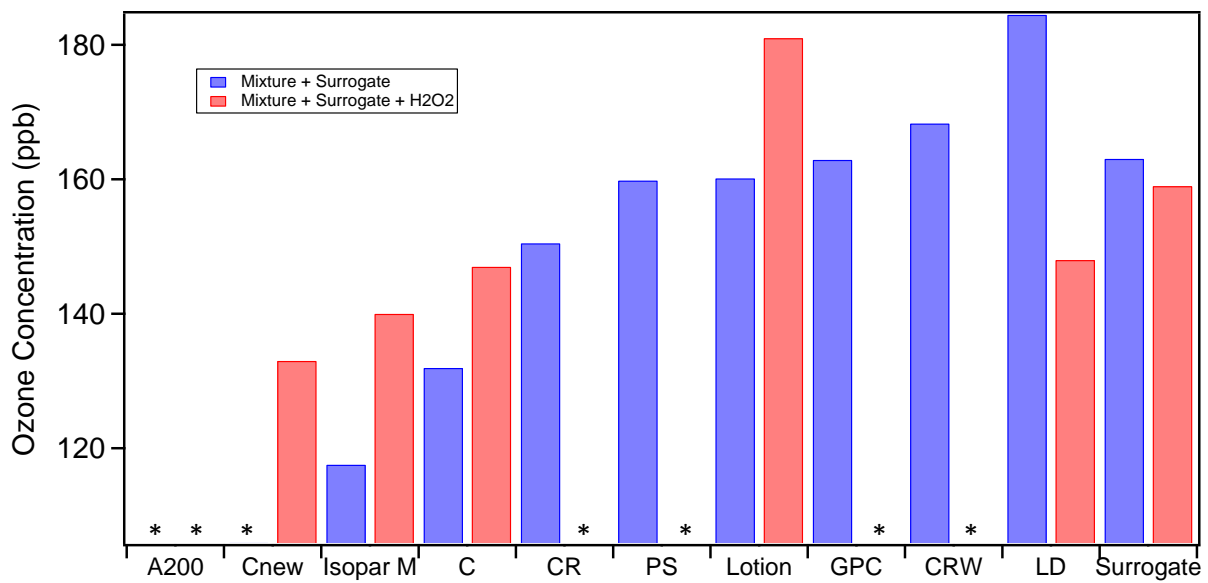
Figure 52 presents SOA formation from individual LVP-VOCs under different conditions. The last column shows the ozone formation from surrogate only and surrogate with H₂O₂ experiments. Generally speaking, addition of H₂O₂ greatly enhanced SOA formation except for n-Heptadecane and DBE-5. The possible reason for slightly lower SOA formation from those two LVP-VOCs with surrogate and H₂O₂ is less LVP-VOCs initial concentration due to injection difficulty. Compared with LVP plus NO experiment, the addition of surrogate enhanced SOA formation. However, compared with LVP plus H₂O₂ only experiment, SOA formation seemed to be suppressed due to the presence of surrogate and NO_x.

Figure 53 presents SOA formation from consumer products and hydrocarbon solvents under different scenarios. Caulk remover with and without water and lotion did not form observable SOA. Compared with surrogate only and surrogate with H₂O₂ experiment, much more SOA was formed due to the presence of LVP-VOCs including paint stripper, Isopar M, Conosol C200*, Conosol C200**, general purpose cleaner, laundry detergent, and Aromatic 200. Lastly, the addition of H₂O₂ greatly enhanced SOA formation.



GT: Glycerol Triacetate
 DG: Diethylene Glycol
 DPGMEA: Dipropylene Glycol Methyl Ether Acetate
 BA: Benzyl Alcohol
 C17: n-Heptadecane
 C13: n-Tridecane
 DEGBE: Diethylene Glycol Monobutyl Ether
 DBE5: Dimethyl Glutarate
 PG: Propylene Glycol
 DEGEE: Diethylene Glycol Ethyl Ether
 T: Triethanolamine

Figure 50: Comparison of ozone formation from individual LVP-VOCs under different scenarios.



CRW: Caulk remover with water

CR: Caulk remover
 PS: Paint striper
 GPC: General purpose cleaner
 LD: Laundry detergent
 C: Conosol C200(*)
 Cnew: Conosol C200(**)
 A200: Aromatic 200
 *: No experiment

Figure 51: Comparison of ozone formation from consumer products and hydrocarbon solvents under different scenarios.

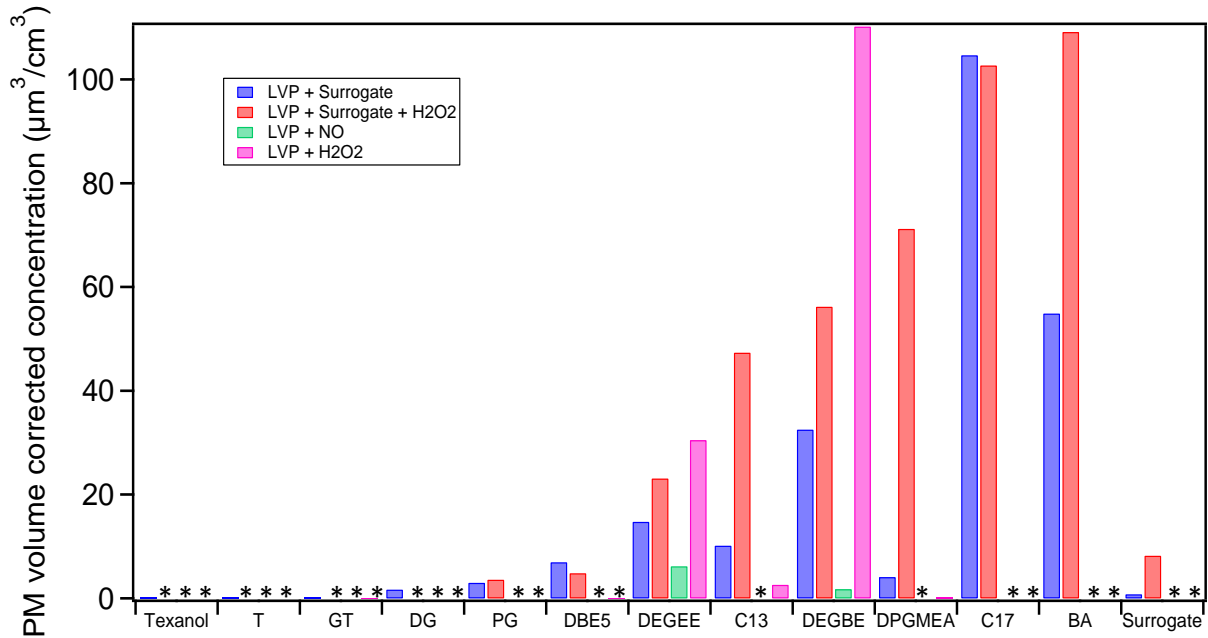


Figure 52: Comparison of SOA formation from individual LVP-VOCs under different scenarios. (*: No experiment)

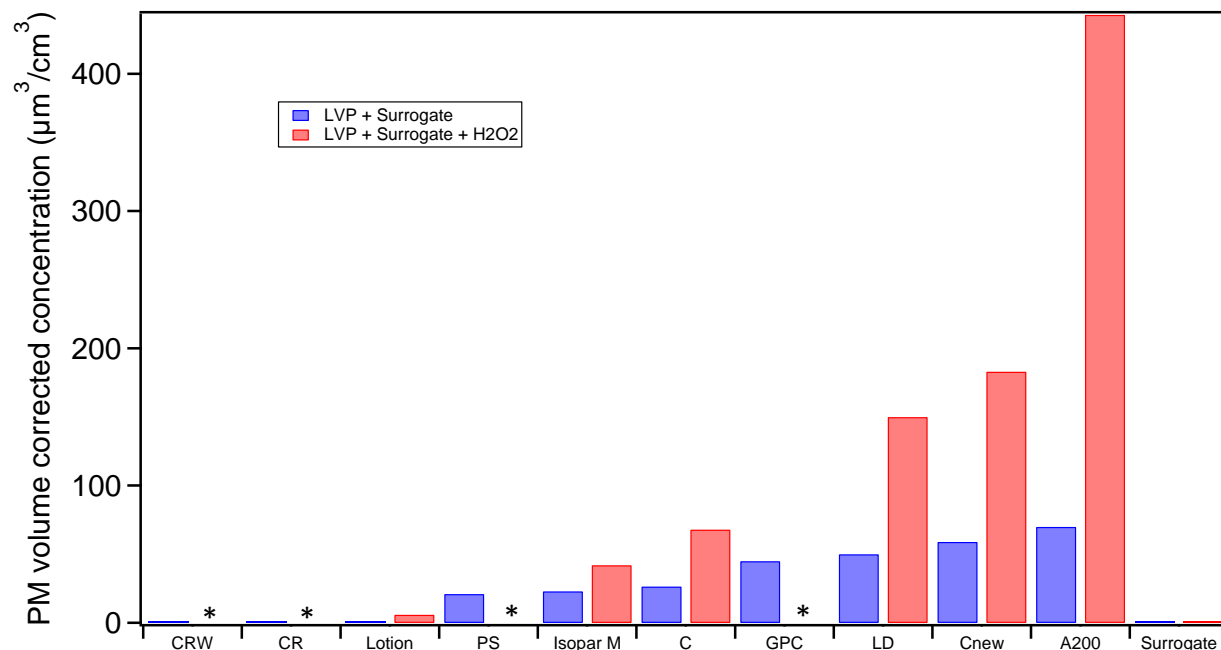


Figure 53: Comparison of SOA formation from consumer products and hydrocarbon solvents under different scenarios. (*: No experiment)

6. Chemical composition characteristics of SOA formation

a. Volume fraction remaining (VFR)

Many organics present in secondary organic aerosol particles are semi-volatile, which means that they can actively partition between the gas and aerosol phase. The more volatile the aerosol, the more likely it will be affected by changes in ambient temperature. The Volume Fraction Remaining (VFR_T) is used to study aerosol volatility. VFR was defined as $VFR_T = (D_T/D_{Ref})^3$ assuming spherical particles. D_{Ref} is the initial particle mode diameter determined at reference temperature (298 K). D_T is the final particle mode diameter after evaporation at 100°C. Information on the aerosol volatility also gives indirect indications of the aerosol composition and provides insights on the vapor pressure of the condensable species. Increasing VFR implies a less volatile aerosol particle. (Emanuelsson, et al. 2013). Final VFR , the VFR measured at the end of an experiment, is summarized in Table 15. Final VFR typically ranged between 0.2 – 0.7, indicating that the SOA formed in the experiments were semi-volatile with 30 – 80% of the aerosol returning to the gas-phase at temperatures of 100°C. Alternatively, this indicates that a significant fraction of the aerosol is available for repartitioning to the gas-phase as the aerosol is diluted in the atmosphere. No correlations are noted between the VFR of the SOA and the starting vapor pressure of the LVP-VOC.

b. Average oxidation state of carbon (OSc)

The oxidation of organic species in the atmosphere is important to several key environmental chemical processes that directly influence human health and global climate. These include the degradation of pollutants, the production of toxic species such as O_3 , and the formation of SOA. The average

oxidation state of carbon is an ideal metric for the degree of oxidation of organic species in the atmosphere, and regarded as a key quantity to describe mixtures of organic aerosol (Kroll, et al. 2011). The OSc increases upon oxidation. The simplified equation that defines OSc is described in the following:

$$\overline{OS}_c = 2O/C - H/C \quad \text{Eq. 5}$$

The O/C and H/C in the SOA are measured using the high resolution aerosol mass spectrometer described in the experimental section above. The SOA OSc from the experiments is summarized in Table 15. While the OSc cannot be used to determine the chemical mechanisms leading to the SOA formation, it does provide insight into the extent of functionalization (e.g., addition of OH, =O, etc.) leading to the SOA formation. The greater the functionalization, the lower the expected vapor pressure (per number of carbon) of the SOA. The OSc of ambient air is a combination of both primary organic aerosol and secondary organic aerosol and is therefore not readily compared to the OSc measured from individual LVP-VOCs. OSc is summarized in Table 15 for the experiments performed.

c. SOA density

The density of the SOA is also reported for each experiment. The density can be used to convert volumetric aerosol formation into aerosol mass concentration ($\mu\text{g m}^{-3}$) by multiplying the volumetric concentration ($\mu\text{m}^3 \text{cm}^{-3}$) by the density (g cm^{-3}). The measured average densities (end of experiment) are summarized in Table 15.

Table 14: SOA characteristics

Run ID	Compound	Average Density	O/C Initial	O/C Final	H/C Initial	H/C Final	VFR Final	\overline{OS}_c
<i>Individual LVP-VOC + NO_x + Surrogate</i>								
EPA1851	Propylene Glycol	1.91	-	-	-	-	0.39	-
EPA1877	Propylene Glycol	1.53	-	-	-	-	0.37	-
EPA1882	Propylene Glycol	1.49	-	-	-	-	0.45	-
EPA1883	Diethylene Glycol	1.54	-	-	-	-	0.44	-
EPA1886	DEGEE	1.52	-	-	-	-	0.34	-
EPA1887	Diethylene Glycol	1.52	-	-	-	-	0.4	-
EPA1888	Propylene Glycol	1.57	-	-	-	-	0.3	-
EPA1891	DEGBE	1.47	-	-	-	-	0.42	-
EPA1892	n-Tridecane	1.32	-	-	-	-	0.41	-
EPA1893	Triethanolamine	1.5	-	-	-	-	0.41	-
EPA1894	Surrogate only	1.37	-	-	-	-	0.44	-
EPA1910	n-Heptadecane	0.99	-	-	-	-	0.3	-
EPA1911	DBE-5	1.37	-	-	-	-	0.36	-
EPA1912	Triethanolamine	-	0.27	0.31	1.83	1.77	0.63	-1.16
EPA1914	Methyl palmitate	-	0.14	0.14	1.71	1.71	0.30	-1.43
EPA1922	DEGEE	1.30	-	-	-	-	0.28	-
EPA1974	DEGEE	1.39	0.27	0.5	1.69	1.75	0.61	-0.75
EPA1987	Benzyl Alcohol	1.51	0.57	0.64	1.46	1.21	0.71	0.07
EPA2023	DPGMEA	1.4	0.33	0.24	1.68	1.3	-	-0.82

EPA2024	Texanol	1.37	0.09	0.32	2.42	1.69	-	-1.05
EPA2025	Glyceryl Triacetate	1.41	0.72	0.63	1.3	1.37	-	-0.11
EPA2172	n-Heptadecane	-	0.28	0.26	1.59	1.67	-	-1.15
Individual LVP-VOC + NO								
EPA1923(B)	DEGEE	1.4	-	-	-	-	-	-
EPA1925	DEGME	1.56	0.18	0.64	1.61	1.61	0.37	-0.33
EPA1926	DEGBE	1.40	-	-	-	-	0.70	-
EPA1985	DEGEE	1.39	-	-	-	-	0.71	-
EPA1986	DEGBE	1.32	-	-	-	-	0.80	-
EPA1993	DEGEE	1.34	0.39	0.60	1.86	1.82	-	-0.61
EPA2048(B)	DEGBE	1.4	-	-	-	-	-	-
EPA2051	DEGBE	-	0.37	0.45	1.39	1.76	-	-0.86
EPA2055	DPGBE	-	2.54	2.58	0.37	0.36	-	4.80
EPA2056	DPGBE	-	0.96	0.87	1.29	1.38	-	0.37
EPA2123(B)	1,3-Diethoxy-2-propanol	1.4	-	-	-	-	-	-
EPA2124(B)	1,3-Diethoxy-2-propanol	1.4	-	-	-	-	-	-
EPA2152(B)	DPGBE	1.4	-	-	-	-	-	-
EPA2154(B)	DEGEE	1.4	-	-	-	-	-	-
Individual LVP-VOC + H₂O₂								
EPA1991	DEGEE	1.58	0.66	0.69	1.77	1.67	-	-0.28
EPA1999	DEGBE	1.43	0.43	0.50	1.81	1.74	-	-0.74
EPA2007	EDGEE	1.51	0.51	0.67	1.64	1.66	-	-0.31
EPA2048	DEGDME	1.40	0.06	0.11	2.35	2.10	-	-1.88
EPA2058	DEGEE	1.43	0.28	0.53	1.93	1.83	-	-0.78
EPA2063	DEGBE	1.28	0.41	0.53	1.74	1.74	-	-0.68
EPA2123	1,3-Diethoxy-2-propanol	1.40	0.51	0.62	1.55	1.65	-	-0.42
EPA2124	3,3-Diethoxy-2-propanol	1.36	0.43	0.68	1.51	1.60	-	-0.23
EPA2152	DPGBE	-	-	-	-	-	-	-
EPA2154	DEGEE	-	-	-	-	-	-	-
Individual LVP-VOC + NO + H₂O₂								
EPA2059	DEGEE	1.35	0.43	0.78	1.87	1.73	-	-0.18
Individual LVP-VOC + NO_x + Surrogate + H₂O₂								
EPA1988	n-Tridecane	1.22	0.21	0.2	1.64	1.66	-	-1.26
EPA2006	Benzyl Alcohol	1.5	0.48	0.59	1.28	1.24	-	-0.06
EPA2027	DBE-5	1.47	1.15	2.5	2.23	1.77	-	3.23
EPA2028	Propylene Glycol	1.47	0.6	0.55	1.42	1.46	-	-0.36
EPA2029	DEGEE	1.4	1.43	1.16	2.46	1.93	-	0.39
EPA2030	DEGBE	1.29	0.68	0.83	2.11	1.92	-	-0.26
EPA2033	DEGEE	1.55	0.2	0.3	1.83	1.81	-	-1.21
EPA2104	n-Heptadecane	1.48	0.31	0.53	1.71	1.44	0.25	-0.39
EPA2173	n-Heptadecane	1.07	0.15	0.23	1.74	1.71	0.22	-1.25
EPA2174	DPGMEA	1.1	0.31	0.17	1.76	1.8	-	-1.46
EPA2243	n-Heptadecane	-	-	-	-	-	-	-

<i>Mixture containing LVP-VOC + NO_x + Surrogate</i>								
EPA2093	Caulk Remover mixture containing DBE-5	1.44	0.2	0.22	2.51	1.35	-	-0.91
EPA2094	Paint Stripper mixture containing DBE-5	1.35	0.44	0.45	1.73	1.51	-	-0.61
EPA2095	General Purpose Spray Cleaner mixture containing DEGBE	1.43	0.15	0.48	2.07	1.65	-	-0.69
EPA2098	Caulk Remover mixture containing DBE-5	-	0.55	0.5	1.52	1.51	-	-0.51
EPA2175	Laundry Detergent	-	0.17	0.25	1.87	1.75	0.04	-1.25
EPA2193	Hand Lotion	1.26	0.38	0.42	1.76	1.59	0.32	-0.75
EPA2194	Hand Lotion	1.23	0.24	0.37	1.69	1.53	-	-0.79
<i>Mixture containing LVP-VOC + NO_x + Surrogate + H₂O₂</i>								
EPA2176	Laundry Detergent	1.36	0.03	0.2	1.96	1.82	-	-1.42
EPA2195	Hand Lotion	N/A	0.54	0.52	1.51	1.48	-	-0.44
EPA2196	Hand Lotion	1.37	0.31	0.48	1.66	1.56	0.27	-0.60
<i>Individual LVP-VOC + Seed+ H₂O₂</i>								
EPA2033	DEGEE	1.55	0.20	0.30	1.83	1.81	-	-1.21
EPA2034	DEGEE	1.54	1.14	1.28	2.33	2.14	-	0.42
EPA2035	DEGBE	1.47	0.66	0.53	1.63	1.73	-	-0.67
EPA2036	DEGEE	1.51	0.69	0.76	1.69	1.62	-	-0.10
EPA2041	DEGEE	1.57	0.62	0.66	1.87	1.63	-	-0.31
EPA2042	n-Tridecane	1.37	0.3	0.19	1.59	1.73	-	-1.35
EPA2096	DBE-5	1.13	0.13	0.18	1.81	1.72	0.12	-1.35
EPA2097	Glyceryl Triacetate	-	0.25	0.27	1.70	1.63	-	-1.08
EPA2099	DBE-5	1.54	0.30	0.31	1.69	1.77	-	-1.16
EPA2100	DPGMEA	1.40	-	-	-	-	-	-
EPA2103	DPGMEA	1.43	-	-	-	-	-	-
<i>Individual LVP-VOC + Seed+ no + H₂O₂</i>								
EPA2101	DBE-5	1.34	-	-	-	-	0.25	-
EPA2102	Glyceryl Triacetate	1.37	0.32	0.50	1.40	1.38	0.30	-0.39
EPA2177	DPGMEA	1.14	0.26	0.23	1.78	1.32	0.14	-0.86
EPA2178	Glyceryl Triacetate	1.15	0.18	0.19	1.68	1.7	0.14	-1.32
EPA2179	DBE-5	1.15	0.19	0.24	1.77	1.68	0.14	-1.20
<i>Hydrocarbon Solvents + NO_x + Surrogate</i>								
EPA2180	Conosol C-200 *	1.18	0.18	0.26	1.77	1.64	0.32	-1.12
EPA2181	Conosol C-200 **	1.16	0.1	0.24	2.04	1.61	0.21	-1.13
EPA2191	Isopar M	1.2	0.2	0.23	1.84	1.75	0.1	-1.29
EPA2192	Isopar M	1.21	0.27	0.24	1.74	1.73	0.17	-1.25
EPA2227	Aromatic 200	1.36	0.24	0.54	1.31	1.17	0.67	-0.09
EPA2228	Aromatic 200	1.38	0.28	0.52	1.61	1.17	0.66	-0.13
<i>Hydrocarbon Solvents + NO_x + Surrogate+ H₂O₂</i>								
EPA2185	Conosol C-200 *	1.18	0.17	0.25	1.67	1.61	0.3	-1.11
EPA2186	Conosol C-200 **	1.2	0.21	0.2	1.63	1.66	0.22	-1.26

EPA2189	Isopar M	1.51	0.22	0.26	1.66	1.7	0.32	-1.18
EPA2190	Isopar M	1.24	0.27	0.27	1.94	1.94	0.12	-1.40
EPA2225	Aromatic 200	1.35	0.38	0.51	1.26	1.1	0.7	-0.08
EPA2226	Aromatic 200	1.33	0.36	0.53	1.16	1.1	0.73	-0.04
<i>Hydrocarbon Solvents + H₂O₂</i>								
EPA2182	Conosol C-70*	1.15	0.16	0.2	1.74	1.66	0.18	-1.26
EPA2183	Conosol C-400*	1.13	0.12	0.15	1.74	1.67	0.16	-1.37
EPA2184	Conosol C-200*	1.13	0.11	0.13	1.78	1.68	0.14	-1.42

-: NO data, *-local vendor, **-major company

Conosol C-70 and Conosol C-400 were obtained through a local vendor. They were used to make Conosol C-200 by blending with a mixing ratio to achieve the viscosity necessary for C-200 and is likely the cause of differences observed between C-200* and C-200**. Experiments with C-200* were performed prior to a major company providing us packaged C-200**.

IV. SUMMARY

This study was designed to evaluate the evaporation rate, of specific compounds in pure form and as part of mixtures as they are used in consumer products and then evaluate the ozone and SOA formation of these compounds once they enter the atmosphere. Ozone and SOA formation impacts from LVP-VOCs and mixtures were evaluated in the presence of a reactive surrogate mixture designed to mimic the reactivity of the atmosphere and more closely simulate atmospheric conditions. Perturbations to the system were made by enhancing hydroxyl radical reactivity to offset losses in the reaction system due to introduction of test species. The enhanced hydroxyl radical levels were also designed to more closely align with the reactive conditions in the outdoor environment. Ozone formation was modeled using SAPRC-11 to identify any LVP-VOC precursors not accurately represented by current models (non were identified). Observed SOA formation varied by a couple orders of magnitude based on the chemical structure of the LVP-VOC precursor. While the results of these experiments are useful to calibrate models and provide SOA formation relative to chemical structure of the compounds, it is noted that atmospheric conditions to vary widely and the results of this work are only for a subset of reactive conditions. Development of predictive models of SOA formation as a function of HO_2/NO or other reactive parameters is still required.

Therefore, the College of Engineering Center for Environmental Research and Technology (CE-CERT) at the University of California, Riverside (UCR) conducted laboratory and environmental chamber experiments to evaluate the volatility and ozone and secondary organic aerosol (SOA) formation potential of selected LVP-VOCs and consumer product-like mixtures containing the LVP-VOCs. The work utilized the advanced environmental chamber facility housed at CE-CERT designed to investigate atmospheric reactivity, ozone formation, and SOA formation at low atmospheric concentrations. Evaporation rates of the individual LVP-VOCs were observed to correlate strongly with vapor pressure and molecular weight. LVP-VOC evaporation rates were influenced by the presence of other chemicals in the consumer product mixtures. The effect appears to be related to mass transfer rates of the LVP-VOC to the air-mixture interface as opposed to significant changes in the thermodynamic equilibrium of those LVP-VOCs studied, as indicated by the observation that increasing surface area increased the partitioning of the LVP-VOC to the air from the consumer product.

Findings:

- a. The evaporation rate of the LVP-VOCs can be modeled according to semi-empirical relationship between evaporation rate, molecular weight, and vapor pressure. Most LVP-VOCs studied in this program evaporated (>95%) in less than six months with the exception of glyceryl triacetate, triethanolamine, and methyl palmitate.
- b. Wall loss of LVP-VOCs studied in this work was found to be negligible for DEGEE, DEGBE, and n-tridecane as additional experiments performed with and without inorganic seed had little impact on SOA formation indicating that the walls were not significantly contributing to losses of LVP-VOC oxidation products. However, wall losses of lower vapor pressure oxidation products of LVP-VOCs were found to be affected for LVP-VOCs with low aerosol formation and nucleation intensity (low number of particles formed during nucleation). The environmental chambers used in this work were deemed suitable to meet the goals of the study of ozone and SOA formation from LVP-VOCs.
- c. SAPRC-11 as evaluated for the LVP-VOCs studied and was found to predict well the gas-phase chemistry and ozone formation from the compounds. No evidence for significant changes to chemical mechanisms was observed.
- d. SOA formation from the LVP-VOCs varied widely. The hypothesis that LVP-VOCs begin with lower vapor pressure than VOCs and therefore will form more secondary aerosol was proven to be generally not true for the compounds studied. Many LVP-VOCs did not form SOA. However,

several selected LVP-VOCs formed appreciable SOA. Chemical structure was found to be a significant driver of SOA formation (e.g., glycol ether case study) The presence and location of –OH in the carbon bond of ethers was found to determine the occurrence of the cyclization mechanism during ether oxidation. Ethers with $-(\text{OCH}_2\text{CH}_2)_2 - \text{OH}$ structure was found to readily form cyclization products and was the dominant structure component driving SOA formation among all ethers. Further detailed studies are required to determine functional relationships of other LVP-VOC compound types to improve forecasting of ability of other LVP-VOC to form SOA.

- e. The addition of lab created generic consumer products (general purpose spray cleaner, paint stripper, caulk remover, laundry detergent, and hand lotion) had a weak influence on ozone formation from the surrogate mixture but strongly affected SOA formation. Other components in the mixtures also strongly contributed to aerosol formation, as the total aerosol formation observed could not be explained solely by the LVP-VOC present. The overall SOA and ozone formation of the generic consumer product could not be explained solely by the results of the pure LVP-VOC experiments.
- f. Ozone and SOA formation from hydrocarbon solvent mixtures (Conosol 200, Isopar M, and Aromatic 200) was also investigated. These mixtures all formed appreciable SOA, which was dramatically enhanced by the addition of H_2O_2 to offset loss of reactivity in surrogate mixture due to the addition of these solvents. The ozone suppression measured in the surrogate mixture in the presence of Isopar M and Conosol 200 are consistent with observations from large alkane molecules. The measurable SOA formation from Isopar M and Conosol 200 are consistent with observations from n-heptadecane suggesting that if sufficient atmospheric reactivity (hydroxyl radical levels) are present that large alkane molecules from a variety of sources may be significant contributors to SOA formation. Aromatic formation from Aromatic-200 is consistent with expectations from aromatic species present with aromatics having higher SOA formation than the other hydrocarbon solvent mixtures.

Suggestions of future work:

- a. SOA formation was found to be highly variable with initial vapor pressures of the LVP-VOC having little influence on the SOA formation from the LVP-VOC. However, the chemical structure of the LVP-VOC within a given class of chemicals (e.g., glycol ethers) was observed to have a profound effect on SOA formation (and to a lesser extent ozone formation). Similar detailed studies of other classes of LVP-VOCs would provide greater predictive measures for evaluating whether the LVP-VOC will form measurable SOA or not.
- b. The evaporation studies in this work provide insight into the governing mechanisms (mass transfer kinetic limitations) for the LVP-VOC to evaporate into the atmosphere. Further exploration of these impacts as it relates to more complex mixtures is suggested to assess the overall availability of the LVP-VOC for evaporation.
- c. Given the strong dependence of SOA formation on hydroxyl radical levels (and therefore likely hydroperoxy levels), further work predicting the influence of these levels on SOA generation as a function of HO_2/NO is suggested, similar to work that has been conducted on aromatic species. Further, this dependence is necessary in more accurately evaluating the behavior of LVP-VOCs as part of a complex mixture where other components of the mixture can influence HO_2/NO levels.
- d. Given the large number of potential sources of large alkanes, a detailed study on their SOA formation as a function of chain length and branching is necessary to provide experimental parameters needed to predict overall ambient impacts of alkanes on SOA formation.
- e. Finally, given the potential importance of chamber wall sorption of aerosol precursors and their oxidation products observed at other facilities (no major effects observed for this work), it is

important to continue to pursue research to understand their potential effects and reasons for observed differences in the importance of wall sorption artifacts on chamber derived SOA formation parameters.

V. REFERENCES

- Carter, W. P. L. (1994): "Development of Ozone Reactivity Scales for Volatile Organic Compounds," *J. Air & Waste Manage. Assoc.*, 44, 881-899.
- Carter, W. P. L., D. Luo, et al. (1995). "Environmental chamber studies of atmospheric reactivities of volatile organic compounds: Effects of varying chamber and light source." Statewide Air Pollution Research Center.
- Carter, W. P. L. (2000): "Documentation of the SAPRC-99 Chemical Mechanism for VOC Reactivity Assessment." Report to the California Air Resources Board, Contracts 92-329 and 95-308, May 8. Available at <http://cert.ucr.edu/~carter/absts.htm#saprc99> and <http://www.cert.ucr.edu/~carter/reactdat.htm>.
- Carter, W. P. L. (2002): "Development of a Next Generation Environmental Chamber Facility for Chemical Mechanism and VOC Reactivity Research." Draft Research Plan and First Progress Report to the United States Environmental Protection Agency Cooperative Agreement CR 827331-01-0, January 3. Available at <http://www.cert.ucr.edu/~carter/epacham>.
- Carter, W. P. L. (2004): "Evaluation of a Gas-Phase Atmospheric Reaction Mechanism for Low NO_x Conditions." Final Report to California Air Resources Board Contract No. 01-305, May 5. Available at <http://www.cert.ucr.edu/~carter/absts.htm#Inoxrpt>.
- Carter, W. P. L. (2007): "Environmental Chamber Studies of Ozone Impacts of Coatings VOCs." Proposal to the California Air Resources Board by the University of California, Riverside, December. (Approved for funding.)
- Carter, W. P. L. (2008a): "Development of the SAPRC-07 Chemical Mechanism and Updated Ozone Reactivity Scales," Final report to the California Air Resources Board Contract No. 03-318. May 28. Available at www.cert.ucr.edu/~carter/SAPRC.
- Carter, W. P. L. (2010): "Updated Maximum Incremental Reactivity Scale and Hydrocarbon Bin Reactivities for Regulatory Applications," Report to the California Air Resources Board, Contract 07-339, January 28, available at <http://www.cert.ucr.edu/~carter/SAPRC/MIR10.pdf>.
- Carter, W. P. L. (2011): "Environmental Chamber Study of Ozone Impacts of Coatings VOCs," Final report to California Air Resources Board Contract No. 07-339, May 11. Available at <http://www.cert.ucr.edu/~carter/absts.htm#coatrpt2>
- Carter, W. P. L., R. Atkinson, A. M. Winer, and J. N. Pitts, Jr. (1982): "Experimental Investigation of Chamber-Dependent Radical Sources." *Int. J. Chem. Kinet.*, 14, 1071.
- Carter, W. P. L., D. R. Cocker III, D. R. Fitz, I. L. Malkina, K. Bumiller, C. G. Sauer, J. T. Pisano, C. Bufalino, and C. Song (2005a): "A New Environmental Chamber for Evaluation of Gas-Phase Chemical Mechanisms and Secondary Aerosol Formation." *Atmos. Environ.* 39:7768-7788.
- Carter, W. P. L., I. L. Malkina, D. R. Cocker III, and C. Song (2005b): "Environmental Chamber Studies of VOC Species in Architectural Coatings and Mobile Source Emissions." Final Report to the South Coast Air Quality Management District Contract No. 03468, July 5. Available at <http://www.cert.ucr.edu/~carter/absts.htm#scaqcham>.
- Carter, W. and I. Malkina (2007). "Investigation of the Atmospheric Impacts of Selected Pesticides." Final Report to the California Air Resources Board Contract: 04-334.
- Carter, W.P.L. (2010): "Development of the SAPRC-07 Chemical Mechanism," *Atmospheric Environment*, 44: 5324-5335.
- Chan, A., Kroll, J., et al. (2007). "Kinetic modeling of secondary organic aerosol formation: effects of particle-and gas-phase reactions of semivolatile products." *Atmospheric Chemistry and Physics*, 7(15): 4135-4147.
- Chan, A. W. H., K. E. Kautzman, et al. (2009). "Secondary organic aerosol formation from photooxidation of naphthalene and alkylnaphthalenes: implications for oxidation of intermediate volatility organic compounds (IVOCs)." *Atmospheric Chemistry and Physics*, 9(9): 3049-3060.

- Chen, J., H. Mao, R.W. Talbot, and R.J. Griffin (2006), "Application of the CACM and MPMPO modules using the CMAQ model for the Eastern United States." *J. Geophys. Res.*, 111, D23S25, doi:10.1029/2006JD007603.
- Cocker, D.R., Flagan, R.C., Seinfeld, J.H.(2001), "State-of-the-art chamber facility for studying atmospheric aerosol chemistry." *Environ. Sci. Technol.*, 35(12): 2594-2601.
- Cocker Iii, D. R., S. L. Clegg, et al. (2001). "The effect of water on gas-particle partitioning of secondary organic aerosol. Part I: α -pinene/ozone system." *Atmospheric Environment*, 35(35): 6049-6072.
- Cocker Iii, D. R., B. T. Mader, et al. (2001). "The effect of water on gas-particle partitioning of secondary organic aerosol: II.m-xylene and 1, 3, 5-trimethylbenzene photooxidation systems." *Atmospheric Environment* 35(35): 6073-6085.
- DeCarlo, Peter F., et al. "Field-deployable, high-resolution, time-of-flight aerosol mass spectrometer." *Analytical chemistry*, 78, no. 24 (2006): 8281-8289.
- Donahue, N., A. Robinson, et al. (2006). "Coupled partitioning, dilution, and chemical aging of semivolatile organics." *Environmental Science & Technology*, 40(8): 2635-2643.
- Donahue, N. (2010). "Organic Aerosols and the Volatility Basis Set:Experimental and Modeling Applications." AAAR tutorial.
- Emanuelsson, E. U., Hallquist, M., Kristensen, K., Glasius, M., Bohn, B., Fuchs, H., Kammer, B., Kiendler-Scharr, A., Nehr, S., Rubach, F., Tillmann, R., Wahner, A., Wu, H.-C., and Mentel, Th. F. "Formation of anthropogenic secondary organic aerosol (SOA) and its influence on biogenic SOA properties." *Atmos. Chem. Phys.*, 13, 2837–2855, 2013.
- Erupe, M. E., A. Liberman-Martin, et al. (2010). "Determination of methylamines and trimethylamine-oxide in particulate matter by non-suppressed ion chromatography." *Journal of Chromatography A*, 1217(13): 2070-2073.
- Griffin, R.J., Cocker, D.R., Flagan, R.C., Seinfeld, J.H. (1999). "Organic Aerosol Formation from the Oxidation of Biogenic Hydrocarbons." *Journal of Geophysical Research*, 104, 3555-3567.
- Griffin, R.J., D. Dabdub, and J.H. Seinfeld (2005). "Development and initial evaluation of a dynamic species resolved model for gas-phase chemistry and size-resolved gas/particle partitioning associated with secondary organic aerosol formation." *J. Geophys. Res.*, 110, D05304, doi:10.1029/2004JD005219.
- Henry, F., C. Couer-Tourneur, F. Ledoux, A. Tomas, D. Menu (2007). "Secondary organic aerosol formation from the gas phase reaction of hydroxyl radicals with m-, o- and p-cresol." *Atmos. Environ.*, 42:13, 3035-3045.
- Henze, D.K., J.H. Seinfeld, N.L. Ng, J.H. Kroll, T.M. Fu, D.J. Jacob, C.L. Heald (2008). "Global modeling of secondary organic aerosol formation from aromatic hydrocarbons: high- vs. low-yield." *Atmos. Chem. Phys.*, 8:9, 2405-2420.
- Hu, D., Tolocka, M., Li, Q., Kamens, R. (2007). "A kinetic mechanism for predicting secondary organic aerosol formation from toluene oxidation in the presence of NO_x and natural sunlight." *Atmos. Env.*, 41(31), 6478-6496.
- Hurley, M.D., Sokolov, O., Wallington, T.J., Takekawa, H., Karasawa, M., Klotz, B., Barnes, I., Becker, K.H. (2001), "Organic aerosol formation during the atmospheric degradation of toluene." *Environ. Sci. Technol.*, 35(7), 1358-1366.
- Izumi, K., Fukuyama, T. (1990). "Photochemical Aerosol Formation from Aromatic-Hydrocarbons in the Presence of NO_x," *Atmospheric Environment*, 24(6), 1433-1441.
- Jang, M.S., Kamens, R.M. (2001), "Characterization of secondary aerosol from the photooxidation of toluene in the presence of NO_x and 1-propene." *Environ. Sci. Technol.*, 35(18), 3626-3639.
- Jeffries, H.E.; Gery, M.W.; and Carter, W.P.L. (1992) Protocol for evaluating oxidant mechanisms for urban and regional models. Report for U.S. Environmental Protection Agency Cooperative Agreement No. 815779, Atmospheric Research and Exposure Assessment Laboratory, Research Triangle Park, NC.

- Johnson, D., Jenkin, M.E., Wirtz, K., Martin-Reviejo, M. (2005). "Simulating the formation of secondary organic aerosol from the photooxidation of aromatic hydrocarbons." *Environmental Chemistry*, 2(1): 35-48.
- Krechmer, E. Jordan., Demetrios Pagonis, Paul J. Ziemann, Jose L. Jimenez (2016). "Quantification of Gas-Wall Partitioning in Teflon Environmental Chambers Using Rapid Bursts of Low-Volatility Oxidized Species Generated in Situ." *Environmental Science & Technology*, 50: 5757-5765.
- Kroll, J. H. & Seinfeld J. H. (2008). "Chemistry of secondary organic aerosol: formation and evolution of low-volatility organics in the atmosphere." *Atmos. Environ.*, 42:3593-3624.
- Lim, Y. B. and P. J. Ziemann (2009). "Effects of molecular structure on aerosol yields from OH radical-initiated reactions of linear, branched, and cyclic alkanes in the presence of NO_x." *Environmental Science & Technology*, 43(7): 2328-2334.
- Mackay, D. and Van Wdsenbeeck (2014). "Correlation of chemical evaporation rate with vapor pressure." *Environ Sci Technol*, 48(17):10259-63.
- Malloy, Q., Nakao, S., Switzer, D., Cocker, D., Hagino, H. (2008). "On-line Density Measurements of Secondary Organic Aerosol Formation." *submitted to Aerosol Science and Technology*.
- Matsunaga, A., K. S. Docherty, et al. (2009). "Composition and yields of secondary organic aerosol formed from OH radical-initiated reactions of linear alkenes in the presence of NO_x: Modeling and measurements." *Atmospheric Environment*, 43(6): 1349-1357.
- Matsunaga, A. and P. J. Ziemann (2010). "Gas-wall partitioning of organic compounds in a Teflon film chamber and potential effects on reaction product and aerosol yield measurements." *Aerosol Science and Technology*, 44(10): 881-892.
- McMurry, P.H., Stolzenburg, M.R., (1989). "On the sensitivity of particle size to relative humidity for Los Angeles aerosols." *Atmospheric Environment*, 23, 497-507.
- Na, K., C. Song, et al. (2006). "Formation of secondary organic aerosol from the reaction of styrene with ozone in the presence and absence of ammonia and water." *Atmospheric Environment*, 40(10): 1889-1900.
- Na, K., C. Song, et al. (2007). "Effect of ammonia on secondary organic aerosol formation from α -pinene ozonolysis in dry and humid conditions." *Environmental Science & Technology*, 41(17): 6096-6102.
- Nakao, S., C. Clark, et al. (2011). "Secondary organic aerosol formation from phenolic compounds in the absence of NO_x." *Atmos. Chem. Phys*, 11(10): 649.
- Nakao, S., L. Qi, et al. (2009). "Secondary organic aerosol formation from m-xylene photooxidation: the role of the phenolic product." *AGU Fall Meeting Abstracts*.
- Ng, N., P. Chhabra, et al. (2007). "Effect of NO_x level on secondary organic aerosol (SOA) formation from the photooxidation of terpenes." *Atmospheric Chemistry and Physics Discussions*, 7(4): 10131-10177.
- Ng, N., J. Kroll, et al. (2007). "Secondary organic aerosol formation from m-xylene, toluene, and benzene." *Atmospheric Chemistry and Physics Discussions*, 7(2): 4085-4126.
- Odum, J.R., Hoffmann, T., Bowman, F., Collins, D., Flagan, R.C., Seinfeld, J.H. (1996). "Gas/particle partitioning and secondary organic aerosol yields." *Environ. Sci. Technol.*, 30(8): 2580-2585.
- Odum, J.R., T.P.W. Jungkamp, R.J. Griffin, R.C. Flagan, and J.H. Seinfeld (1997). "The atmospheric aerosol-forming potential of whole gasoline vapor." *Science*, 276:96-99.
- Pankow JF. (1994a). "An absorption model of gas-particle partitioning of organic compounds in the atmosphere." *Atmospheric Environment* 28 (2): 185-188.
- Pankow JF. (1994b). "An absorption model of the gas-aerosol partitioning involved in the formation of secondary organic aerosol." *Atmospheric Environment*, 28(2): 189-193.
- Pathak, R., A. Presto, et al. (2007). "Ozonolysis of α -pinene: parameterization of secondary organic aerosol mass fraction." *Atmospheric Chemistry and Physics Discussions*, 7(1): 1941-1967.

- Rader, D. and P. McMurry (1986). "Application of the tandem differential mobility analyzer to studies of droplet growth or evaporation." *Journal of Aerosol Science*, 17(5): 771-787.
- Sato, K., S. Hatakeyama, T. Imamura (2007). "Secondary organic aerosol formation during the photooxidation of toluene: NO_x dependence of chemical composition." *J. Phys. Chem.*, 111, 9796-9808.
- Silva, P. J., M. E. Erupe, et al. (2008). "Trimethylamine as precursor to secondary organic aerosol formation via nitrate radical reaction in the atmosphere." *Environmental Science & Technology*, 42(13): 4689-4696.
- Song, C., K. Na, and D.R. Cocker III (2005). "Impact of the hydrocarbon to NO_x ratio on secondary organic aerosol formation." *Environ.Sci. Technol.*, 39:3143-3149.
- Song, C., Na, K., Warren, B., Malloy, Q., Cocker, D.R. (2007a). "Impact of Propene on Secondary Organic Aerosol Formation from m-Xylene." *Environ. Sci. Technol.*, 41:6990-6995.
- Song, C., Na, K., Warren, B., Malloy, Q., Cocker, D.R. (2007b). "Secondary Organic Aerosol Formation from m-Xylene in the absence of NO_x." *Environ. Sci. Technol.*, 41:7409-7416.
- Song, C., Na, K., Warren, B., Malloy, Q., Cocker, D.R. (2007c). "Secondary Organic Aerosol Formation from the Photooxidation of p- and o-Xylene." *Environ. Sci. Technol.*, 41:7403-7408.
- Võ, U. and Morris, M. (2012). "Non-Volatile, Semi-Volatile, or Volatile: Redefining Volatile for Volatile Organic Compounds." South Coast Air Quality Management District.
- Vuilleumier, L, Bamer, J., Harley, R., Brown, N. (2001), "Evaluation of Nitrogen Dioxide Photolysis Rates in an Urban Area Using Data from the 1997 Southern California Ozone Study.", *Atmos. Environ.*, 35:36, 6525-6537.
- Warren, B., C. Song, et al. (2008). "Light intensity and light source influence on secondary organic aerosol formation for the m-xylene/NO_x photooxidation system." *Environmental Science & Technology*. 42(15): 5461-5466.
- Warren, B., Cocker, D.R., Song, C., Carter, W.P.L., (2007). "Predicting Secondary Organic Aerosol Formation from Aromatics: m-Xylene Case Study." American Association for Aerosol Research 26th Annual Conference.
- Warren, B., Song, C., Carter, W.P.L., Cocker, D.R. (2008). "Predicting Secondary Organic Aerosol Formation: PM-SAPRC08." American Association for Aerosol Research 27th Annual Conference.
- Warren, B., Volkamer, R., J.L. Jimenez, F. San Martini, K. Dzepina, Q. Zhang, D. Salcedo, L.T. Molina, D.R. Worsnop, and M.J. Molina (2006). "Secondary organic aerosol formation from anthropogenic air pollution: Rapid and higher than expected." *Geophys. Res. Letters*, 33, L16804, doi:10.1029/2006GL026310.
- Ye, P., Ding, X., Hakala, Jani., Hofbauer, Victoria., Ellis S. Robinson, Neil M. Donahue (2016). "Vapor wall loss of semi-volatile organic compounds in a Teflon chamber." *Aerosol Science and Technology*, 50(8):822-834.
- Yeh, G. K., and Ziemann, P. J. (2014). "Alkyl Nitrate Formation from the Reactions of C₈-C₁₄ n-Alkanes with OH Radicals in the Presence of NO_x: Measured Yields with Essential Corrections for Gas-Wall Partitioning." *J. Phys. Chem. A*, 118:8147-8157.
- Zhang, Q., Jimenez, J. L. Canagaratna, M. R., Allan, J. D., Coe, H. Ulbrich, I. Alfarra, M. R., Takami, A. Middlebrook, A. M., Sun, Y. L., et al.(2007). "Ubiquity and dominance of oxygenated species in organic aerosols in anthropogenically-influenced Northern Hemisphere midlatitudes." *Geophys. Res. Let.*, 34:13, L13801.
- Zhang, X, Christopher D. Cappa, Shantanu H. Jathar, Renee C. McVay, Joseph J. Ensberg, Michael J. Kleeman, and John H. Seinfeld (2014). "Influence of vapor wall loss in laboratory chambers on yields of secondary organic aerosol." *PNAS*. 111(16):5802-5807.